ผลกระทบขององค์ประกอบของของไหลในแหล่งกักเก็บต่อการอัดก๊าซคาร์บอนไดออกไซด์ในแหล่งกักเก็บก๊าซธรรมชาติเหลว

นางสาว ปฐมาภรณ์ ทิตอร่าม

วิทยานิพนธ์นี้เป็นส่วนหนึ่งของการศึกษาตามหลักสูตรปริญญาวิศวกรรมศาสตรมหาบัณฑิต
สาขาวิชาวิศวกรรมปิโตรเลียม ภาควิชาวิศวกรรมเหมืองแร่และปิโตรเลียม
คณะวิศวกรรมศาสตร์ จุฬาลงกรณ์มหาวิทยาลัย
ปีการศึกษา 2552

EFFECT OF RESERVOIR FLUID COMPOSITION ON CARBON DIOXIDE INJECTION IN GAS CONDENSATE RESERVOIRS

Ms. Patamaporn Thitaram

A Thesis Submitted in Partial Fulfillment of the Requirements
for the Degree of Master of Engineering Program in Petroleum Engineering
Department of Mining and Petroleum Engineering
Faculty of Engineering
Chulalongkorn University
Academic Year 2009

Thesis Title	EFFECT OF RESERVOIR FLUID COMPOSITION ON CARBON DIOXIDE INJECTION IN GAS CONDENSATE RESERVOIRS
By	Ms. Patamaporn Thitaram
Field of Study	Petroleum Engineering
Thesis Advisor	Assistant Professor Suwat Athichanagorn, Ph.D.

Accepted by the Faculty of Engineering, Chulalongkorn University in Partial Fulfillment of the Requirements for the Master's Degree

.... Dean of the Faculty of Engineering
(Associate Professor Boonsom Lerdhirunwong, Dr.Ing.)

THESIS COMMITTEE

....Chairman
(Assistant Professor Jirawat Chewaroungroaj, Ph.D.)

Suwat Athichanagorn
....Thesis Advisor
(Assistant Professor Suwat Athichanagorn, Ph.D.)

Witsarut T.
....External Examiner
(Witsarut Thungsuntonkhun, Ph.D.)

ปฐมาภรณ์ ทิตอร่าม : ผลกระทบขององค์ประกอบของของไหลในแหล่งกักเก็บต่อการอัดก๊าซคาร์บอนไดออกไซด์ในแหล่งกักเก็บก๊าซธรรมชาติเหลว (EFFECT OF RESERVOIR FLUID COMPOSITION ON CARBON DIOXIDE INJECTION IN GAS CONDENSATE RESERVOIRS) อ. ที่ปรึกษาวิทยานิพนธ์หลัก: ผศ. ดร. สุวัฒน์ อธิชนากร, 163 หน้า.

แหล่งกักเก็บก๊าซธรรมชาติเหลวมักพบปัญหาการกีดขวางโดยก๊าซธรรมชาติเหลวเมื่อความดันภายในแหล่งกักเก็บลดลงต่ำกว่าความดันกลั่นตัว ปริมาณของของเหลวที่เกิดขึ้น ขึ้นกับองค์ประกอบของของไหลในแหล่งผลิต ถ้าปริมาณของของเหลวมีมากขึ้น จะทำให้เกิดการกีดขวางการผลิต การอัดก๊าซลงไปในแหล่งกักเก็บเป็นวิธีที่มีประสิทธิภาพในการแก้ปัญหานี้และยังเพิ่มผลผลิตก๊าซธรรมชาติเหลว

จุดประสงค์ของการศึกษานี้คือ ศึกษาผลกระทบของความหลากหลายขององค์ประกอบของของไหลในแหล่งกักเก็บก๊าซธรรมชาติเหลวต่อการอัดก๊าซคาร์บอนไดออกไซด์ องค์ประกอบของของไหล 10 ตัวอย่าง ถูกใช้ในการศึกษานี้ แบบจำลองชนิดพิจารณาองค์ประกอบถูกใช้ในการจำลองการอัดก๊าซคาร์บอนไดออกไซด์ จากผลการจำลองพบว่าความหลากหลายขององค์ประกอบของของไหลในแหล่งกักเก็บมีผลกระทบต่อเวลาที่เริ่มการอัดก๊าซคาร์บอนไดออกไซด์เพื่อให้ได้ผลผลิตก๊าซธรรมชาติเหลวสูงสุด เวลาที่เริ่มที่ดีที่สุดในการอัดก๊าซคาร์บอนไดออกไซด์คือเวลาที่ช้าที่สุดที่ทำให้ของเหลวที่กลั่นตัวออกมาระเหยไปหมดก่อนที่ความเข้มข้นของก๊าซคาร์บอนไดออกไซด์จะถึงขีดจำกัด เมื่อความดันกลั่นตัวมีค่าสูงหรือปริมาณของเหลวที่เกิดขึ้นมีค่าต่ำ เวลาเริ่มต้นที่ดีที่สุดในการอัดก๊าซจะเร็วขึ้น ในกรณีที่ความดันเริ่มต้นของแหล่งกักเก็บเท่ากับความดันกลั่นตัว อัตราการอัดก๊าซคาร์บอนไดออกไซด์ควรจะมากกว่าอัตราการผลิต จึงจะทำให้ได้ผลผลิตก๊าซธรรมชาติเหลวสูงสุด อัตราการอัดก๊าซที่สูงจะทำให้ความดันของแหล่งกักเก็บยังคงมีค่าสูง ดังนั้นของเหลวที่กลั่นตัวอยู่รอบๆหลุมผลิตจะระเหยไปหมด อย่างไรก็ดี ถ้าอัตราการอัดก๊าซสูงเกินไป ก๊าซคาร์บอนไดออกไซด์จะเข้าถึงหลุมผลิตเร็ว และการผลิตจะสิ้นสุดเร็วเนื่องจากความเข้มข้นที่สูงของก๊าซคาร์บอนไดออกไซด์ในก๊าซที่ผลิตได้ เมื่อปริมาณของเหลวที่เกิดขึ้นมีค่าต่ำ อัตราการอัดก๊าซที่ดีที่สุดจะมีค่าสูง

ภาควิชา วิศวกรรมเหมืองแร่และปิโตรเลียม..........ลายมือชื่อนิสิต.......ปฐมาภรณ์ ทิตอร่าม.......
สาขาวิชา วิศวกรรมปิโตรเลียม.........................ลายมือชื่อ อ.ที่ปรึกษาวิทยานิพนธ์หลัก...........
ปีการศึกษา 2552..

5071611521: MAJOR PETROLEUM ENGINEERING

KEYWORDS: /INJECTION/CO2/COMPOSITION/GAS CONDENSATE

PATAMAPORN THITARAM. EFFECT OF RESERVOIR FLUID COMPOSITION ON CARBON DIOXIDE INJECTION IN GAS CONDENSATE RESERVOIRS. THESIS ADVISOR: ASST. PROF. SUWAT ATHICHANAGORN, Ph.D., 163 pp.

Gas condensate reservoirs encounter a condensate blockage problem when the pressure around the wellbore falls below the dew point pressure. The amount of the liquid dropout depends on the composition of the reservoir fluid. If the percentage of liquid increases, it will restrict the production. Gas injection is the effective method to solve this problem and help increase recovery of the valuable condensate liquid.

The objective of this study is to evaluate the effect of different reservoir fluid compositions on CO_2 injection in a gas condensate reservoir. Ten sets of reservoir compositions were selected. A compositional reservoir simulation was used to simulate the performance of CO_2 injection. The results show that composition of reservoir fluid has a significant effect on the optimum starting time for CO_2 injection. In order to maximize condensate recovery, the time to start CO_2 injection is the latest time that CO_2 injection can revaporize liquid dropout before CO_2 concentration reaches the limit. When the dew point pressure is high or maximum liquid dropout is low, the most optimum time of injection will be quite early. In the case that the initial reservoir pressure is equal to the dew point pressure, CO_2 injection rate has to be higher than the production rate in order to maximize condensate recovery. The higher injection rate will keep the reservoir pressure high. Thus, liquid dropout around the wellbore can be completely revaporized. However, if the injection rate is too high, early CO_2 breakthrough at the producer will cause an early abandonment of the production due to high CO_2 content in the produced gas. When the maximum liquid dropout is low, the most optimum injection rate will generally be high.

Department: Mining and Petroleum Engineering.....Student's signature: Patamaporn
Field of study: Petroleum Engineering.................Advisor's signature: Suwat Athichanagorn
Academic Year: 2009.....................................

Acknowledgements

First of all, I would like to thank Asst. Prof. Suwat Athichanagorn, my thesis advisor, for giving knowledge of petroleum engineering and invaluable guidance during this study.

Secondly, I would like to thank all faculty members in the Department of Mining and Petroleum Engineering who have offered petroleum knowledge, technical advice, and invaluable consultation. I wish to thank the thesis committee members for their comments and recommendations that make this thesis formally complete.

I am indebted to Mr. Chaibhorn Kittirattanapaiboon for providing some important data used in this work. I would also like to thank Mr. Phakphum Tangkaprasert, for invaluable discussions, encouragement and provide some important data used in this work.

Finally, I would like to express my deep gratitude and thank to my parents who have always been my inspiration, hope, and faith.

Contents

CHAPTER

List of Tables

List of Figures

Page

List of Abbreviations

AIM	Adaptive IMplicit
bbl	barrel (bbl/d : barrel per day)
BCF	billion cubic foot
BHP	bottomhole pressure
BICs	binary interaction coefficients
BTU	British thermal unit
CGR	condensate-gas ratio
C_1	methane
C_2	ethane
C_3	propane
$i\text{-}C_4$ or $I\text{-}C_4$	isobutane
$i\text{-}C_5$ or $I\text{-}C_5$	isopentane
$n\text{-}C_4$ or $N\text{-}C_4$	normal butane
$n\text{-}C_5$ or $N\text{-}C_5$	normal pentane
C_6	hexane
C_{7+}	alkane hydrocarbon account from heptanes forward
CO_2	carbon dioxide
D	darcy
EOS	equation of state
FVF	formation volume factor
GPR	gas production rate
OPR	oil production rate
IRR	internal rate of return
LGR	local grid refinement
M	^{1} thousand (1,000 of petroleum unit), ^{2} million (dollar)
MSCF/D	thousand standard cubic feet per day
NaCl	sodium chloride
NEI	non-equilibrium initialisation
NPV	net present value
PR	Peng-Robinson

PVT	pressure-volume-temperature
PSIA or psia	pounds per square inch absolute
SCAL	special core analysis
SCF	standard cubic foot
SGAS	gas saturation
SGFN	gas saturation function
SOFN	oil saturation function
SRK	Soave Redlich-Kwong
STB or stb	stock-tank barrel
STB/D	stock-tank barrels per day
SWAT	water saturation
SWFN	water saturation function
THP	tubing head pressure
TVD	true vertical depth or total vertical depth
VLP	vertical lift performance

Nomenclature

B	formation volume factor
C	salinity of brine in weight percent of solid
E	sweep efficiency
k	permeability
k_{rg}	gas relative permeability
k_{rw}	water relative permeability
k_{rog}	oil relative permeability for a system with oil, gas and connate water
k_{row}	oil relative permeability for a system with oil and water only
k_{rowg}	oil relative permeability for a system with oil and water at $S_g = 0$
K_i	vapor liquid equilibrium ratio or the equilibrium vaporization ratio
M	molecular weight
p	pressure
p_c	capillary pressure
p_d	dew point pressure
R	solubility of CO_2 in water
S	saturation
T	temperature
x	distance
z	compressibility factor
Z	mole fraction of component

GREEK LETTER

ϕ	porosity
ρ	fluid density (mass/volume)
$\mathrm{\rho}$	density
Δ	difference operator
$\mathrm{\omega}$	Pitzer acentric factor

SUBSCRIPTS

A	areal
atm	at standard pressure

c	critical
d	displacement
g	gas
i	vertical
o	oil
sb	brine
sc	*at* standard condition
sw	distilled water
w	water

CHAPTER I

INTRODUCTION

In gas condensate reservoirs, condensate liquid can drop out and build up in the near wellbore region when the flowing bottomhole pressure declines below the dew point pressure. This phenomenon is called condensate blockage or condensate banking. The liquid percentage will increase and may eventually restrict production and also cause the loss of heavy component recovery.

The amount of the liquid dropout around the wellbore depends not only on the pressure and temperature, but also on the composition of the reservoir fluid. What should be well understood are the fluid phase properties, formation flow characteristics and pressure in the formation and in the wellbore. If these factors are not understood at the beginning of the field development, sooner or later production performance can suffer.

There are several techniques to solve the condensate blockage problem. Gas injection is an alternative technique to enhance gas and condensate recoveries by re-pressurization which maintains the reservoir pressure above the dew point pressure. Furthermore, the injected gas can re-vaporize the liquid dropout around the wellbore.

The purpose of this study is to investigate the effect of reservoir fluid composition on hydrocarbon recovery in gas condensate reservoirs. The results of this study will provide more understanding about the effect of reservoir fluid composition on CO_2 injection in gas condensate reservoirs and also provides the guideline for selecting the candidate reservoir for CO_2 injection.

1.1 Outline of Methodology

The thesis studies the effect of reservoir fluid composition on CO_2 injection in gas condensate reservoir to maximize the condensate recovery. The compositional simulation is used as a tool to study two initial reservoir conditions as listed below:

(a) The initial reservoir pressure is equal to 3,500 psia. Each reservoir fluid will reach the dew point pressure at different production times.

(b) The initial reservoir pressure is equal to the dew point pressure. In this scenario, liquid dropout around the wellbore will occur at the beginning of the production.

Two production and injection strategies which are natural depletion and CO_2 injection were simulated for each case as listed below:

(a) In natural depletion scenario, the production is simulated with one production well produced until condensate or gas production rate drops below the economic limit.

(b) In CO_2 injection scenario, the production is from one of the wells and then CO_2 injection is performed with different starting times on the other well until condensate or gas production rate drops below the economic limit or CO_2 concentration in the produced gas reaches its concentration limit.

In this study, the economic limits are set by condensate production rate, gas production rate and CO_2 concentration limit. The concentration limit of CO_2 is 23%. The 23% limit is the common CO_2 concentration limit in Gulf of Thailand. Then, the economic analysis will be performed in order to investigate the feasibility of CO_2 injection project.

1.2 Thesis Outline

This thesis consists of six chapters.

Chapter II outlines a list of related works/studies on CO_2 injection into gas condensate reservoir to reduce the condensate blockage and enhance hydrocarbon recovery.

Chapter III describes the overview of gas condensate reservoir and hydrocarbon production from gas condensate reservoir.

Chapter IV describes the principle of reservoir simulation model used in this study.

Chapter V discusses the results of reservoir simulation obtained from different sets of reservoir fluid composition.

Chapter VI provides conclusion and recommendation for further study.

CHAPTER II

LITERATURE REVIEW

This chapter discusses previous works that are related to the effect of gas injection on reduction of condensate blockage in gas condensate reservoir, the pressure/composition behavior of gas condensate and optimal injection/production strategy in gas condensate reservoir.

2.1 Previous works

The evaluation of pressure maintenance schemes by adding gas to gas condensate reservoirs was introduced by Chaback, and Williams [1]. The p-x behavior was studies by use of a rich gas condensate with CO_2 and equimolar mixture of N_2+CO_2 at 215 and 316 ^oF. The author revealed that addition of CO_2 can reduce the retrograde liquid formation than addition of N_2+CO_2 in both temperatures. They also studied the revaporization process of retrograde liquid. CO_2 was significantly more effective than the mixed gases in revaporizing retrograde liquid.

Shtepani [2] investigated CO_2 gas / condensate behavior. A p-x experiment was performed by collecting liquid and gas samples from separators. The different mole% CO_2 with 20, 40, 60 and 80 mole% CO_2 were used to investigate the phase behavior. The author revealed that at higher mole % CO_2, there was no retrograde liquid occurred and the mixture was in single phase gas.

He also performed CO_2 injection core flood test to identify CO_2 breakthrough characteristics. He has defined the width of dispersion zone as the distance between the locations at which the CO_2 concentration is 0.1 and 0.9 mole fraction. He concludes that the dispersion width is proportional to square root of time. For constant injection rate, the dispersion width is proportional to the square root of the mean distance traveled.

Many researchers have focused on the effect of the injected gas. Zaitsev et. al. [3] investigated the effect of different injection gases (methane, carbon dioxide, nitrogen, dry separator gas and wet separator gas) to maintain the reservoir pressure and reduce the condensate blockage around the wellbore. They concluded that the most effective injection gases were separator gases or carbon dioxide.

Ahmed et. al. [4] investigated ‘Huff and Puff ‘gas injection technique to remove liquid dropout in and around the wellbore. Different types of gas such as nitrogen, carbon dioxide, and methane and different combinations of gases were used in the investigation. They found that injecting pure carbon dioxide was the most effective injection gas to reduce liquid dropout around the wellbore. They also showed that the liquid blockage can be increased when injected with insufficient volume.

The study of optimum time of one-time produced gas injection to remove the condensate bank and improve well productivity was introduced by Marokane et. al. [5]. The gas condensate fluid with liquid dropout 6 %, 11% and 21% were used to investigate. The reservoir simulation results indicated that, the optimization of injection time for rich gas is to start injection before the maximum liquid dropout is attained. For lean gas, gas injection should start after the maximum liquid dropout is attained.

Tangkaprasert [6] studied optimal production and injection strategy of CO_2 injection in gas condensate reservoirs in order to maximize hydrocarbon recovery. A compositional simulation (ECLIPSE 300) was used as a tool to predict gas and condensate production under different strategies. The results show that the hydrocarbon recovery depends on the bottomhole pressure when the CO_2 injection starts. Injecting CO_2 within a short duration after the bottomhole pressure falls below the dew point pressure provides the maximum oil recovery and injecting CO_2 after the bottomhole pressure reaches the BHP limit increases gas recovery but decreases oil recovery. Starting injecting CO_2 after the bottomhole pressure reaches the BHP limit has no effect on oil and gas recovery.

The understanding of the composition change of reservoir fluid and the development methodology to increase the productivity of gas and condensate from gas condensate reservoir was introduced by Shi and Horne [7]. The effects of different bottomhole pressure, relative permeability and production rate have been compared, and the optimum producing sequences are suggested for maximum recovery. They concluded that the composition and condensate saturation change significantly as a function of relative permeability and interfacial tension effect. The higher the BHP, the less condensate banking and the smaller the amount of heavy component in the reservoir. In the case of lower production rate, the amount of heavy component left in the reservoir is lower. They also suggested that gas productivity can be maximized with proper production strategy.

Chang et. al. [8] proposed a significant parameter that cannot be neglected in the simulation, the solubility of CO_2 in water, by generating a new empirical correlation. The correlation determines the solubility of CO_2 in distilled water as a function of temperature and pressure. In the effect of salinity, the solubility in distilled water can be adjusted to obtain the solubility of CO_2 in NaCl brine. Furthermore, correlations for computing other properties of CO_2 saturated-water are presented in this paper.

CHAPTER III

THEORY AND CONCEPT

This chapter discusses the fundamental of gas condensate reservoir and related theories involved with the mechanism of CO_2 injection in gas condensate reservoir.

3.1 Review of Gas Condensate Reservoir

The type of reservoir fluids can divided into five types; black oil, volatile oil, retrograde gas, wet gas and dry gas. Each type of reservoir fluids has unique characteristics which can be confirmed only by observation in the laboratory. The characteristics used to identify the type of reservoir fluid are the *initial producing gas oil ratio*, the *gravity of the stock tank liquid*, the *color of the stock tank liquid*, *oil formation volume factor*, and *mole fraction of hepthane plus*.

Gas condensate reservoir is one of the reservoirs which can be considered as the most complex reservior. The initial reservoir condition is a single phase gas. As the reservoir produces, the reservoir pressure will decrease until reaching the dewpoint and liquid starts to drop out of the gas.

3.1.1 Gas Condensate Phase Behavior

Gas condensate or retrograde gas is one of the various types of reservoir fluid which has unique characteristics of phase diagram as illustrated in Figure 3.1. The region of retrograde condensation occurs at temperatures between the critical temperature (T_C) and the cricondentherm. The cricondenterm is the highest temperature on saturated envelope.

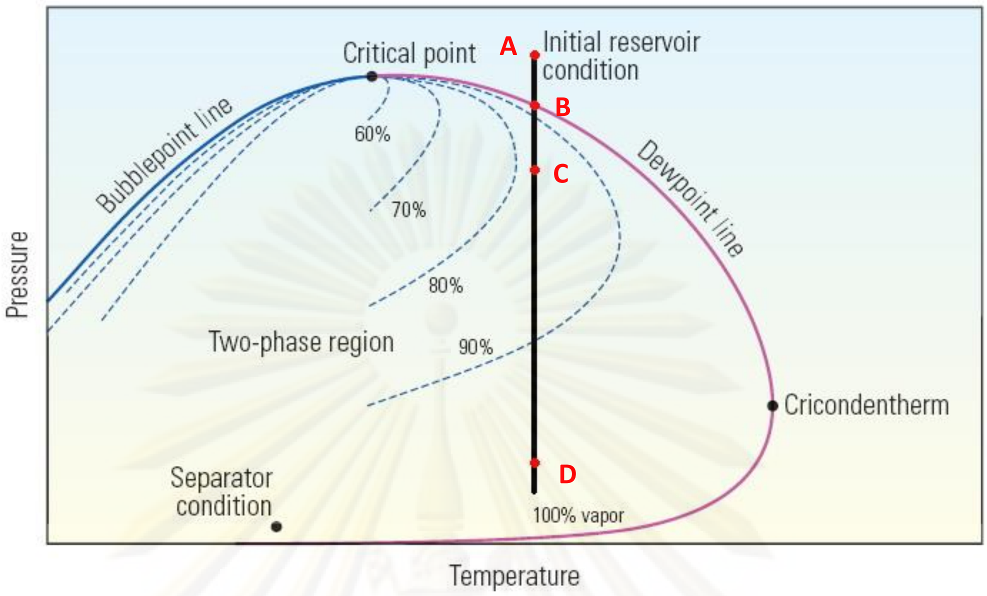

Figure 3.1: Pressure-Volume-Temperature diagram of condensate (after Fan et. al. [9]).

The gas condensate is a single-phase gas at original reservoir condition (point A). Under certain conditions of temperature and pressure, the fluid will separate into gas and liquid that is called a retrograde condensate (point B). The liquid dropout in the pore space will lead to the formation of a liquid phase and a consequent reduction in the gas production of the well. This phenomenon continues until a point of maximum liquid volume is reached (point C). Lowering the pressure will cause the re-vaporization process (point D) but this process is typically below the economic life of the field, and this stage will not be reached.

The amount of the liquid dropout does not only depend on the temperature and pressure, but also depends on the composition of the reservoir fluid. The condensate gas can be classified into three types; poor, middle and rich content condensate gas. The classifications and the physical characteristics are listed in Table 3.1 [10].

Table 3.1: Physical characteristics of condensate gas (after Yisheng et. al. [10]).

Fluid Type	Heavier Hydrocarbon Content C7+	Reservoir Fluid Density (g/cm$^{3)}$	Production GOR (m^3/m$^{3)}$	Condensate Content (g/m$^{3)}$
Poor	0.5~2.0	0.2~0.25	18000~5000	<150
Middle	2.0~4.0	0.25~0.30	5000~2000	150~350
Rich	4.0~9.0	0.30~0.45	2000~1000	350~600
Near Critical	9.0~12.5	0.45~0.50	1000~700	600~800

A rich gas condensate forms a higher percentage of liquid than a lean gas condensate. The phase diagrams of poor, middle and rich content condensate gas are shown in Figures 3.2, 3.3, and 3.4, respectively.

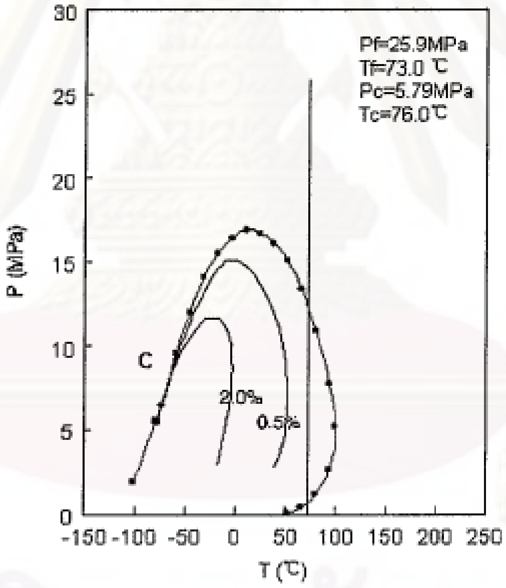

Figure 3.2: Pressure-Volume-Temperature diagram of poor condensate content (after Yisheng et. al. [10]).

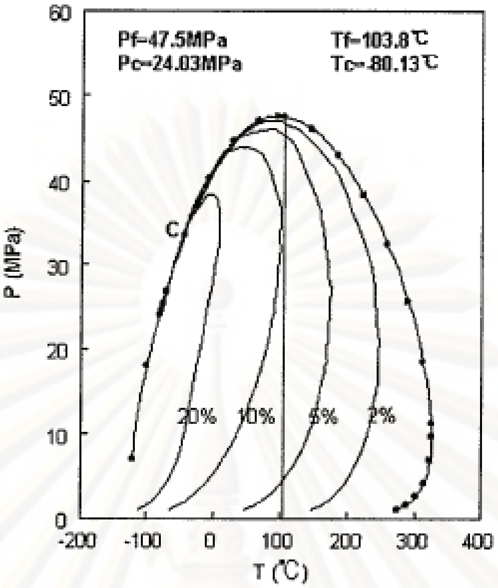

Figure 3.3: Pressure-Volume-Temperature diagram of middle condensate content (after Yisheng et. al. [10]).

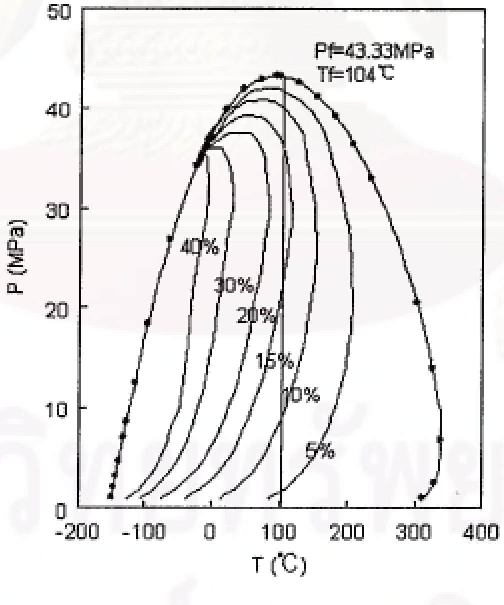

Figure 3.4: Pressure-Volume-Temperature diagram of rich condensate content (after Yisheng et. al. [10]).

3.1.2 Regions around Gas Condensate Wellbores

The flow in gas condensate fields can be divided into three regions. The two regions closet to a producing well exist when the pressure is below the dew point pressure and the third region exist when its pressure is above the dew point pressure as shown in Figure 3.5 [9].

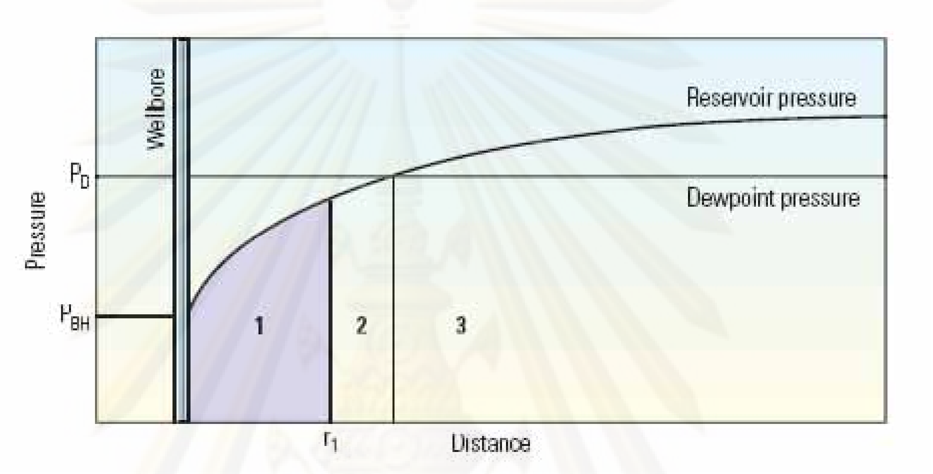

Figure 3.5: Three regions of gas condensate reservoir (after Fan et. al. [9]).

Regions 1: This region is close to a producing well where both gas and condensate are flowing simultaneously at different velocities. The condensate saturation of this region is greater than the critical condensate saturation, both gas and condensate flow. The oil relative permeability increases with saturation while gas relative permeability decreases, which illustrates the blockage effect.

Regions 2: In the second region, the liquid drops out of the gas phase. The condensate saturation of this region is less than the critical saturation, only gas phase is flowing.

Regions 3: This region is away from the producing well where only gas phase is present and flowing. Gas velocity in this region is generally low because the cross sectional area is high. Composition in this region is equal to the original reservoir gas.

There may also exist a fourth region immediately near wellbore where low interfacial tension at high gas velocity leads to decreased condensate saturation and increased gas mobility. This phenomenon is referred to as *positive coupling*.

3.1.3 Dew point Pressure of Condensate Fluid

The retrograde dew point occurs when a gas mixture containing heavy hydrocarbons is depressured until a liquid is formed. The retrograde dew point is significant in interpreting the reservoir behavior. A possible method of calculating the dew point pressure would be to employ a set of equilibrium ratios (K-values). The K-values depend on composition as well as temperature and pressure.

The dew point pressure can be calculated from a correlation proposed by Nemeth and Kennedy [11]

$\ln P_d = A_1\left[z_{C_2} + z_{CO_2} + z_{H_2S} + z_{C_6} + 2\left(z_{C_3} + z_{C_4}\right) + z_{C_5} + 0.4z_{C_1} + 0.2z_{N_2}\right] +$
$A_2\,\rho_{C_{7+}} + A_3\left[z_{C_1}/\left(z_{C_{7+}} + 0.002\right)\right] + A_4\,T + A_5\left(z_{C_{7+}} \times M_{C_{7+}}\right) + A_6\left(z_{C_{7+}} \times\right.$
MC7+2+A7zC7+×MC7+3+ A8 MC7+/ρC7++0.0001+ A9
$\left[M_{C_{7+}}/\left(\rho_{C_{7+}} + 0.0001\right)\right]^2 + A_{10}\left[M_{C_{7+}}/\left(\rho_{C_{7+}} + 0.0001\right)\right]^3 + A_{11}$
(3.1)

where

P_d	=	dew point pressure, psia	T	=	temperature, ^{o}R
Z	=	mole fraction of component	M	=	molecular weight
ρ	=	density, gm/ml	A_1	=	-2.0623054
A_2	=	6.6259728	A_3	=	$-4.4670559 \times 10^{-3}$
A_4	=	1.0448346×10^{-4}	A_5	=	3.2673714×10^{-2}
A_6	=	$-3.6453277 \times 10^{-3}$	A_7	=	7.4299951×10^{-5}
A_8	=	$-1.1381195 \times 10^{-1}$	A_9	=	6.2476497×10^{-4}
A_{10}	=	$-1.0716866 \times 10^{-6}$	A_{11}	=	1.0746622×10

3.2 Two Phase Equilibrium

Equilibrium is a static condition which no changes occur in the macroscopic properties of a system with time. The area bounded by the bubble point and dewpoint curves on the phase diagram of a multicomponent mixture defines the conditions for vapor and liquid to exist in equilibrium. There are two methods commonly used to calculate the vapor liquid equilibrium which are flash calculation and equation of state.

3.2.1 Flash calculation

Flash calculations involve solving simple material balance equations for multiphase systems in order to establish the phase compositions as well as amounts upon equilibrium seperation.

Consider F moles of a hydrocarbon mixture of composition (z_i) entering a seperation unit. At the operating conditions of seperator, it splits into L moles of liquid of composition (x_i), and V moles of vapor of composition (y_i). Then, by the law of conservation of mass:

$$F = L + V \tag{3.2}$$

And

$$Fz_i = Lx_i + Vy_i \qquad \text{for each component i} \tag{3.3}$$

The vapor liquid distribution coefficient, commonly known as the vapor liquid equilibrium ratio or the equilibrium vaporization ratio, K_i, is defined by

$$K_i = \frac{y_i}{x_i} \tag{3.4}$$

This quantity is known as the K-value for component *i*. The mole fractions of component *i* in liquid phase (x_i) and vapor phase (y_i) are given as

$$x_i = \frac{Z_i}{[1+\propto(K_i-1)]} \tag{3.5}$$

$$y_i = \frac{Z_i K_i}{[1+\propto(K_i-1)]} \tag{3.6}$$

where $$\propto = \frac{\text{V(lb mole of the vapor leaving the seperator)}}{\text{F(lb mole of the fluid stream entering the seperator)}} \tag{3.7}$$

Equilibrium ratio values can be determined by laboratory equilibrium flash experiments by analyzing the mole fractions of the different components in the vapor and liquid phases.

3.2.2 Equations of State

Though the K-value approach is easily the most common representative of two-phase equilibrium, it suffers from a lack of generality and may result in inaccuracies particularly near the convergence pressure. Equation of state (EOS) seems to be more common since there are potentially able to work near the critical point and yield internally consistent densities and molar volumes.

In 1873, Van Der Waals [12] introduced the first equation of state derived by the assumption of a finite volume occupied by the constituent molecules. His new formula revolutionized the study of equation of state, and was most famously continued via the Redlich-Kwong equation of state and the Soave modification of Redlich-Kwong. Two popularly accepted equations of state in the petroleum industry are Redlich-Kwong and Peng-Robinson.

Redlich-Kwong

Redlich and Kwong [13] proposed an equation of state which takes into account the temperature dependencies of the molecular attraction term in a manner.

$$p = \frac{RT}{V_m - b} - \frac{a}{\sqrt{T} V_m (V_m + b)} \tag{3.8}$$

Where

$$a = 0.42747 \frac{R^2 T_c^{2.5}}{P_c} \text{ and } b = 0.08664 \frac{RT_c}{P_c} \tag{3.9}$$

Soave [14] suggested that $a/\sqrt{T}$ be replaced with a temperature dependent term, a_T. This modification is often called the Soave Redlich-Kwong (SRK) equation of state.

$$p = \frac{RT}{V_m - b} - \frac{a_T}{V_m (V_m + b)} \tag{3.10}$$

$$a_c = 0.42747 \frac{R^2 T_c^2}{P_c} \text{ and } b = 0.08664 \frac{RT_c}{P_c} \tag{3.11}$$

The equation for a_T is

$$a_T = a_c \alpha \tag{3.12}$$

where a_c is the value of a_T at the critical temperature and α is a nondimensional temperature-dependent term which has a value of 1.0 at the critical temperature. The values of α is obtained from

$$\alpha^{1/2} = 1 + m\left(1 - T_r^{1/2}\right) \tag{3.13}$$

$$m = 0.480 + 1.574\omega - 0.17\omega^2 \tag{3.14}$$

$$\omega = -(\log P_{vr} + 1) \quad \text{at} \quad T_r = 0.7 \tag{3.15}$$

where ω is the Pitzer acentric factor for each pure substance and P_{vr} is the reduced vapor pressure.

Peng-Robinson

Peng and Robinson [15] proposed a slightly different form of the molecular attraction term.

$$p = \frac{RT}{V_m - b} - \frac{a_T}{V_m^2 + 2bV_m - b^2} \tag{3.16}$$

$$a_c = 0.45724 \frac{R^2 T_c^2}{P_c} \text{ and } b = 0.07780 \frac{RT_c}{P_c} \tag{3.17}$$

The equation for a_T is

$$a_T = a_c \alpha \tag{3.18}$$

The values of α is obtained from

$$\alpha^{1/2} = 1 + m\left(1 - T_r^{1/2}\right) \tag{3.19}$$

$$m = 0.37464 + 1.5422\omega - 0.26992\omega^2 \tag{3.20}$$

3.3 Hydrocarbon Production from Gas Condensate Reservoirs

The key to develop a gas condensate reservoir is to select the suitable development scheme based on gas condensate phase behavior. In general, it is difficult and complicated to develop a gas condensate reservoir effectively. The reasons are as follows:

(a) Low condensate recovery when the reservoir pressure is lower than the dewpoint pressure.

(b) There are complicated multiphase flows in the gas condensate reservoir with oil ring or with bottom oil or with edge/bottom water.

(c) The complicated surface processing technologies, such as gathering, transferring and boosting, are required.

The hydrocarbon production from gas condensate reservoirs can be natural depletion or gas cycling or gas injection which is described as follows:

(a) In natural depletion, the reservoir is produced from one production well without any injection. The main disadvantage is low condensate recovery for the gas reservoir with high condensate content. The condensate recovery factor of natural depletion is only 20~40% [10].

(b) The reservoir pressure maintenance by gas cycling or gas injection can reduce the condensate loss, enhance the condensate recovery, and increase the economic profit. Gas injection can re-pressurize the reservoir pressure to be above the dew point pressure that would avoid gas changing to liquid in the reservoir. Furthermore, the injected gas can re-vaporize the liquid dropout around the wellbore when the reservoir pressure is below the dew point pressure. It is estimated that the recovery is 19~25% higher than the natural depletion development [10].

3.3.1 Flooding Pattern and Sweep Efficiency

There are several patterns of production wells and injection wells for enhanced recovery project. The patterns are

(a) Two-spot

(b) Three-spot

(c) Regular four-spot and skewed four-spot

(d) Normal five-spot and inverted five-spot

(e) Normal seven-spot and inverted seven -spot

(f) Normal nine-spot and inverted nine -spot

(g) Direct line drive

(h) Staggered line drive

Different flooding patterns will result in different areal sweep efficiencies. The normal five-spot pattern is the highest areal sweep efficiency and most common flooding pattern. The areal sweep efficiencies at breakthrough for several of flooding patterns are listed in Table 3.2 [16].

Table 3.2: Areal sweep efficiency for various flooding patterns (after Forrest [16]).

Flooding Pattern	**Mobility Ratio**	**Areal sweep efficiency at breakthrough (%)**
Isolated two-spot	1.0	52.5 – 53.8
Isolated three-spot	1.0	78.5
Skewed four-spot	1.0	55.0
Inverted five-spot	1.0	80.0
Normal seven-spot	1.0	74.0-82.0
Inverted seven-spot	1.0	82.2

The overall efficiency at breakthrough is defined as

$$E = E_A \cdot E_i \cdot E_d \tag{3.21}$$

where E_A is areal sweep efficiency, E_i is vertical sweep efficiency, and E_d is displacement efficiency.

In this study, the injectors and producers are arranged as normal five-spot pattern which consists of a injection well surrounded by four production wells. An inverted pattern has an production well surrounded by four injection wells. The schematic of five spot flooding pattern is shown in Figure 3.6.

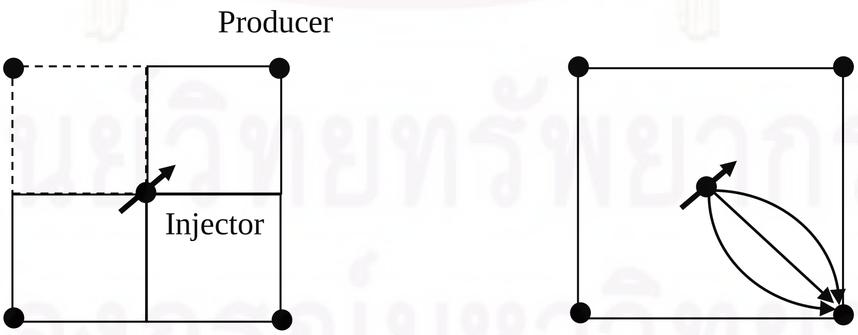

Figure 3.6: Five spot flooding pattern.

3.3.2 CO_2 Dispersion

The efficiency of CO_2 injection in gas condensate reservoirs depends on the phase behavior of mixtures of the gas with the liquid. CO_2 is miscible with hydrocarbon gas. Components in the gas may dissolve in the condensate and in the water, while some components present in the condensate and some water transfer to the vapor phase.

For CO_2 injection into gas condensate fields, the important issues involve the effect of miscible mixing of the gases by dispersion. The dispersion is a contribution of convection and molecular diffusion. The width of dispersion zone as the distance between the locations at which the CO_2 concentration is 0.1 and 0.9 mole fraction. The width of dispersion zone can be calculated from the correlation proposed by E. Shtepani [2].

$$x_{0.1-}x_{0.9} = 3.625\sqrt{K_l t} \qquad (3.22)$$

K_l is the longitudinal dispersion coefficient, and t is time after CO_2 injection begin.

3.3.3 CO_2 Solubility in water

The solubility of CO_2 in water is much higher than that of hydrocarbon components and is a factor that cannot be neglected in the simulation process. CO_2 solubility is a function of pressure, temperature, and water salinity. The solubility of CO_2 will increase with pressure and decrease with temperature. An increase in salinity of the reservoir water decreases the solubility of CO_2. The CO_2 solubility in water can be calculated from the correlation proposed by Chang et. al. [8].

The solubility of CO_2 in distilled water may be estimated as

$$R_{sw} = a \cdot p \cdot \left[1 - b \cdot \sin\left(\frac{\pi}{2} \cdot \frac{c \cdot p}{c \cdot p + 1}\right)\right] \qquad \text{if } p < p^0 \qquad (3.23)$$

$$R_{sw} = R_{sw}^0 + m \cdot (p - p^o) \qquad \text{if } p \geq p^0 \qquad (3.24)$$

where

$$a = \sum_{i=0}^{4} a_i \cdot 10^{-3i} \cdot T^i \tag{3.25}$$

$$b = \sum_{i=0}^{4} b_i \cdot 10^{-3i} \cdot T^i \qquad 0 < b < 1 \tag{3.26}$$

$$c = 10^{-3} \cdot \sum_{i=0}^{4} c_i \cdot 10^{-3i} \cdot T^i \tag{3.27}$$

$$p^0 = \frac{2}{\pi} \cdot \frac{\sin^{-1}(b^2)}{c \cdot \left[1 - \frac{2}{\pi} \cdot \sin^{-1}(b^2)\right]} \tag{3.28}$$

$$R_{sw}^0 = a \cdot p^0 \cdot (1 - b^3) \tag{3.29}$$

$$m = a\left\{1 - b\left[\sin\left(\frac{\pi}{2} \cdot \frac{c \cdot p^0}{c \cdot p^0 + 1}\right) + \frac{\pi}{2} \frac{c \cdot p^0}{(c \cdot p^0 + 1)^2} \cos\left(\frac{\pi}{2} \cdot \frac{c \cdot p^0}{c \cdot p^0 + 1}\right)\right]\right\} \tag{3.30}$$

R_{sw} is CO_2 solubility in scf of CO_2 per STB of water, T is temperature (^oF), p is pressure (psia), and the coefficients are shown in Table 3.3.

Table 3.3: Values of Coefficient in Eqs 3.25 to 3.27.

	a_i	**b_i**	**c_i**
i = 0	1.163	0.965	1.28
i = 1	-16.63	-0.272	-10.757
i = 2	111.073	0.0923	52.696
i = 3	-376.859	-0.1008	-222.395
i = 4	524.889	0.0998	462.672

The calculated solubility in distilled water can be adjusted further for the effects of salinity to obtain the solubility of CO_2 in brine:

$$\log\left(\frac{R_{sb}}{R_{sw}}\right) = -0.028 \cdot S \cdot T^{-0.12} \tag{3.31}$$

R_{sb} is CO_2 solubility in scf of CO_2 per STB of brine, S is the salinity of brine in weight percent of solid, and T is temperature (^oF).

The formation volume factor of CO_2-saturated water (or brine) is calculated with

$$B_w = \frac{\rho_{w,sc} + 0.02066 \cdot R_{sb}}{\rho_{w,atm} + 0.0058 \cdot R_{sb}} \tag{3.32}$$

B_w is water formation volume factor in reservoir barrel per STB of water (rb/STB), $\rho_{w,sc}$ is water density at standard temperature and pressure in lb/ft^3, and $\rho_{w,atm}$ is water density at reservoir temperature and 14.7 psia in lb/ft^3.

CHAPTER IV

RESERVOIR SIMULATION MODEL

In this chapter, the reservoir simulation model that is used to predict the performance of gas condensate reservoir is presented. Three main sections of reservoir simulation model are

1. **PVT*i* section.** PVT*i* generates the phase behavior of the reservoir fluid and calculates the binary interaction coefficients between components.
2. **ECLIPSE section.** ECLIPSE 300 is used to simulate the performance of the gas condensate reservoir.
3. **VFP section.** VFP constructs the wellbore model and calculates the vertical performance.

This chapter describes each section in details and how properties in each section were gathered. The detail of the simulation input is shown in Appendix A.

4.1 PVTi Section

PVT*i* is a compositional PVT equation of state based program used for characterizing a set of fluid samples. The component type is *user defined*. In this type, the physical properties of each component such as critical pressure, critical temperature, and acentric factors can be defined by the user, so the phase diagram and the binary interaction coefficients (BICs) will be generated.

The initial fluid compositions used in this study are actual field data from Society of Petroleum Engineering papers, as shown in Table 4.1 [17].

Table 4.1: Initial composition of reservoir fluid.

Component	**Fraction Case 1**	**Fraction Case 2**	**Fraction Case 3**	**Fraction Case 4**	**Fraction Case 5**	**Fraction Case 6**	**Fraction Case 7**	**Fraction Case 8**	**Fraction Case 9**	**Fraction Case 10**
Methane (CH_4)	0.59991	0.6481	0.7426	0.8358	0.832	0.834	0.7351	0.7104	0.6072	0.6372
Ethane (C_2H_6)	0.084326	0.0527	0.0818	0.0595	0.074	0.072	0.0623	0.0757	0.081	0.0575
Propane (C_3H_8)	0.063988	0.0623	0.0395	0.0291	0.028	0.0274	0.0301	0.0348	0.0637	0.0437
Iso-Butane (C_4H_{10})	0.034127	0.0167	0.0104	0.0045	0.0063	0.0054	0.0289	0.0064	0.0398	0.0498
Normal-Butane (C_4H_{10})	0.038989	0.0309	0.0158	0.0111	0.0094	0.009	0.0365	0.0143	0.0445	0.0315
Iso-Pentane (C_5H_{12})	0.014286	0.0137	0.0074	0.0036	0.0048	0.0042	0.024	0.005	0.0291	0.0341
Normal-Pentane (C_5H_{12})	0.013988	0.0131	0.0087	0.0048	0.004	0.003	0.0111	0.0056	0.0252	0.0302
Hexane (C_6H_{14})	0.072718	0.0159	0.0098	0.006	0.0064	0.0058	0.0174	0.0075	0.0179	0.0109
Heptane (C_7H_{16})	0.065366	0.1339	0.0656	0.008	0.0074	0.0049	0.0138	0.0107	0.0885	0.104
Octane (C_8H_{18})	-	-	-	0.0076	0.0048	0.0054	0.0097	0.0136	-	-
Nonane (C_9H_{20})	-	-	-	0.0047	0.0036	0.0043	0.0077	0.0086	-	-
Decane ($C_{10}H_{22}$)	-	-	-	0.0103	0.0026	0.0033	0.0048	0.0061	-	-
Undecane ($C_{11}H_{24}$)	-	-	-	-	0.0099	0.0147	0.0143	0.0041	-	-
Dodecane ($C_{12}H_{26}$)	-	-	-	-	-	-	-	0.0202	-	-
Carbon dioxide (CO_2)	0.012302	0.0106	0.004	0.0065	0.002	0.0019	0.0021	0.0708	0.0018	0.0008
Nitrogen (N_2)	-	0.0021	0.0144	0.0085	0.0048	0.0047	0.0022	0.0062	0.0013	0.0003

The physical properties of each component were acquired from Engineering Data Book, GPSA 1987, as shown in Table 4.2 [18].

Table 4.2: Physical properties of each component.

Comp.	Boiling Point (^oR)	Critical Pressure (psia)	Critical Temp. (^oR)	Critical Volume (ft^3/lb-mole)	Molecular Weight	Acentric factor
C_1	201.280	667.0	343.34	0.0988	16.043	0.0108
C_2	332.540	707.8	550.07	0.0783	30.070	0.0972
C_3	416.270	615.0	665.92	0.0727	44.097	0.1515
i-C_4	470.780	527.9	734.41	0.0714	58.123	0.1852
n-C_4	491.080	548.8	765.51	0.0703	58.123	0.1981
i-C_5	542.090	490.4	828.96	0.0684	72.150	0.2286
n-C_5	556.890	488.1	845.70	0.0695	72.150	0.2510
C_6	615.700	439.5	911.80	0.0688	86.177	0.2990
C_7	669.070	397.4	970.90	0.0682	100.204	0.3483
C_8	718.170	361.1	1023.50	0.0673	114.231	0.3978
C_9	763.400	330.7	1070.80	0.0693	128.258	0.4425
C_{10}	805.400	304.6	1112.20	0.0702	142.285	0.4881
C_{11}	844.800	287.2	1150.20	0.0366	156.310	0.5370
C_{12+}	881.160	263.9	1184.40	0.0398	170.340	0.5760
CO_2	350.765	1069.5	547.73	0.0342	44.010	0.2667
N_2	139.564	492.8	227.51	0.0510	28.013	0.0370

The phase behavior of all ten initial compositions and the binary interaction coefficient between components are shown in Appendix B.

4.2 ECLIPSE Section

Reservoir simulation can be used to predict the performance of gas condensate reservoir. The fluid description of the reservoir simulation can divided to *Black oil*, *Equation of state (EOS)-compositional*, and *Chemical*. The black oil model assumes that there are only two hydrocarbon components (oil and gas) in the fluid. This model is inappropriate when the composition changes with time, such as gas injection. In this case, the compositional model (ECLIPSE 300) with multiple hydrocarbon components is necessary. The required data for the compositional model are described as follows:

4.2.1 Grid

The reservoir model is plane geometry and homogenous. The selected grid system is Cartesian coordinate. The dimensions of the reservoir are 2,250 ft x 2,250 ft x 120 ft and 8,000 ft TVD (depth of top face). The number of block is 15 x 15 x 3. The quarter five-spot injection pattern with an injector at one of the corners and a producer at the opposite corner was selected for this study.

The most accurate way to determine near well behavior of a gas condensate field is to use local grid refinement (LGR). The local grid refinement of the producer is shown in Table 4.3. The top view, side view, and 3D view of this model are shown in Figures 4.1, 4.2, and 4.3, respectively.

Table 4.3: Local grid refinement of the producer.

LGR Name	LGR Coordinate			Number of refined cells		
	I	J	K	X	Y	Z
Producer	1-2	1-2	1-3	8	8	3

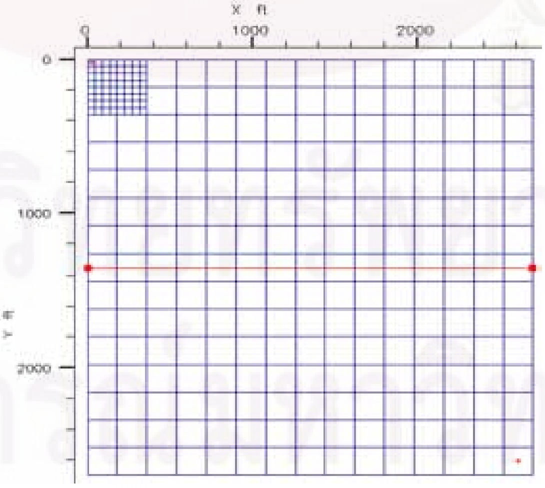

Figure 4.1: Top view of the reservoir model.

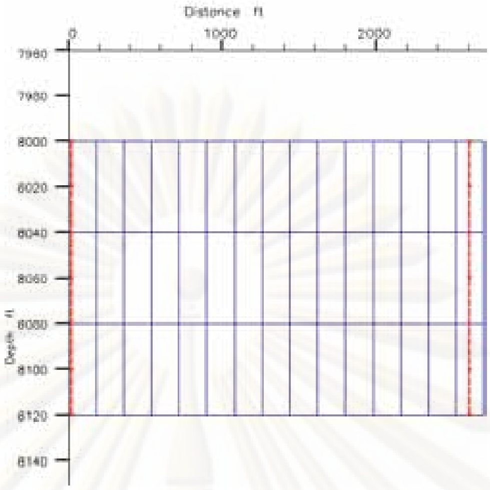

Figure 4.2: Side view of the reservoir model.

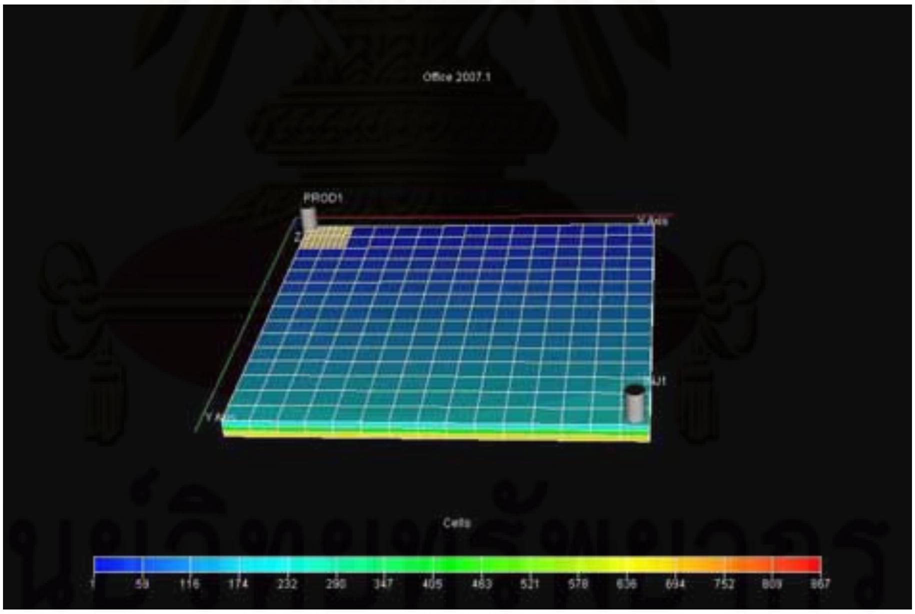

Figure 4.3: 3D view of the reservoir model.

The porosity of the reservoir is assumed to be 16.5%, the horizontal permeability is 10.85 mD, and vertical permeability is 1.27 mD.

4.2.2 Reservoir fluids

The initial fluid compositions in gas condensate reservoir are the actual field data from Society of Petroleum Engineering papers and the injected fluid is pure CO_2. The initial fluid composition is specified in Non-Equilibrium Initialization (NEI) section which is used to generate consistent oil and gas compositions for each cell. The equation of state used in this study is Peng-Robinson.

The maximum liquid dropout and dew point pressure are obtained from the PVTi section as shown in Table 4.4

Table 4.4: Maximum liquid dropout and dew point pressure of gas condensate reservoir.

Case	**Maximum liquid dropout (%)**	**Dew point pressure (psi)**
1	19	2020
2	25	2440
3	1	1680
4	1	2150
5	2	2550
6	2	2990
7	10	2800
8	12	3500
9	15	2010
10	20	2180

The initial water saturation and initial gas saturation is 0.11 and 0.89, respectively. These values are average value from one gas field in the Gulf of Thailand.

In this study, two different cases of initial reservoir pressure were investigated in order to determine the effect of the difference between initial reservoir pressure and dew point pressure. In the model, the two initial reservoir conditions are

(a) The initial reservoir pressure is equal to 3,500 psia.

(b) The initial reservoir pressure is equal to the dew point pressure.

The volume of gas and oil at the surface in the case that the initial reservoir pressure is above the dew point pressure and in the case that the initial reservoir pressure equal to the dew point pressure as shown in Table 4.5 and Table 4.6, respectively.

Table 4.5: Volume of gas and oil at the surface in the case that the initial reservoir pressure is above the dew point pressure.

Case	**Gas (BCF)**	**Oil (STB)**
1	18.38	1643854.9
2	17.35	2565996.5
3	17.79	682364.44
4	17.11	571871.38
5	17.17	591461.31
6	17.09	782433.69
7	17.86	1317020.5
8	17.55	1693049.6
9	18.36	1622917.4
10	17.95	1958095.1

Table 4.6: Volume of gas and oil at the surface in the case that the initial reservoir pressure is equal to the dew point pressure.

Case	**Gas (BCF)**	**Oil (STB)**
1	12.51	1119160
2	13.82	2043028.8
3	8.90	341225.44
4	10.84	362288.63
5	12.89	444244.5
6	14.92	683153
7	15.12	1114824.8
8	17.55	1693049.6
9	12.39	1078750.6
10	13.06	1379677.3

The solubility of CO_2 in water can be calculated using a correlation developed by Chang et. al. [8]. The percent by weight of NaCl is three. This value of salinity is commonly seen in the Gulf of Thailand. The solubility of CO_2 in water as a function of pressure is shown in Table 4.7 and Figure 4.4.

Table 4.7: CO_2 solubility in water.

Pressure (psi)	**CO_2 Solubility (scf/stb)**	**Pressure (psi)**	**CO_2 Solubility (scf/stb)**
14.7	1.6022420	2000	128.7121799
200	20.6106981	2200	135.4247293
400	38.8621564	2400	141.5094212
600	55.0491457	2600	147.0410961
800	69.4314589	2800	152.0850902
1000	82.2365873	3000	156.6985265
1200	93.6629441	3200	160.9314247
1400	103.8831835	3400	164.8276528
1600	113.0473766	3600	168.4257452
1800	121.2859265	3800	171.7596043

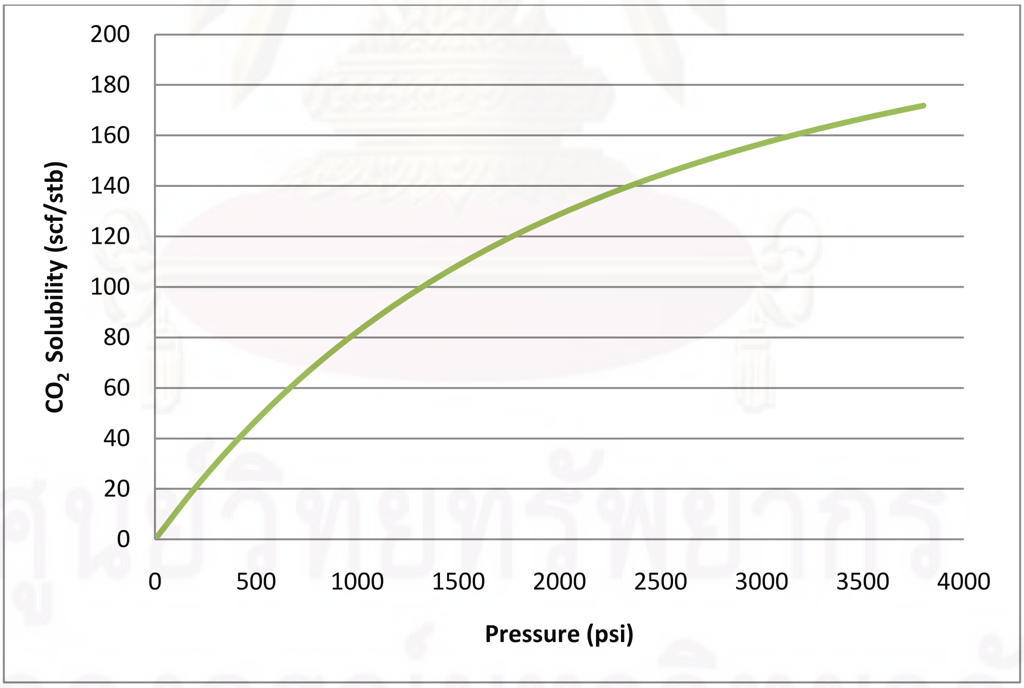

Figure 4.4: CO_2 solubility in water.

4.2.3 SCAL (Special Core Analysis) Section

Gas condensate reservoir properties in this compositional simulation were obtained from average values of special core analysis data of samples collected from one of the gas fields in the Gulf of Thailand. The relation between oil saturation and oil relative permeability are tabulated in Table 4.8 and shown in Figure 4.5. k_{row} is the oil relative permeability for a system with oil and water only, and k_{rowg} is the oil relative permeability for a system with oil, water, and gas.

Table 4.8: Oil saturation and oil relative permeability.

S_o	k_{row}	k_{rowg}
0	0	0
0.2	0	0
0.32	0.00463	0.015625
0.44	0.037037	0.125
0.56	0.125	0.421875
0.68	0.296296	1
0.95	1	1

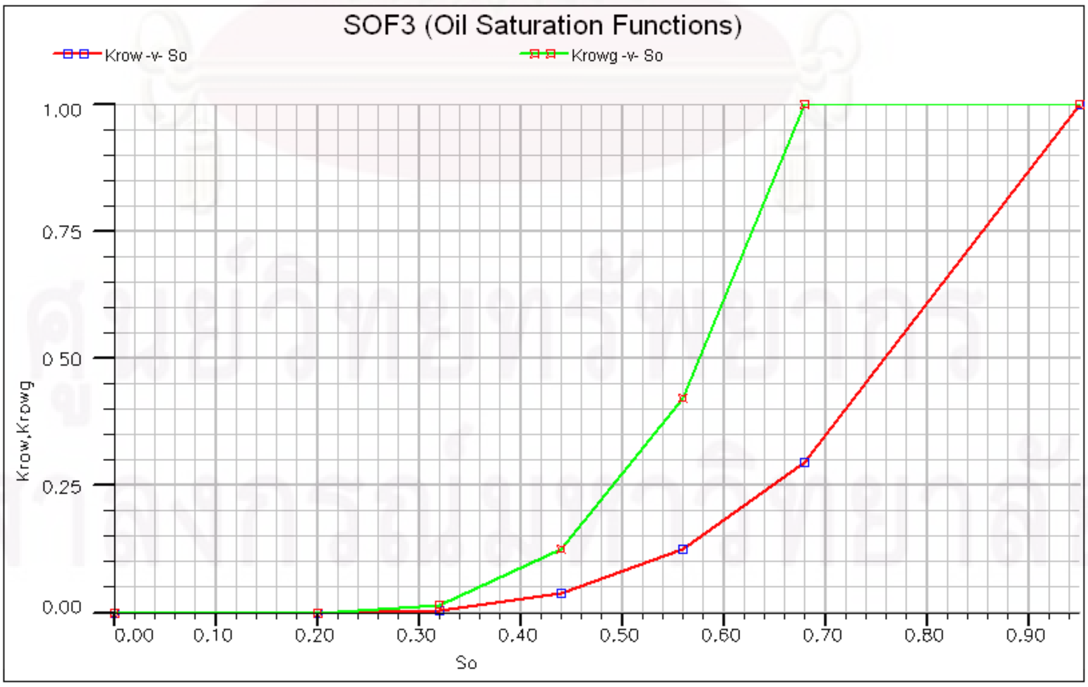

Figure 4.5: Oil relative permeability function.

The relation between water saturation and water relative permeability are tabulated in Table 4.9 and shown in Figure 4.6.

Table 4.9: Water saturation and water relative permeability.

S_w	k_{rw}
0.11	0
0.157	0
0.216	0
0.313	0.02
0.44	0.06
0.56	0.10
0.68	0.15
0.80	0.30
0.90	0.65

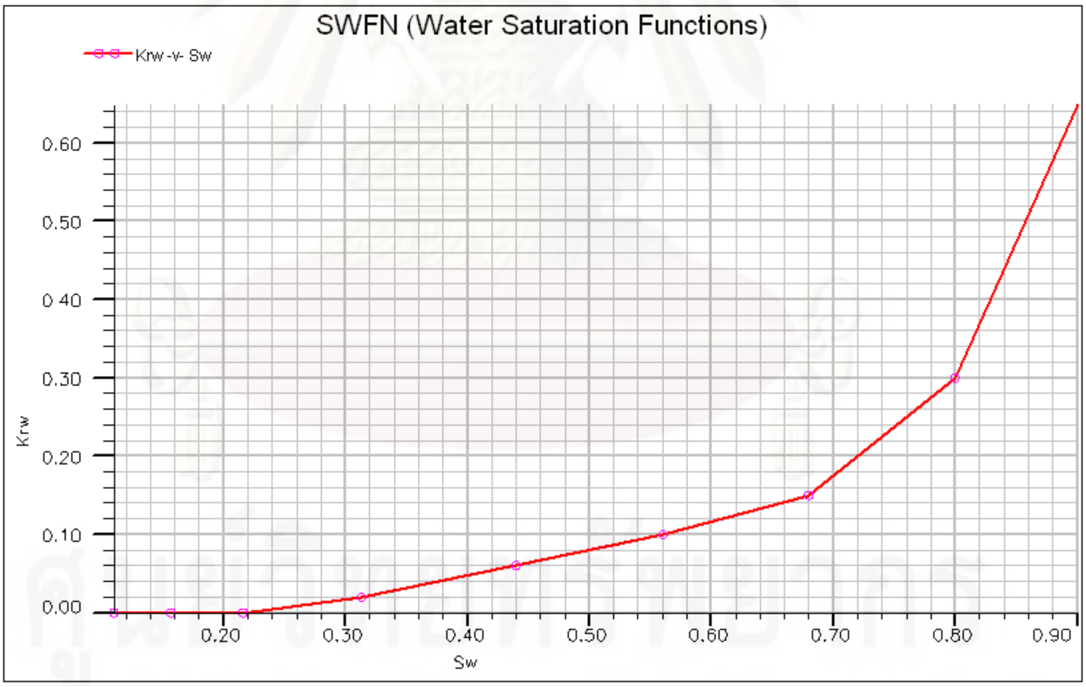

Figure 4.6: Water relative permeability as a function of water saturation.

The relation between gas saturation and gas relative permeability are tabulated in Table 4.10 and shown in Figure 4.7.

Table 4.10: Gas saturation function and relative gas permeability.

S_g	k_{rg}
0	0
0.10	0
0.20	0
0.30	0.20
0.40	0.40
0.60	0.85
0.70	0.90
0.80	0.92
0.90	0.95
0.95	0.95

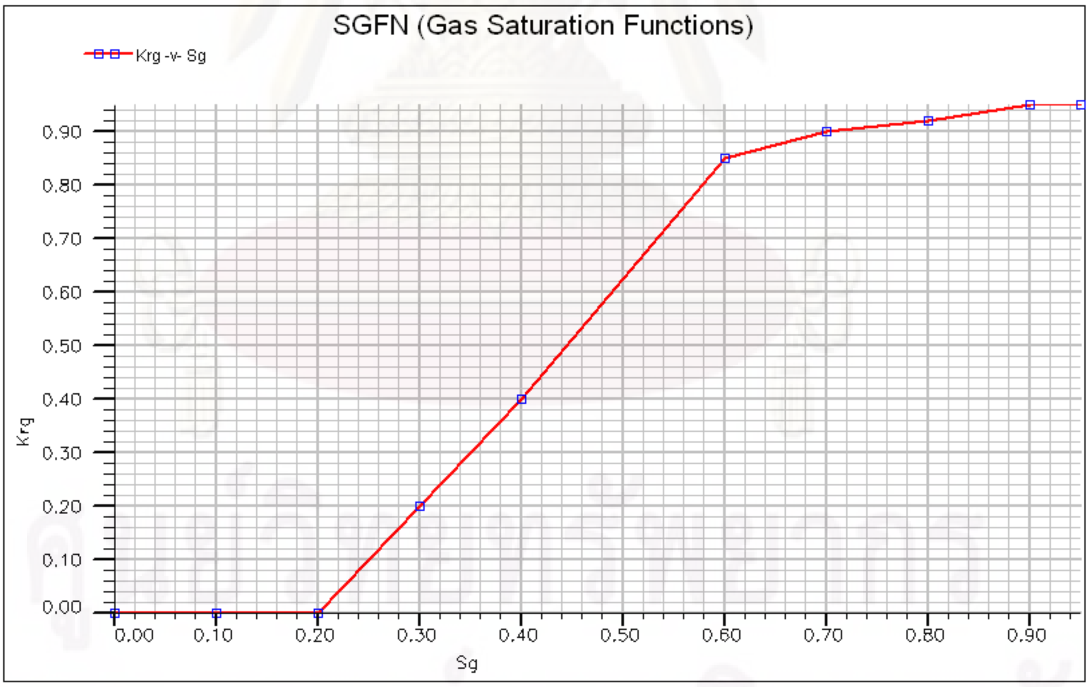

Figure 4.7: Gas relative permeability as a function of gas saturation.

The relation between water saturation and capillary pressure are tabulated in Table 4.11 and shown in Figure 4.8.

Table 4.11: Water saturation function and capillary pressure.

Sw	Pc (psia)
0.11	250
0.157	53
0.216	13
0.313	1
0.44	0
0.56	0
0.68	0
0.80	0
0.90	0

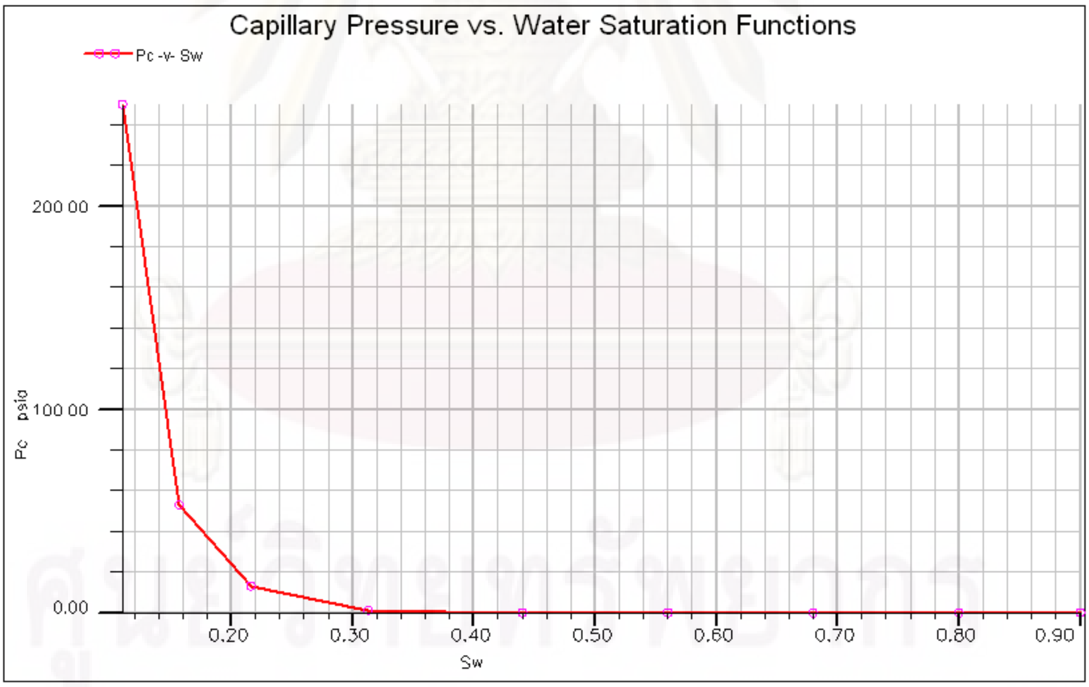

Figure 4.8: Capillary pressure as a function of water saturation.

4.3 VFP Section

The production and injection wells of the model have the wellbore diameter of 3-1/2 inches with an inside diameter of 2.992 inches. The well is perforated from 8,000 ft to 8,120 ft and the perforation interval is from the top to the bottom of the reservoir. The schematic of wellbore configuration is shown in Figure 4.9.

The vertical flow performance of all ten fluid compositions was generated by PROduction and Systems PERformance analysis software (PROSPER). The vertical lift correlation is Fancher Brown. For a gas condensate well, the flow regime is normally mist flow; so the slip between liquid and gas is minimal. Fancher Brown is a no-slip hold-up correlation which gives the lowest possible value of VLP. The vertical flow performance used in this study is shown in Appendix C.

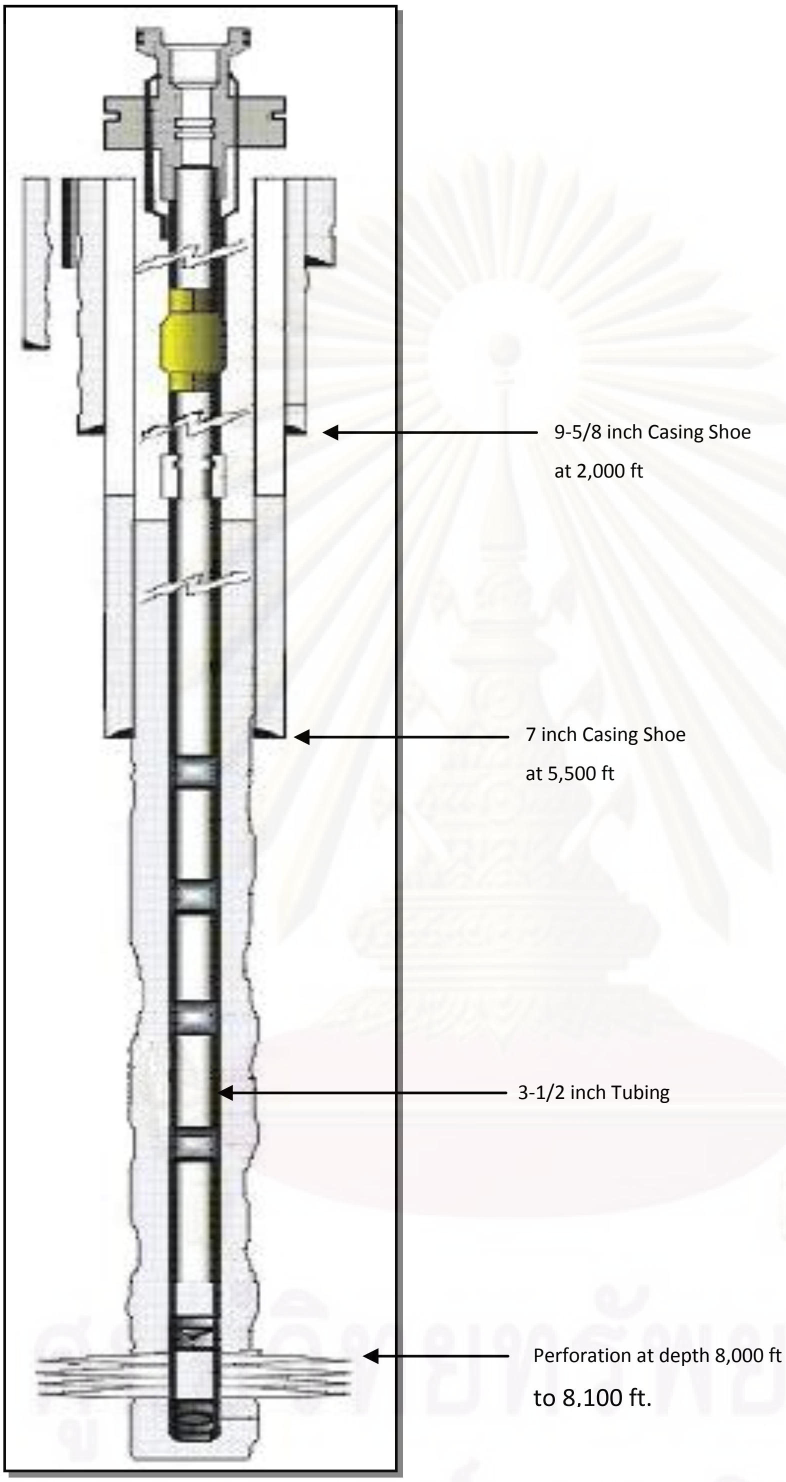

Figure 4.9: Casing and tubing flow model used in this study.

CHAPTER V

RESULTS AND DISCUSSION

In this chapter, the analysis and discussion of the reservoir simulation results under different production and injection strategies and fluid compositions are reported. The results are analyzed and discussed in term of CO_2 injection mechanism and the effect of composition on the most optimum production and injection scenarios. In this study, there are two different initial reservoir conditions which are

(a) The initial reservoir pressure is equal to 3,500 psia. In this case, each reservoir fluid will reach the dew point pressure at different production times.
(b) The initial reservoir pressure is equal to the dew point pressure. In this case, liquid dropout around the wellbore will occur at the beginning of the production.

Two production and injection strategies which are natural depletion and CO_2 injection were simulated for each case. In natural depletion scenario, the production is simulated with one production well that produces until the condensate or gas production rate drops below the economic limit. In CO_2 injection scenario, the production is initially from two wells. Then, CO_2 injection is carried out at different starting times on one of the wells until the condensate or gas production rate drops below the economic limit or CO_2 concentration in the produced gas reaches its concentration limit. The minimum tubing head pressure of producer is 200 psia. This limit is a common tubing head pressure limit used in Gulf of Thailand when a booster compressor is installed. The economic limit for gas production rate is 100 MSCF/D and the economic limit for condensate production rate is 5 STB/D for production by natural depletion and 13.32 STB/D for production with CO_2 injection. The economic limit at 5 STB/D for production with natural depletion is used by assuming a typical daily operating cost. The economic limit at 13.32 STB/D for production with CO_2 injection is calculated by accounting for the operating cost of compressor at 235,394 US$/yr or 645 US$/day and equal to 8.32 STB/D of condensate at 77.5 US$/ STB.

The economic evaluations were performed in order to investigate the feasibility of CO_2 injection project.

5.1 Scenario 1: Initial reservoir pressure is 3,500 psia

In this scenario, the initial reservoir pressure of each reservoir fluid composition is equal to 3,500 psia. The liquid dropout around the wellbore will occur at different times because each case has different dew point pressures. Three types of production and injection scenarios: natural depletion, CO_2 injection at the beginning and CO_2 injection when the pressure around the wellbore reaches the dew point pressure were simulated.

5.1.1 Production with Natural Depletion

In this scenario, gas condensate reservoirs having different compositions were simulated by natural depletion strategy. The maximum gas production rate is set at 10,000 MSCF/D. And, the economic limit for condensate production rate is 5 STB/D.

The gas production rate and the tubing head pressure (THP) are shown in Figures 5.1 and 5.2, respectively. In all cases, the gas production rate is constant at the beginning. The gas production rate starts to decline when the tubing head pressure reaches its limit at 200 psia. The simulation stops when the gas or condensate production rate reaches the economic limit.

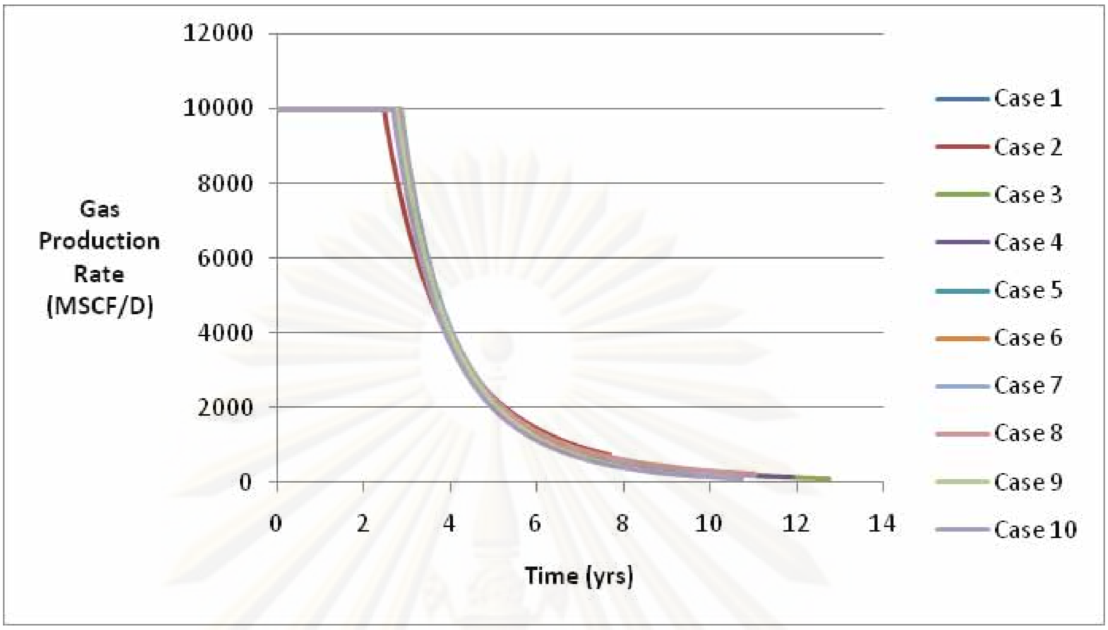

Figure 5.1: Gas production rate for producing with natural depletion with initial reservoir pressure equal to 3,500 psia.

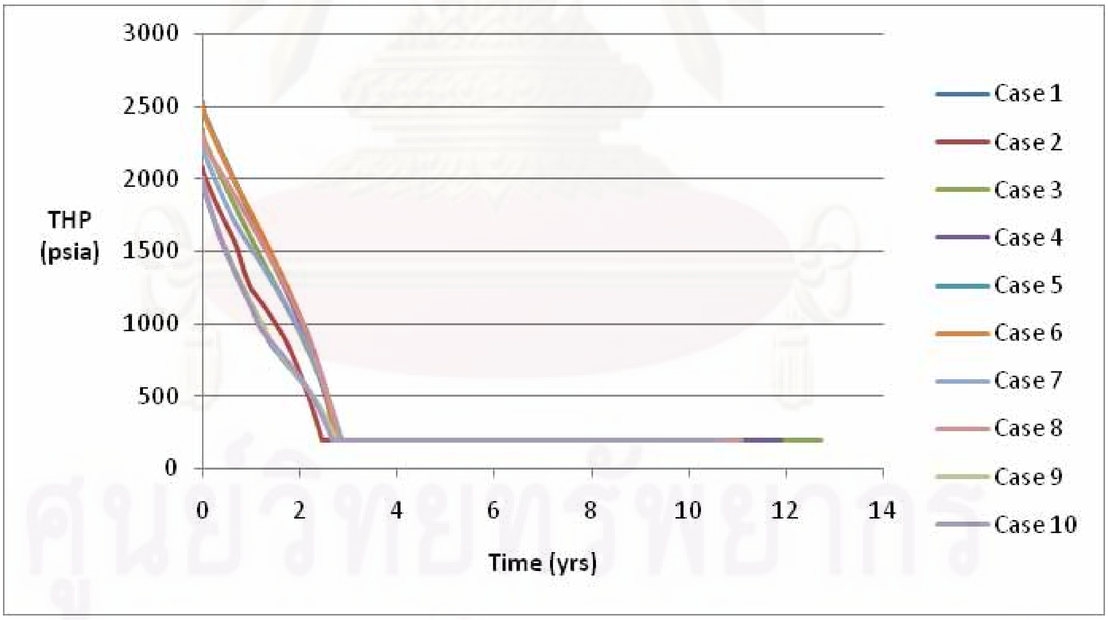

Figure 5.2: Tubing head pressure for producing with natural depletion with initial reservoir pressure equal to 3,500 psia.

The producing time before reaching the tubing head pressure limit, cumulative production of gas, recovery factor, and the production life of natural depletion are summarized in Table 5.1. The producing time before reaching THP limit ranges from 2.46 to 2.87 years. The production life ranges from 7.7 to 12.8 years. Case 2 reaches THP limit faster than other cases, so the total gas production of this case is lowest and the production life of this case is shortest. Case 3 reaches THP limit slower than other cases, so the production life of this case is longest.

Table 5.1: Producing time before reaching THP limit, cumulative production of gas, recovery factor, and production life for producing with natural depletion with initial reservoir pressure equal to 3,500 psia.

Case	Producing time before reaching THP limit (years)	Total gas production (BCF)	Gas recovery factor (%)	Production life (years)
1	2.74	15.42	84%	10.6
2	2.46	14.85	86%	7.7
3	2.87	15.88	89%	12.8
4	2.75	15.55	91%	11.9
5	2.77	15.58	91%	10.8
6	2.76	15.52	91%	10.7
7	2.86	16.01	90%	11.1
8	2.80	15.92	91%	11.1
9	2.75	15.47	84%	10.8
10	2.68	15.08	84%	10.8

The condensate production rate and the bottomhole pressure (BHP) are shown in Figures 5.3 and 5.4, respectively. The condensate production rates for the ten cases are different because the condensate-gas ratios (CGR) are different. At the early time, the condensate production rates remain constant for certain durations before starting to decline except case 8, in which the condensate production rate starts to decline at the beginning. In general, the condensate production rate declines because the bottomhole pressure drops below the dew point pressure and liquid starts to condense in the pore space. Case 8 has the initial reservoir pressure below the dew point pressure. Therefore, liquid dropout occurs at the beginning.

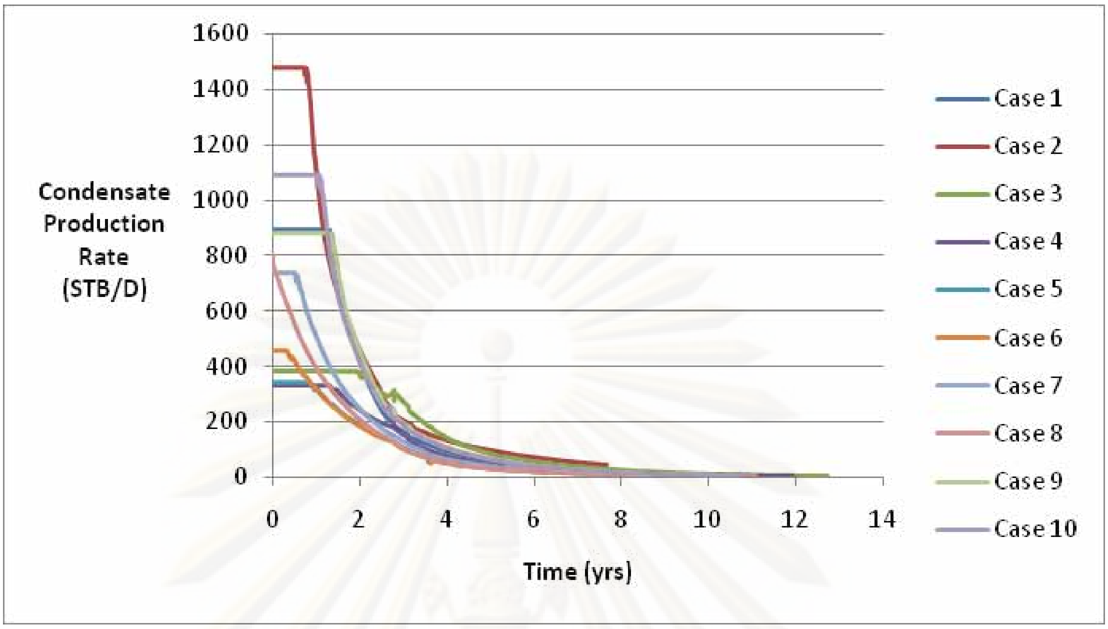

Figure 5.3: Condensate production rate for producing with natural depletion with initial reservoir pressure equal to 3,500 psia.

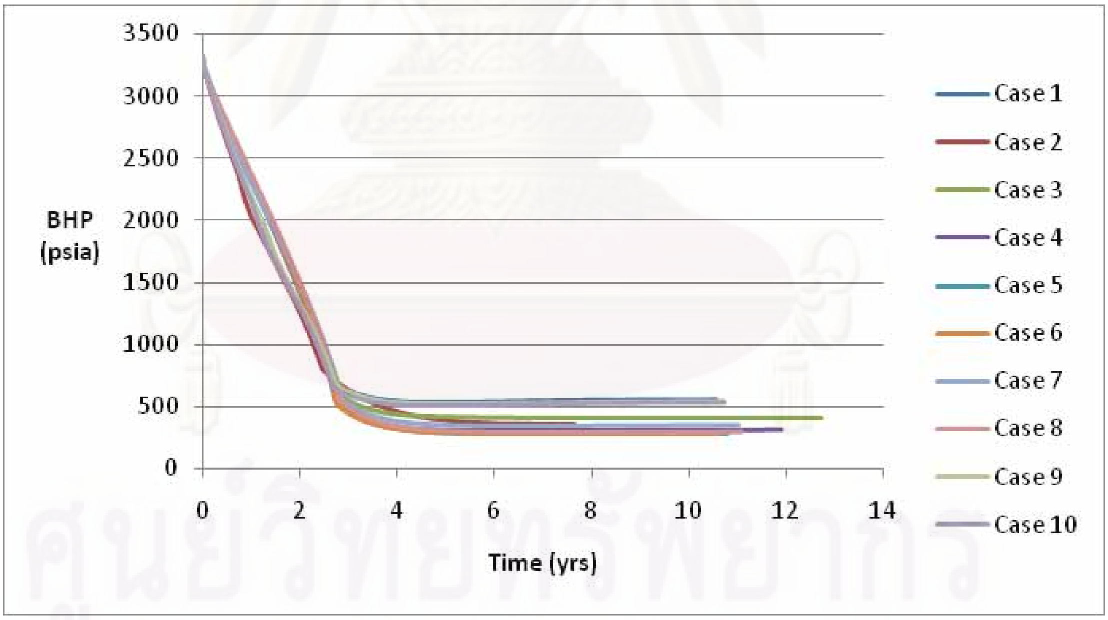

Figure 5.4: Bottomhole pressure for producing with natural depletion with initial reservoir pressure equal to 3,500 psia.

The condensate-gas ratio (CGR), mole fraction of heptanes plus, producing time before reaching the dew point pressure, cumulative production of condensate, and recovery factor of natural depletion are summarized in Table 5.2. The condensate-gas ratio ranges from 33 to 148 STB/MMSCF. The highest condensate-gas ratio is obtained in case 2 because this case has highest mole fraction of heptanes plus. Case 4 and case 5 have almost equal condensate-gas ratio and can be considered as the lowest compared to the other cases because these cases have highest mole fraction of methane and lowest mole fraction of heptanes plus. The producing time before reaching the dew point pressure of case 8 equal to 0 because this case has the dew point pressure equal to 3500 psia, which is the initial reservoir pressure. The producing time before reaching the dew point pressure of case 3 is higher than other cases because this case has lowest dew point pressure (1680 psia).

Table 5.2: Condensate-gas ratio, mole fraction of heptanes plus, producing time before reaching the dew point pressure, cumulative production of condensate, and recovery factor for producing with natural depletion with initial reservoir pressure equal to 3,500 psia.

Case	**CGR (STB/MMSCF)**	**Mole fraction of heptanes plus**	**Producing time before reaching the dew point (years)**	**Total condensate production (STB)**	**Condensate recovery factor (%)**
1	89	0.0654	1.25	799,840	49%
2	148	0.1339	0.73	1,060,405	41%
3	38	0.0656	1.95	585,901	86%
4	33	0.0306	1.31	409,266	72%
5	34	0.0283	0.84	341,421	58%
6	46	0.0326	0.33	359,280	46%
7	74	0.0503	0.51	532,119	40%
8	80	0.0633	0.00	442,274	26%
9	88	0.0885	1.26	829,142	51%
10	109	0.1040	1.02	887,478	45%

From the simulation results, we can see that the condensate recovery factor depends on dew point pressure and maximum liquid dropout. From Table 4.4 we separate the reservoir fluids into two main categories which are moderate-high maximum liquid dropout and low maximum liquid dropout. Cases 1, 2, 7, 8, 9, and 10 are moderate-high maximum liquid dropout case and case 3, 4, 5, and 6 are low maximum liquid dropout case. The condensate recovery factor as a function of dew point pressure for moderate-high maximum liquid dropout and low maximum liquid dropout are shown in Figure 5.5 and 5.6, respectively. The condensate recovery factor decrease when the dew point pressure increase. The dew point pressure has effect to the time before liquid dropping out. Higher the dew point pressure results in shorter the time before liquid dropping out. The maximum liquid dropout also has effect to the condensate recovery factor. Higher the maximum liquid dropout results in more condensate left in the reservoir and lower the condensate recovery factor. When compare between case 4 and case 10 which have similar dew point pressure but case 10 has the maximum liquid dropout higher than case 4. The condensate recovery factor of case 10 has 27% lower than case 4.

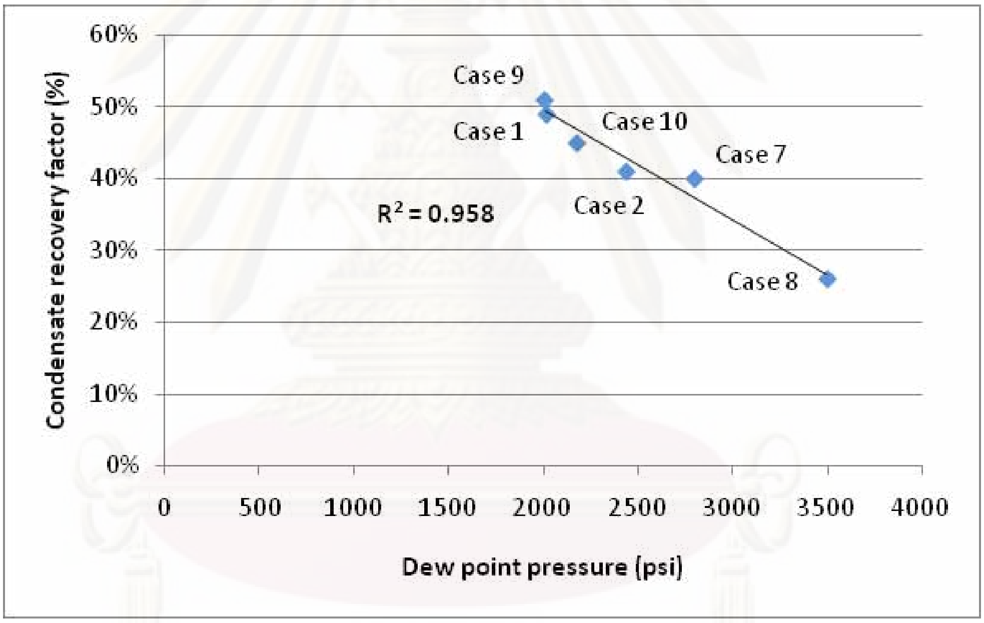

Figure 5.5: Condensate recovery factor as a function of dew point pressure for producing with natural depletion with initial reservoir pressure equal to 3,500 psia (moderate-high maximum liquid dropout).

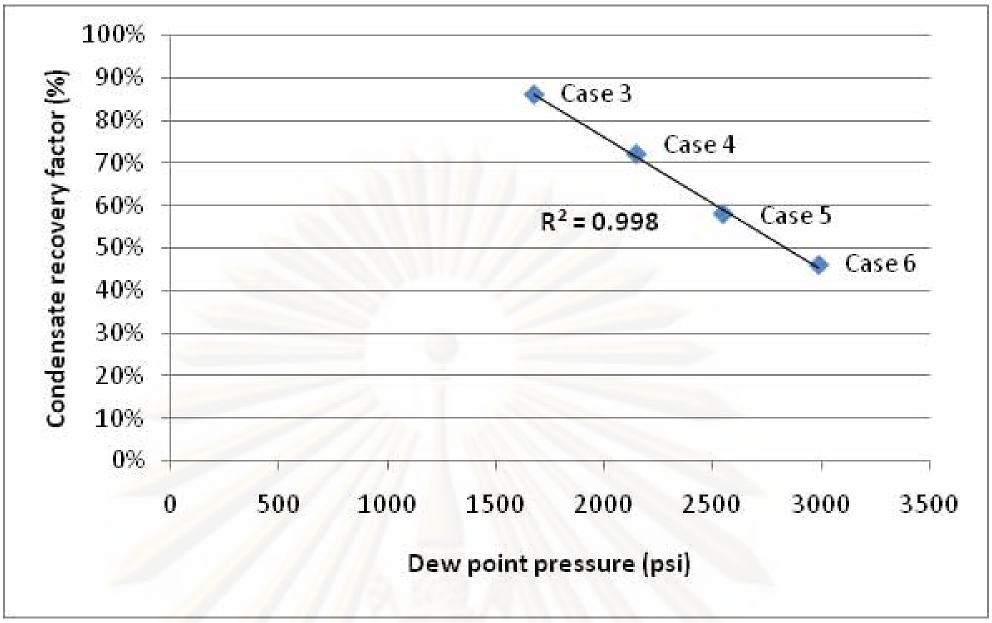

Figure 5.6: Condensate recovery factor as a function of dew point pressure for producing with natural depletion with initial reservoir pressure equal to 3,500 psia (low maximum liquid dropout).

The performance of gas condensate reservoirs with natural depletion can be summarized as follows:

(a) The total gas production ranges from 14.85 to 16.01 BCF. The gas recovery factor ranges from 84 to 91%.

(b) The total condensate production ranges from 341,421 to 1,060,405 STB. The condensate recovery factor ranges from 26 to 86%.

(c) The highest recovery factor of total condensate production is 86% and is obtained in case 3. This case has the longest producing time before the bottomhole pressure reaches the dew point pressure since the initial reservoir pressure is much higher than the dew point pressure. The liquid dropout occurs slower than the other cases.

(d) The lowest recovery factor of total condensate production is 26% and is obtained in case 8. This case has the shortest producing time before the bottomhole pressure reaches the dew point pressure since the reservoir pressure is the same as the dew point pressure (zero day). The liquid dropout in case 8 occurs at the beginning of the production.

5.1.2 Production of gas condensate reservoir with CO_2 injection at the beginning

In this scenario, the gas condensate reservoirs are produced together with CO_2 injection at the beginning in order to maintain the reservoir pressure above the dew point pressure. The schematic of injection well and production well on the five-spot pattern is shown in Figure 5.7. The producer is located at coordinate 1, in LGR grid representing the producer (located at coordinate (1, 1) in the global grid), and the injector is located at coordinate (15, 15) in the global grid in order to simulate a quarter five-spot pattern. The CO_2 injection rate is 10,000 MSCF/D which is equal to the production rate. The economic limit for condensate production rate is 13.32 STB/D. This economic limit is calculated from the daily operating cost of injection and production. The CO_2 concentration limit in this simulation is 23% which is the limit commonly used in the Gulf of Thailand.

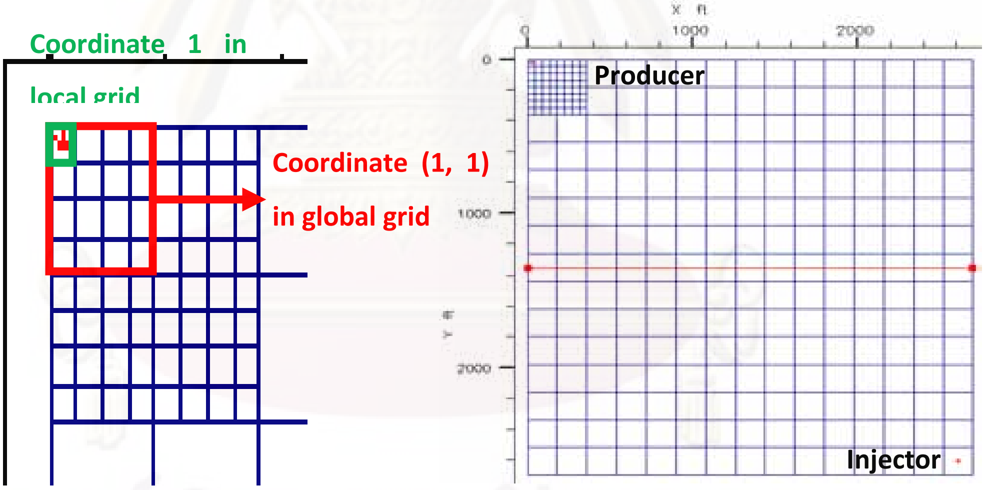

Figure 5.7: Injection well and production well on five-spot pattern.

The gas production rate and the tubing head pressure (THP) for production with CO_2 injection at the beginning are shown in Figures 5.8 and 5.9, respectively. In all cases, the gas production rate is constant at the initial period. The gas production rate starts to decline when CO_2 breaks through the producer. The simulation stops when CO_2 concentration reaches the economic limit of 23%. The production with

CO_2 injection can keep the reservoir pressure to be high, so the tubing head pressure (THP) does not reach the limit of 200 psia.

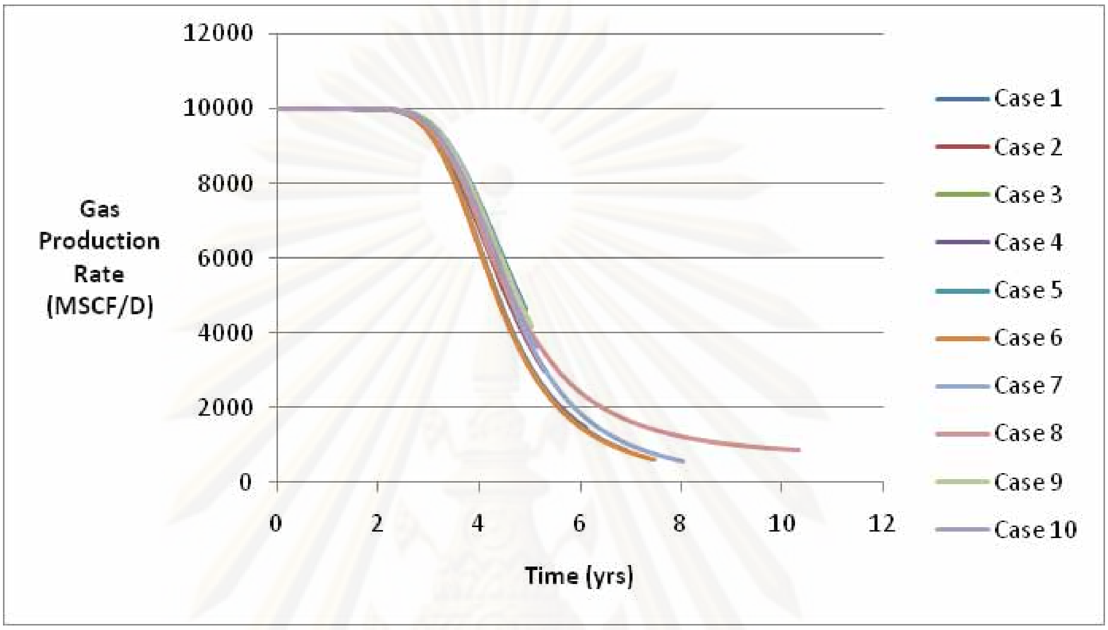

Figure 5.8: Gas production rate for producing with CO_2 injection at the beginning with initial reservoir pressure equal to 3,500 psia.

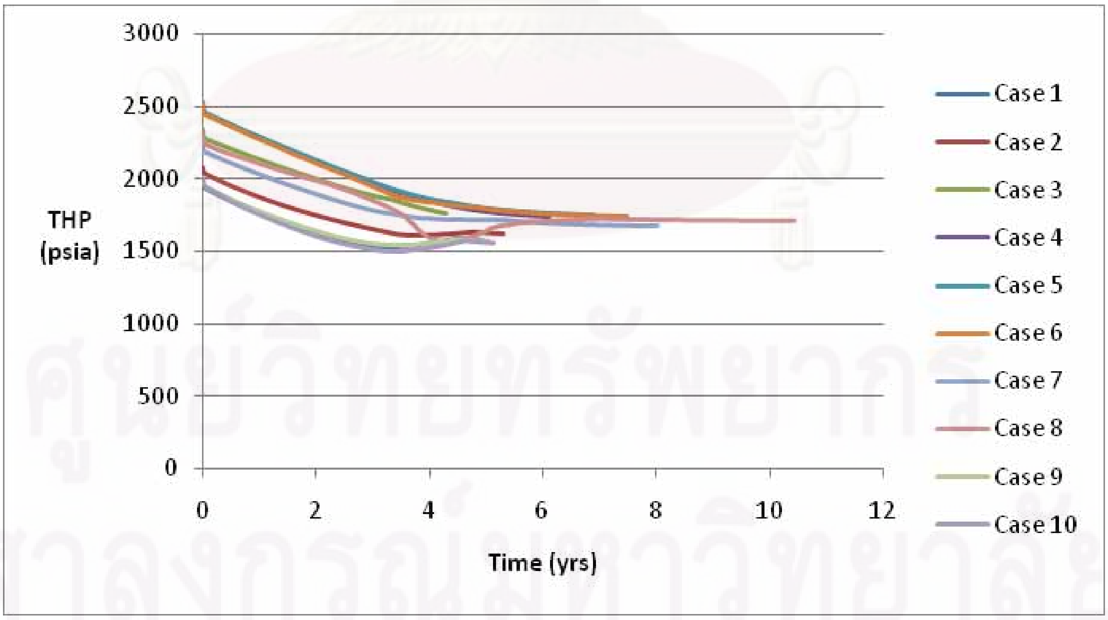

Figure 5.9: Tubing head pressure for producing with CO_2 injection at the beginning with initial reservoir pressure equal to 3,500 psia.

The production life between no CO_2 concentration limit and 23% CO_2 concentration limit of injecting CO_2 at the beginning are summarized in Table 5.3. The highest and lowest production life of no CO_2 concentration limit is obtained in case 8 and case 3, respectively. The production lives of 23% CO_2 concentration limit of all cases are not much different. This result shows that the times for CO_2 to reach the producer and raise the CO_2 concentration to 23% are not much different. So, the composition of reservoir fluid does not have significant effect on the speed of CO_2 traveling in the reservoir.

Table 5.3: Production life for producing with CO_2 injection at the beginning with initial reservoir pressure equal to 3,500 psia.

Case	**Production life (years)**	
	No limit	**23% CO_2 limit**
1	4.9	3.9
2	5.3	3.7
3	4.3	3.8
4	6.2	3.6
5	6.9	3.6
6	7.5	3.6
7	8.1	3.8
8	10.5	3.6
9	5.1	3.9
10	5.2	3.8

The total gas production and the gas recovery factor for the case with no CO_2 concentration limit and 23% CO_2 concentration limit for CO_2 injection at the beginning are summarized in Table 5.4. The total gas production and gas recovery factor of 23% CO_2 concentration limit of all cases are not much different except case 8. The total gas production and gas recovery factor depend on the production life and the gas production rate. And, both the production life and the gas production rate are not much different among each case.

Table 5.4: Total gas production and recovery factor for producing with CO_2 injection at the beginning with initial reservoir pressure equal to 3,500 psia.

Case	**Total gas production (BCF)**		**Gas recovery factor (%)**	
	No limit	**23% CO_2 limit**	**No limit**	**23% CO_2 limit**
1	16.12	13.82	88%	75%
2	16.20	13.16	93%	76%
3	14.65	13.34	82%	75%
4	16.36	12.81	96%	75%
5	16.69	12.88	97%	75%
6	16.81	12.84	98%	75%
7	17.70	13.45	99%	75%
8	16.56	11.82	94%	67%
9	16.30	13.87	89%	76%
10	16.26	13.62	91%	76%

The condensate production rate and the bottomhole pressure (BHP) for production with CO_2 injection at the beginning are shown in Figures 5.10 and 5.11, respectively. The condensate production rates for different cases are different because the condensate-gas ratios (CGR) are different. At the early time, the condensate production rates remain constant for certain durations before starting to decline except case 8, in which the condensate production rate starts to decline at the beginning. In general, the condensate production rate starts to decline when the injected CO_2 breaks through the producer. The decline of condensate production rate in case 8 is due to the fact that the initial reservoir pressure is the same as the dew point pressure and liquid dropout occurs at the initial period of the production. When the liquid dropout around the wellbore is revaporized by CO_2 injection, the condensate production rate shoots up.

The comparison of condensate production profile between production by natural depletion and production by CO_2 injection at the beginning can be made by inspecting Figure 5.3 and Figure 5.10. CO_2 injection can maintain condensate production rate to be constant longer than the natural depletion case because injecting

CO_2 at the beginning can maintain the bottomhole pressure to be higher than the dew point pressure.

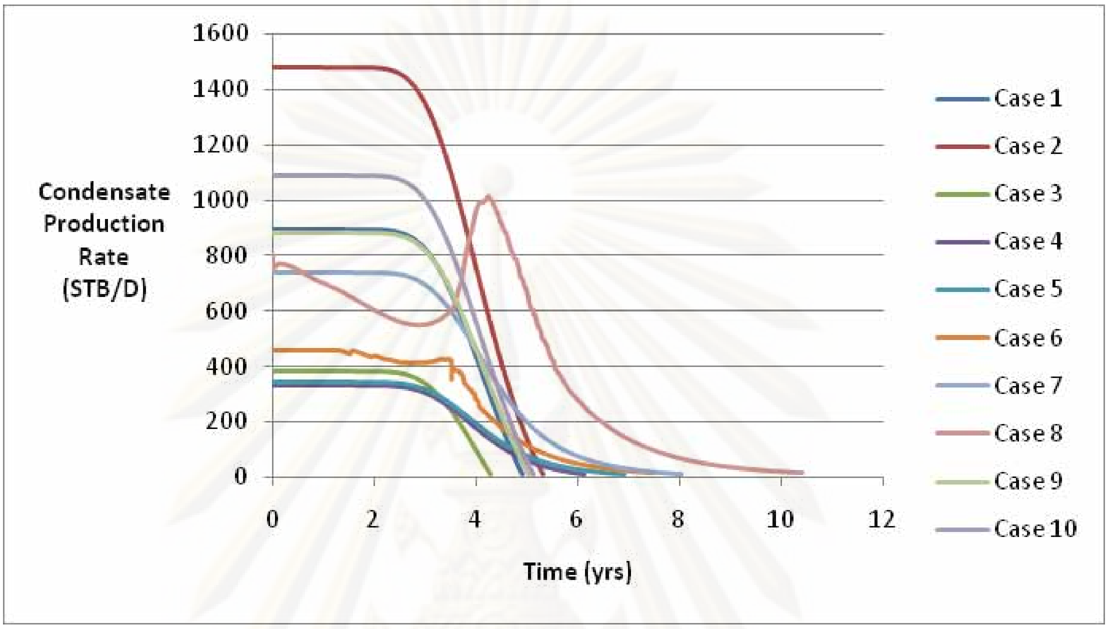

Figure 5.10: Condensate production rate for producing with CO_2 injection at the beginning with initial reservoir pressure equal to 3,500 psia.

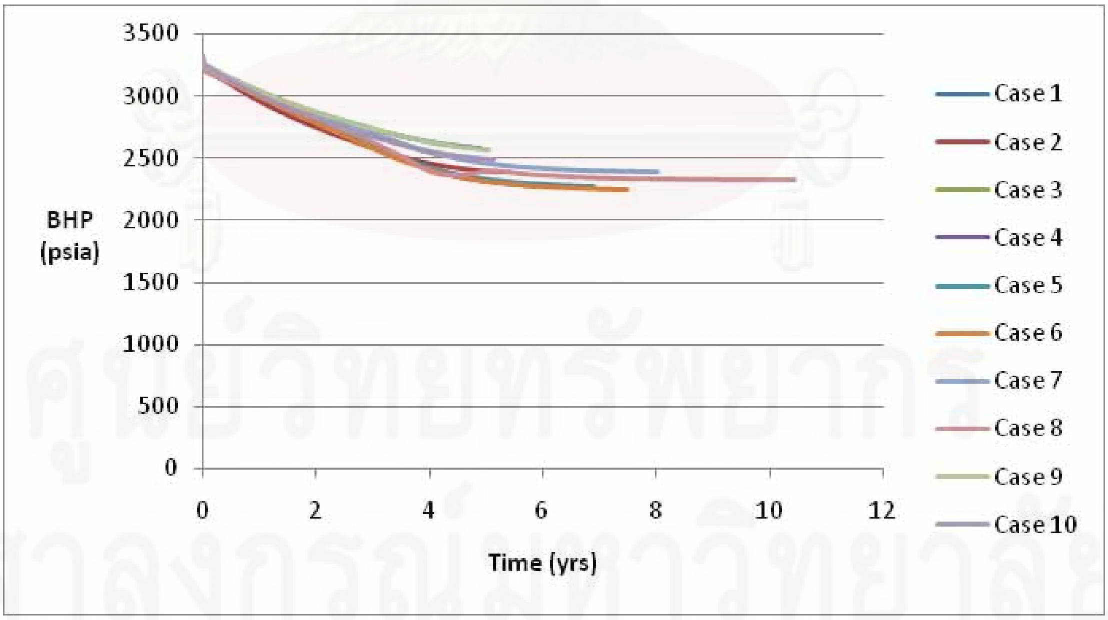

Figure 5.11: Bottomhole pressure for producing with CO_2 injection at the beginning with initial reservoir pressure equal to 3,500 psia.

The condensate saturation at local grid block (1, 1, 1), which is the producer, is shown in Figure 5.12. Injecting CO_2 at the beginning can maintain the reservoir pressure above the dew point pressure, so liquid dropout at the producer does not occur except for cases 6 and 8. Cases 6 and 8 have relatively high dew point pressure, injecting CO_2 cannot prevent the liquid dropout. If the reservoir is produced without CO_2 concentration limit, the liquid dropout can be completely revaporized, resulting in condensate saturation of 0. When the CO_2 concentration limit of 23% is applied, the liquid dropout around the well bore cannot be completely revaporized.

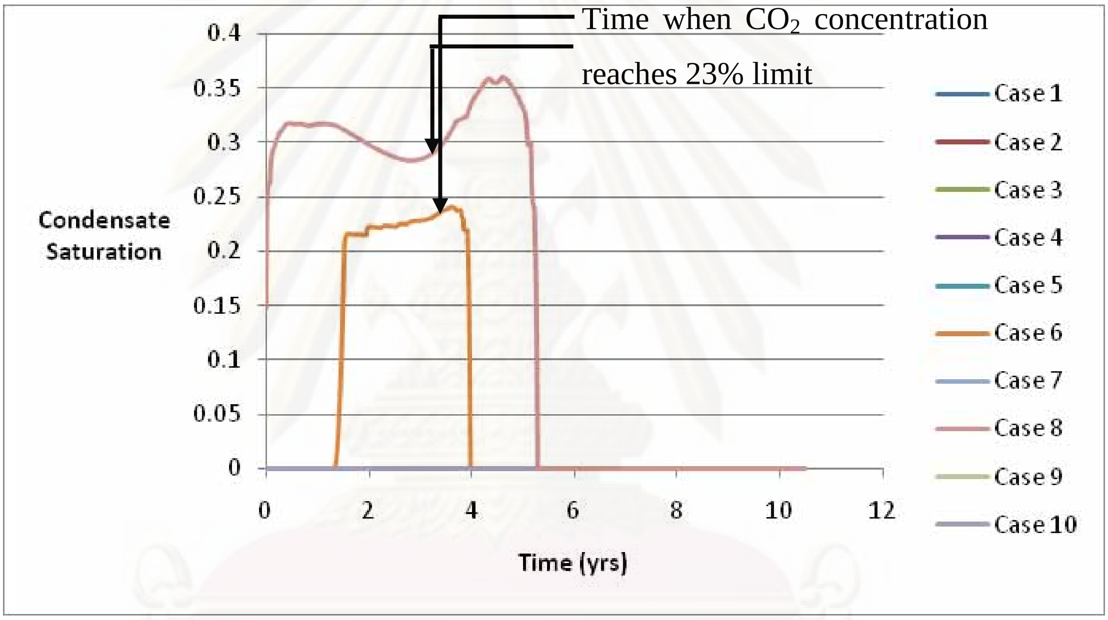

Figure 5.12: Condensate saturation for producing with CO_2 injection at the beginning with initial reservoir pressure equal to 3,500 psia.

The total condensate production and the condensate recovery factor for the case with no CO_2 concentration limit and 23% CO_2 concentration limit for CO_2 injection at the beginning are summarized in Table 5.5. The condensate recovery factor of 23% CO_2 concentration limit of all cases are not much different except case 8. CO_2 injection at the beginning can prevent the liquid drop out around the wellbore. So, the condensate recovery factor depends only on the production life and the production life of each case is not different.

Table 5.5: Total condensate production and recovery factor for producing with CO_2 injection at the beginning with initial reservoir pressure equal to 3,500 psia.

Case	**Total condensate production (STB)**		**Condensate recovery factor (%)**	
	No limit	**23% CO_2 limit**	**No limit**	**23% CO_2 limit**
1	1,284,227	1,195,409	78%	73%
2	2,162,279	1,910,289	84%	74%
3	507,733	489,917	74%	72%
4	509,656	424,462	89%	74%
5	544,548	440,866	92%	75%
6	735,016	579,076	94%	74%
7	1,210,278	982,394	92%	75%
8	1,582,471	833,376	93%	49%
9	1,293,208	1,191,262	80%	73%
10	1,594,891	1,449,278	81%	74%

The performance of gas condensate reservoirs with CO_2 injection at the beginning can be summarized as follows:

(a) In the case of 23% CO_2 concentration limit, the total gas production ranges from 11.82 to 13.87 BCF, yielding gas recovery factor between 67 to 76%.

(b) In the case of 23% CO_2 concentration limit, the total condensate production ranges from 424,462 to 1,910,289 STB, yielding condensate recovery factor between 49 to 75%.

(c) The lowest recovery factor of total condensate production and total gas production are 49% and 67%, respectively in case 8 because the liquid dropout occurs at the beginning of the production.

The comparisons of the simulation results between production with natural depletion and production with CO_2 injection at the beginning are reported. The difference in cumulative gas production, cumulative condensate production, and recovery factors of 23% CO_2 concentration limit are summarized in Table 5.6.

Table 5.6: The difference in cumulative gas production, cumulative condensate production, and recovery factors of 23% CO_2 concentration limit between natural depletion and CO_2 injection at the beginning with initial reservoir pressure equal to 3,500 psia.

Case	**ΔGp (BCF)**	**ΔRF for gas (%)**	**ΔNp (STB)**	**ΔRF for condensate (%)**
1	-1.60	-9%	395,569	24%
2	-1.69	-10%	849,884	33%
3	-2.54	-14%	-95,984	-14%
4	-2.74	-16%	15,196	3%
5	-2.70	-16%	99,445	17%
6	-2.68	-16%	219,796	28%
7	-2.56	-15%	450,275	34%
8	-4.10	-24%	391,102	23%
9	-1.60	-8%	362,120	22%
10	-1.46	-8%	561,800	29%

The performance of gas condensate reservoirs with CO_2 injection at the beginning compared with production by natural depletion can be summarized as follows:

(a) In all cases, injecting CO_2 at the beginning of the production decreases the total gas production compared with production by natural depletion. When producing with natural depletion, most of the reservoir fluid is produced as gas but the produced reservoir fluid is changed from gas to condensate when producing with CO_2 injection at the beginning. When injecting CO_2 at the beginning, the reservoir can be produced until reaching the economic limit of CO_2 concentration even though the economic limit of gas production may not be reached yet. But in the natural depletion case, the reservoir can be produced until reaching the economic limit of condensate and gas production rates.

(b) Injecting CO_2 at the beginning of the production increases the total condensate production compared with production by natural depletion in all cases except case 3. Since injecting CO_2 at the beginning can maintain the reservoir pressure to be above the dew point pressure, the liquid dropout around the producer does not occur and condensate can be recovered at surface.

(c) In case 3, the total condensate production with production by CO_2 injection at the beginning is lower than production by natural depletion. From the phase diagram shown in Figure 5.13, the reservoir fluid in this case has a dew point pressure of 1680 psia which is the lowest among the 10 cases in this study. The maximum liquid dropout is only 1%. The liquid dropout can be completely revaporized even in natural depletion case when the reservoir pressure drops below 620 psia. CO_2 injection will cause an early termination of gas production due to high CO_2 concentration at the producer (CO_2 limit = 23%), resulting in lower recovery factor.

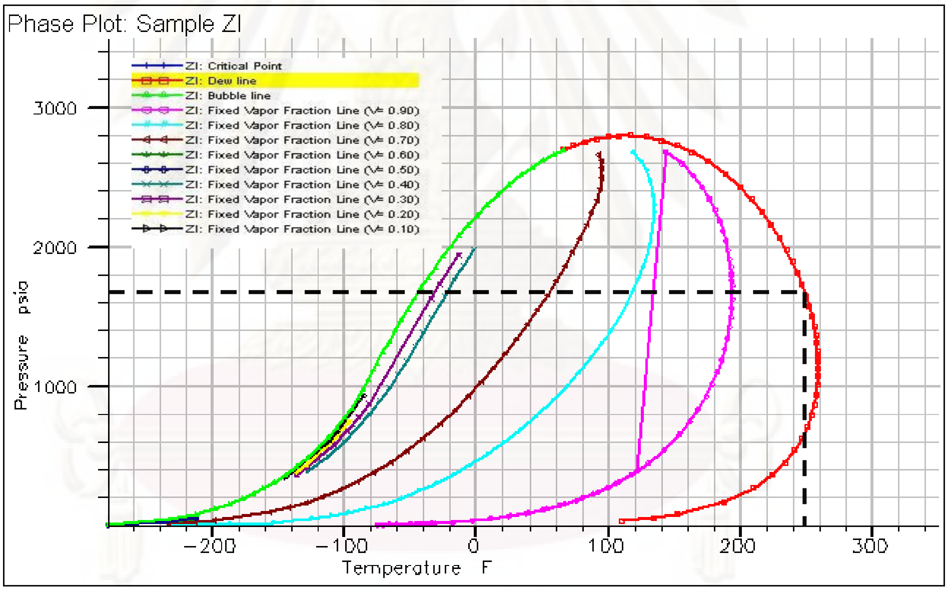

Figure 5.13: Phase diagram of reservoir fluid in case 3.

(d) As already mentioned, the gas and condensate recovery factor of each case are not different when producing with CO_2 injection at the beginning except case 8. The gas and condensate recovery factor gained from the CO_2 injection at the beginning depends only on the gas and condensate recovery factor when producing with natural depletion.

5.1.3 Production of gas condensate reservoir with CO_2 injection at the dew point pressure

In this scenario, the gas condensate reservoirs are produced without CO_2 injection at the beginning, and then we start injecting CO_2 when the well block pressure reaches the dew point pressure. In previous study, Tangkaprasert [6] concludes that the best time to start CO_2 injection is when the bottomhole pressure reaches the dew point pressure. In this scenario, we try to study the effect of reservoir fluid compositions on the optimum time to start CO_2 injection.

The gas production rate and the tubing head pressure (THP) for production with CO_2 injection at the dew point pressure are shown in Figures 5.14 and 5.15, respectively. In all cases, the gas production rates are constant at the early state. The gas production rate starts to decline when CO_2 breaks through the producer. The simulation stops when CO_2 concentration reaches the economic limit of 23%. CO_2 injection can maintain the reservoir pressure so the tubing head pressure (THP) does not reach the limit of 200 psia.

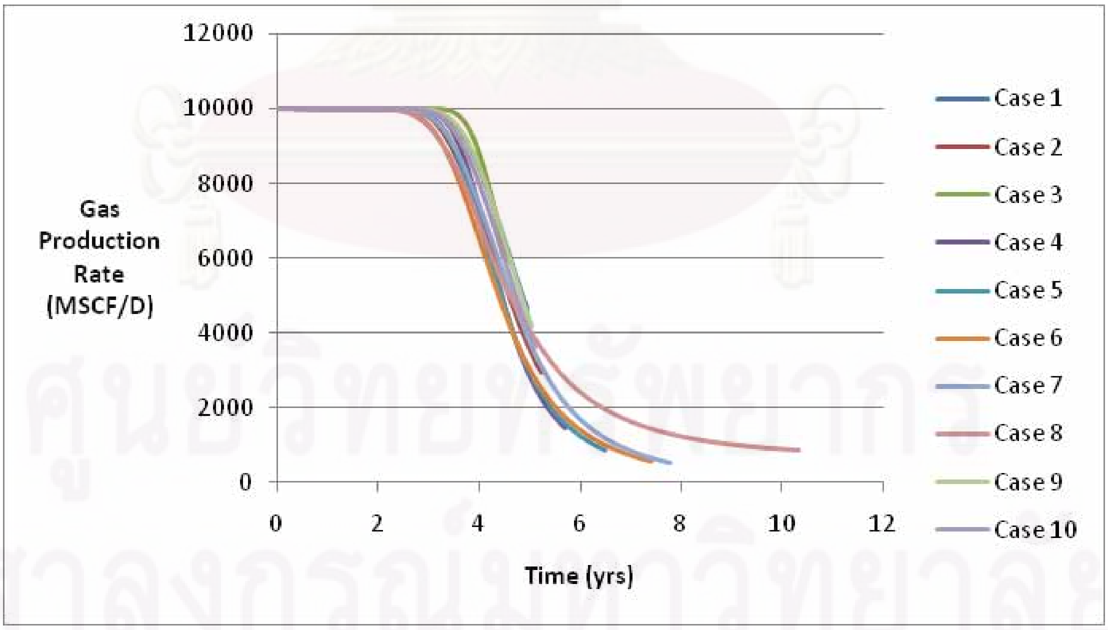

Figure 5.14: Gas production rate for producing with CO_2 injection at the dew point pressure with initial reservoir pressure equal to 3,500 psia.

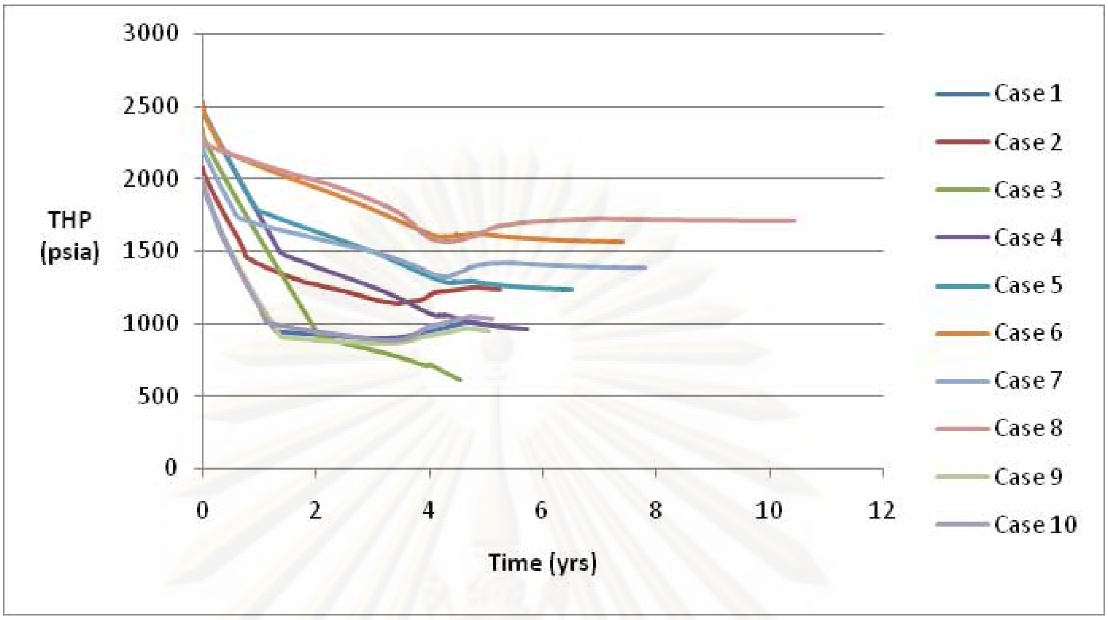

Figure 5.15: Tubing head pressure for producing with CO_2 injection at the dew point pressure with initial reservoir pressure equal to 3,500 psia.

The production life for the case of no CO_2 concentration limit and 23% CO_2 concentration limit of injecting CO_2 at the dew point pressure are summarized in Table 5.7. The highest and lowest production life of no CO_2 concentration limit is obtained in case 8 and case 3, respectively. The production life of 23% CO_2 concentration limit depends on the dew point pressure. In the case that the dew point pressure is high, the CO_2 injection will start early. So, the CO_2 will reach the producer early, causing the production life to be short.

Table 5.7: Producing time before reaching the dew point pressure and production life for producing with CO_2 injection at the dew point pressure with initial reservoir pressure equal to 3,500 psia.

Case	**Producing time before reaching the dew point pressure (years)**	**Production life (years)**	
		No limit	**23% CO_2 limit**
1	1.25	5.0	4.2
2	0.73	5.3	3.9
3	1.95	4.6	4.2
4	1.31	5.8	3.9
5	0.84	6.5	3.8
6	0.33	7.4	3.7
7	0.51	7.8	3.9
8	0.00	10.5	3.6
9	1.26	5.1	4.2
10	1.02	5.2	4.1

The total gas production and gas recovery factor for the case with no CO_2 concentration limit and 23% CO_2 concentration limit for CO_2 injection at the dew point pressure are summarized in Table 5.8. With CO_2 concentration limit, the gas recovery factors with no CO_2 concentration limit are not much different and almost equal 100%. For the case with 23% CO_2 concentration limit, the gas recovery factor seems to depend on the dew point pressure. The gas recovery factor is the results of production rate multiply by the production life. The gas production rates of each case are very similar. So, gas recovery factor will depend on the production life. When the dew point pressure is higher, the CO_2 injection will starts earlier and make the production life shorter. Therefore, the gas recovery factor will be higher when the dew point pressure is lower.

Table 5.8: Total gas production and recovery factor for producing with CO_2 injection at the dew point pressure with initial reservoir pressure equal to 3,500 psia.

Case	**Total Gas Production (BCF)**		**Gas recovery factor (%)**	
	No limit	**23% CO_2 limit**	**No limit**	**23% CO_2 limit**
1	16.68	14.91	91%	81%
2	16.42	13.79	95%	79%
3	15.95	15.17	90%	85%
4	16.57	14.03	97%	82%
5	16.81	13.72	98%	80%
6	16.87	13.15	99%	77%
7	17.72	13.93	99%	78%
8	16.56	11.82	94%	67%
9	16.85	15.03	92%	82%
10	16.64	14.55	93%	81%

The condensate production rate and the bottomhole pressure (BHP) for production with CO_2 injection at the dew point pressure are shown in Figures 5.16 and 5.17, respectively. The condensate production rates at the beginning are different because the condensate-gas ratios (CGR) are different. In case 1, 3, 9 and 10, the condensate production rate can remain nearly constant after CO_2 injection starts and starts decline when CO_2 breaks through the producer. In case 2, 4, 5, 6, 7 and 8, the condensate production rate slowly declines and increases as a result of pressure maintenance by CO_2 injection and then slowly declines again after CO_2 breaks through the producer. Injecting CO_2 at the dew point pressure can maintain the bottomhole pressure to be almost constant in case 1, 9, and 10. Case 3 has the lowest dew point pressure with a maximum liquid dropout of 1%. So, the liquid does not drop out much in the pore space. In case 2, 4, 5, 6, 7 and 8, injecting CO_2 at the dew point pressure cannot maintain the bottomhole pressure to be higher than the dew point. So, the liquid dropout occurs in the pore space around the wellbore. In case 1, 3, 9 and 10, the liquid dropout occurs only in the well block. The increase in condensate production rate when CO_2 breaks through is the results of liquid revaporization by CO_2 which will be discussed in more detail later in this chapter.

The condensate production profile of production by natural depletion, production by CO_2 injection at the beginning and production by CO_2 injection at the dew point pressure can be compared by inspecting Figure 5.3, Figure 5.10, and Figure 5.16. The behavior of condensate production rate of CO_2 injection at the dew point pressure is similar to that of CO_2 injection at the beginning cases. CO_2 injection at the dew point pressure can maintain the condensate production rate to be constant longer than the natural depletion case because injecting CO_2 at the dew point pressure can maintain the bottomhole pressure to be high as shown in Figure 5.17.

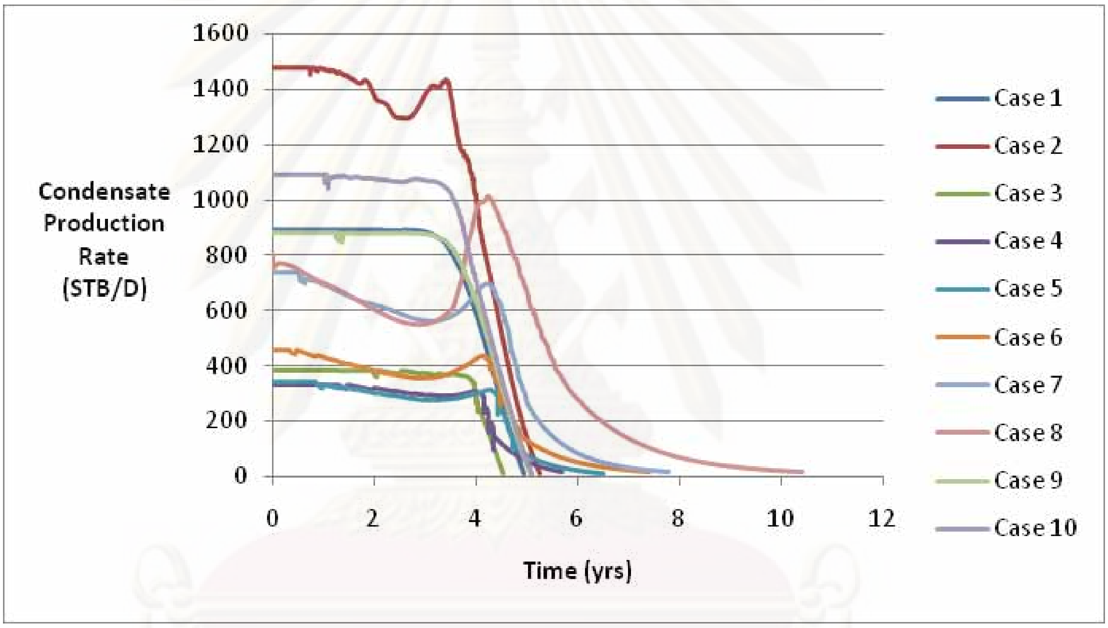

Figure 5.16: Condensate production rate for producing with CO_2 injection at the dew point pressure with initial reservoir pressure equal to 3,500 psia.

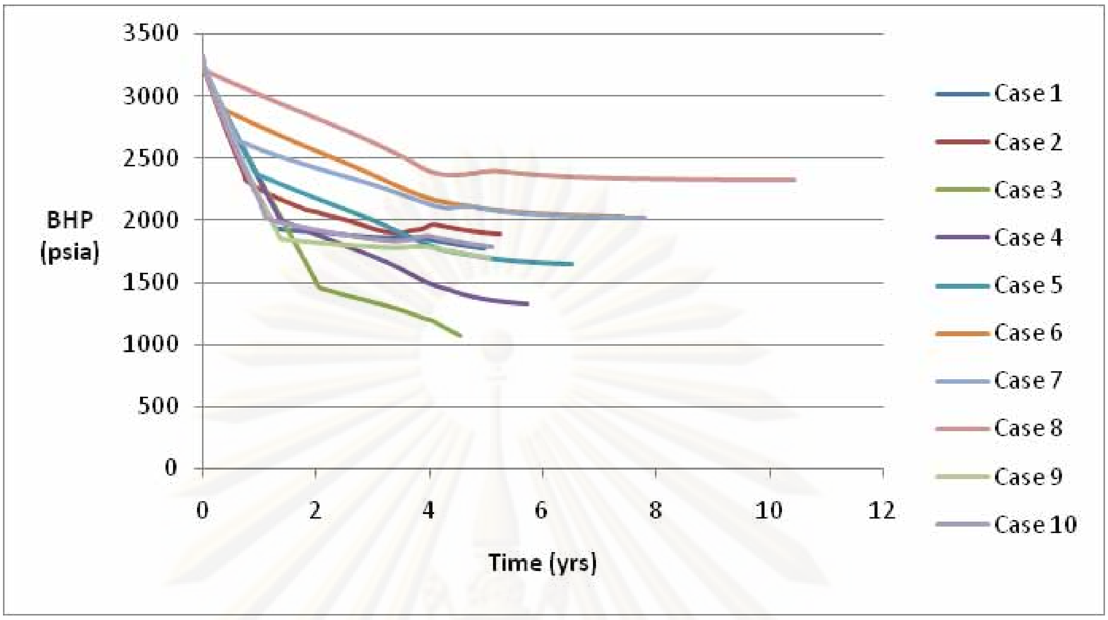

Figure 5.17: Bottomhole pressure for producing with CO_2 injection at the dew point pressure with initial reservoir pressure equal to 3,500 psia.

The condensate saturation at grid block (1, 1, 1), which is the producer, for the case with 23% CO_2 concentration limit and no CO_2 concentration limit is shown in Figures 5.18 and 5.19, respectively. In the case of 23% CO_2 concentration limit, the liquid dropout can be completely revaporized in cases 1, 3, 9 and 10 as depicted in Figure 5.18. Case 3 has the lowest dew point pressure with the maximum liquid dropout of only 1%. So, the liquid does not drop out much in the pore space. As shown in Table 4.4, the dew point pressures of case 1, 9 and 10 are relatively low when compared to the other cases. So, the reservoir pressure is easier to be maintained. The liquid dropout can be completely revaporized. For cases 2, 4, 5, 6, 7 and 8, the liquid dropout cannot be completely revaporized due to high dew point pressure. As shown in Table 4.4, the dew point pressures of case 2, 7 and 8 are relatively high, making it difficult to maintain the reservoir pressure above the dew point pressure. In the case of no CO_2 concentration limit, the liquid dropout can be completely revaporized in all cases. When producing with no CO_2 concentration limit, the CO_2 mole fraction can be high enough to completely revaporized the liquid in the reservoir.

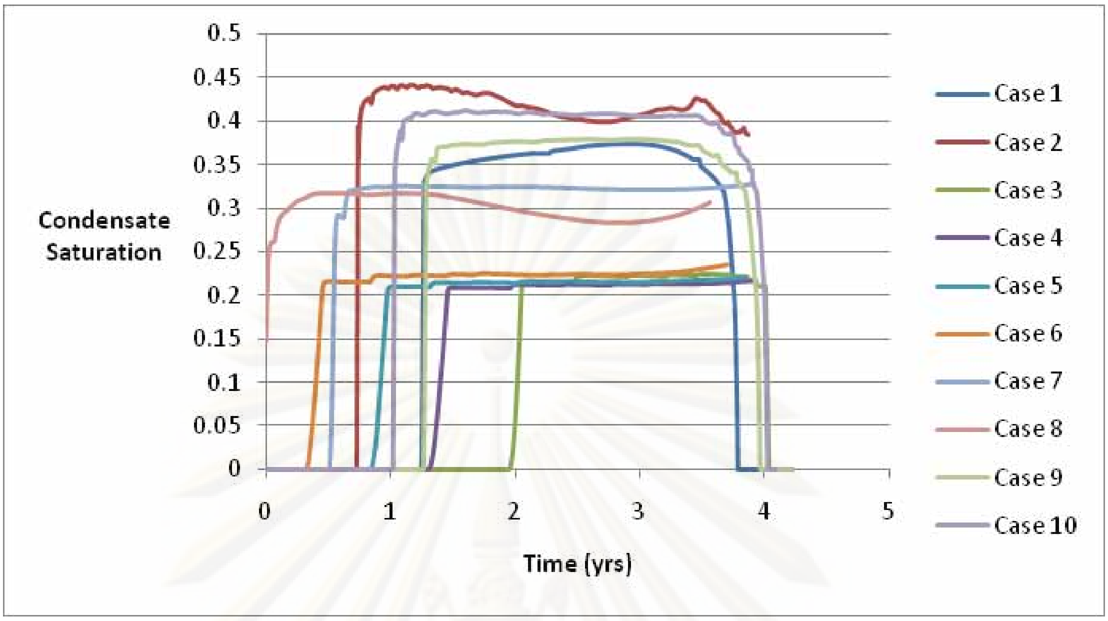

Figure 5.18: Condensate saturation for producing with CO_2 injection at the dew point pressure with initial reservoir pressure equal to 3,500 psia (23% CO_2 concentration limit).

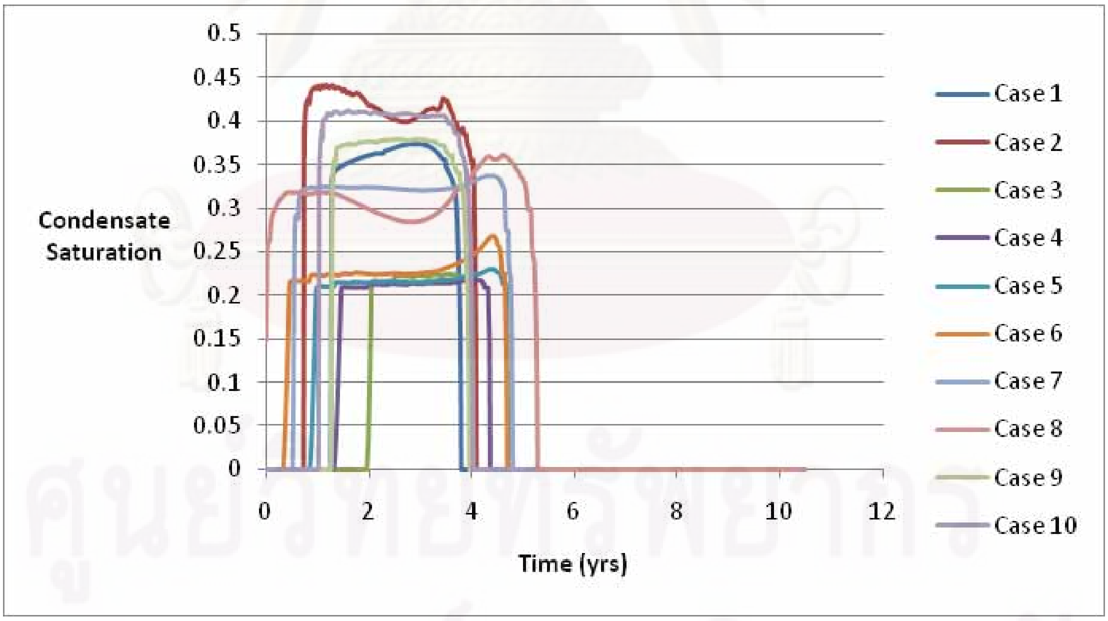

Figure 5.19: Condensate saturation for producing with CO_2 injection at the dew point pressure with initial reservoir pressure equal to 3,500 psia (no CO_2 concentration limit).

The total condensate production and the condensate recovery factor for the case with no CO_2 concentration limit and 23% CO_2 concentration limit for CO_2 injection at the dew point pressure are summarized in Table 5.9.

Table 5.9: Total condensate production and recovery factor for producing with CO_2 injection at the dew point pressure with initial reservoir pressure equal to 3,500 psia.

Case	**Total condensate production (STB)**		**Condensate recovery factor (%)**	
	No limit	**23% CO_2 limit**	**No limit**	**23% CO_2 limit**
1	1,370,993	1,302,462	83%	79%
2	2,221,391	1,973,242	87%	77%
3	579,081	568,525	85%	83%
4	526,720	453,765	92%	79%
5	551,794	434,278	93%	73%
6	735,914	538,865	94%	69%
7	1,212,879	912,999	92%	69%
8	1,582,471	833,376	93%	49%
9	1,378,361	1,301,819	85%	80%
10	1,673,198	1,557,479	85%	80%

The performance of gas condensate reservoirs with CO_2 injection at the dew point pressure can be summarized as follows:

(a) In the case of 23% CO_2 concentration limit, the total gas production ranges from 11.82 to 15.17 BCF, yielding gas recovery factor between 67 to 85%.

(b) In the case of 23% CO_2 concentration limit, the total condensate production ranges from 434,278 to 1,973,242 STB, yielding condensate recovery factor between 49 to 83%.

(c) The lowest recovery factor of total condensate production and total gas production are 49% and 67%, respectively in case 8 because the liquid dropout occurs at the beginning of the production.

The comparisons of the simulation results between production with natural depletion and production with CO_2 injection at the dew point pressure are reported.

The difference in cumulative gas production, cumulative condensate production, and recovery factors of 23% CO_2 concentration limit are summarized in Table 5.10.

Table 5.10: The difference in cumulative gas production, cumulative condensate production, and recovery factors of 23% CO_2 concentration limit between natural depletion and CO_2 injection at the dew point pressure with initial reservoir pressure equal to 3,500 psia.

Case	**ΔGp (BCF)**	**ΔRF for gas (%)**	**ΔNp (STB)**	**ΔRF for condensate (%)**
1	-0.51	-3%	502,622	31%
2	-1.06	-7%	912,837	36%
3	-0.71	-4%	-17,376	-3%
4	-1.52	-9%	44,499	8%
5	-1.86	-11%	92,857	16%
6	-2.37	-14%	179,585	23%
7	-2.08	-12%	380,880	29%
8	-4.10	-24%	391,102	23%
9	-0.44	-2%	472,677	29%
10	-0.53	-3%	670,001	34%

The performance of gas condensate reservoirs with CO_2 injection at the dew point pressure compared with production by natural depletion can be summarized as follows:

(a) In all cases, injecting CO_2 at the dew point pressure decreases the total gas production compared with production by natural depletion. When producing with natural depletion, most of the reservoir fluid is produced as gas but the produced reservoir fluid is changed from gas to condensate when producing with CO_2 injection at the dew point pressure. When injecting CO_2 at the dew point pressure, the reservoir can be produced until reaching the economic limit of CO_2 concentration even though the economic limit of gas production may not be reached yet. But in the natural depletion case, the reservoir can be produced until reaching the economic limit of condensate and gas production rates.

(b) Injecting CO_2 at the dew point pressure increases the total condensate production compared with production by natural depletion in all cases except case 3. Since injecting CO_2 at the dew point pressure can minimize the reservoir pressure drop and liquid dropout around wellbore.

(c) In case 3, the total condensate production with production by CO_2 injection at the dew point pressure is lower than production by natural depletion. From the phase diagram shown in Figure 5.13, the reservoir fluid in this case has a dew point pressure of 1680 psia which is the lowest among the 10 cases in this study. The maximum liquid dropout is only 1%. The liquid dropout can be completely revaporized even in natural depletion case when the reservoir pressure drops below 620 psia. CO_2 injection will cause an early termination of gas production due to high CO_2 concentration at the producer (CO_2 limit = 23%), resulting in lower recovery factor.

5.1.4 Comparison between Production with Natural Depletion and CO_2 injection

In this section, comparisons between the simulation results of production with natural depletion, CO_2 injection at the beginning and CO_2 injection at the dew point pressure are discussed in term of total condensate and gas production. The dew point pressure and total gas productions for natural depletion, CO_2 injection at the beginning and CO_2 injection at the dew point pressure of 23% CO_2 concentration limit are shown in Table 5.11.

Table 5.11: Dew point pressure, total gas production for natural depletion, injecting CO_2 at the beginning and injecting CO_2 at the dew point pressure of 23% CO_2 concentration limit with initial reservoir pressure equal to 3,500 psia.

Case	**Dew point pressure (psia)**	**Total gas production (BCF)**		
		Natural depletion	**Injecting CO_2 at the beginning**	**Injecting CO_2 at the dew point pressure**
1	2020	15.42	13.82	14.91
2	2440	14.85	13.16	13.79
3	1680	15.88	13.34	15.17
4	2150	15.55	12.81	14.03
5	2550	15.58	12.88	13.72
6	2990	15.52	12.84	13.15
7	2800	16.01	13.45	13.93
8	3500	15.92	11.82	11.82
9	2010	15.47	13.87	15.03
10	2180	15.08	13.62	14.55

The dew point pressure and total condensate productions for natural depletion, CO_2 injection at the beginning and CO_2 injection at the dew point pressure of 23% CO_2 concentration limit are shown in Table 5.12.

Table 5.12: Dew point pressure, total condensate production for natural depletion, injecting CO_2 at the beginning and injecting CO_2 at the dew point pressure of 23% CO_2 concentration limit with initial reservoir pressure equal to 3,500 psia.

Case	Dew point pressure (psia)	Total condensate production (STB)		
		Natural depletion	Injecting CO_2 at the beginning	Injecting CO_2 at the dew point pressure
1	2020	799,840	1,195,409	1,302,462
2	2440	1,060,405	1,910,289	1,973,242
3	1680	585,901	489,917	568,525
4	2150	409,266	424,462	453,765
5	2550	341,421	440,866	434,278
6	2990	359,280	579,076	538,865
7	2800	532,119	982,394	912,999
8	3500	442,274	833,376	833,376
9	2010	829,142	1,191,262	1,301,819
10	2180	887,478	1,449,278	1,557,479

The performance comparison between gas condensate reservoirs with natural depletion, CO_2 injection at the beginning and CO_2 injection at the dew point pressure can be summarized as follows:

(a) In all cases, production with natural depletion has the highest total gas production. When producing with natural depletion, most of the reservoir fluid is produced as gas but the produced reservoir fluid is changed from gas to condensate when producing with CO_2 injection at the beginning and dew point pressure. In the natural depletion case, the reservoir can be produced until reaching the economic limit of condensate and gas production rates. In the CO_2 injection case, the reservoir can be produced until reaching the economic limit of CO_2 concentration even though the economic limit of gas production may not be reached yet.

(b) Injecting CO_2 at the beginning gives lower total gas production than injecting CO_2 at the dew point pressure because injecting CO_2 at the dew point pressure causes the CO_2 level at the producer to reach the CO_2 concentration limit slower than injecting CO_2 at the beginning.

(c) Injecting CO_2 at the beginning and at the dew point pressure yields higher total condensate production than production with natural depletion except case 3.

(d) In case 3, injecting CO_2 at the beginning has lower total condensate production than production with natural depletion and CO_2 injection at the dew point pressure because this case has the lowest dew point pressure with the maximum liquid dropout of only 1%. The liquid dropout can be completely revaporized even production with natural depletion. Injecting CO_2 will accelerate the breakthrough leading to a shorter production life.

(e) For cases 1, 2, 4, 9 and 10, injecting CO_2 at the dew point pressure gives higher total condensate production than injecting CO_2 at the beginning because injecting CO_2 at the dew point pressure causes the CO_2 level at the producer to reach the CO_2 concentration limit slower than injecting CO_2 at the beginning.

(f) For cases 5, 6 and 7, injecting CO_2 at the beginning gives higher total condensate production than injecting CO_2 at the dew point pressure. Cases 5, 6 and 7 have relatively high dew point pressure when compare to the other cases. Injecting CO_2 at the beginning is better in maintaining the reservoir pressure and minimizing the liquid dropout around the wellbore.

5.1.5 Production of gas condensate reservoir with CO_2 injection starting above the dew point pressure

The objective of this scenario is to optimize the time to start CO_2 injection before reaching the dew point pressure, which should be the time that can completely revaporize liquid dropout around the wellbore. In this section, cases 1, 3, 9 and 10 will not be studied because the liquid dropout around the wellbore can be revaporized when starting CO_2 injection at the dew point pressure. Case 8 will also not be studied because the bottomhole pressure reaches the dew point pressure at the beginning of the simulation. In order to determine the most appropriate time to start CO_2 injection, three different scenarios are studied i.e, the injection starts when the bottomhole pressure is 200, 300, and 400 psia above the dew point.

The total gas production and total condensate production with CO_2 injection starting at 200, 300, and 400 psia above the dew point pressure is summarized in Tables 5.13 and 5.14, respectively. In case 6, CO_2 injection cannot be start at 300 and 400 psia above the dew point pressure. Although, the initial reservoir pressure is equal to 3,500 psia, but the bottomhole pressure needed to be 3,300 psia in order to have 10,000 Mscf/day at the beginning as already shown in Figure 5.17. Therefore, start injection at 300 psia above the dew point pressure is the same time at start injection at the beginning.

Table 5.13: Total gas production for producing with CO_2 injection starting above the dew point pressure with initial reservoir pressure equal to 3,500 psia.

Case	**Gas production total (BCF)**		
	200 psia above the dew point pressure	**300 psia above the dew point pressure**	**400 psia above the dew point pressure**
2	13.65	13.58	13.51
4	13.80	13.73	13.65
5	13.49	13.33	13.26
6	12.99	-	-
7	13.75	13.67	13.59

Table 5.14: Total condensate production for producing with CO_2 injection starting above the dew point pressure with initial reservoir pressure equal to 3,500 psia.

Case	**Condensate production total (STB)**		
	200 psia above the dew point pressure	**300 psia above the dew point pressure**	**400 psia above the dew point pressure**
2	1,986,792	1,976,124	1,965,244
4	458,612	456,070	453,361
5	456,078	456,785	454,231
6	563,412	-	-
7	997,659	998,885	993,038

The performance of gas condensate reservoirs when starting CO_2 injection above the dew point pressure can be summarized as follows:

(a) In all cases, starting CO_2 injection at 200 psia above the dew point pressure yields the highest total gas production because CO_2 concentration at the producer reaches the CO_2 concentration limit slower than other scenarios.

(b) In case 2 and case 4, starting CO_2 injection at 200 psia above the dew point pressure gives the highest total condensate production. And, in case 5 and case 7, starting CO_2 injection at 300 psia above the dew point pressure gives the highest total condensate production.

In order to obtain the maximum condensate recovery, we found that liquid dropout around the wellbore has to be completely revaporized before the economic limit is reached. The details of revaporization process are discussed as follows:

Condensate revaporization

From the previous section, we observed that if there is liquid dropout in the reservoir, the condensate production rate will increase when CO_2 reaches the producer. This is the results of condensate revaporization. We choose case 7 to study the revaporization process in detail. The condensate gas ratio as a function of time for producing with natural depletion, CO_2 injection at the beginning, and CO_2 injection at the dew point pressure of case 7 is shown in Figure 5.20. For producing with natural depletion, the condensate gas ratio decreases rapidly when the bottomhole pressure reaches the dew point pressure. And then, the condensate gas ratio gradually increases because the percent of liquid dropout starts to increase. For producing with CO_2 injection at the beginning, the condensate gas ratio remains constant for certain duration before starting to decline after CO_2 concentration in the produced gas increases. For producing with CO_2 injection at the dew point pressure, the condensate gas ratio decreases when the bottomhole pressure reaches the dew point pressure. And then, the condensate gas ratio increases when CO_2 reaches the producer.

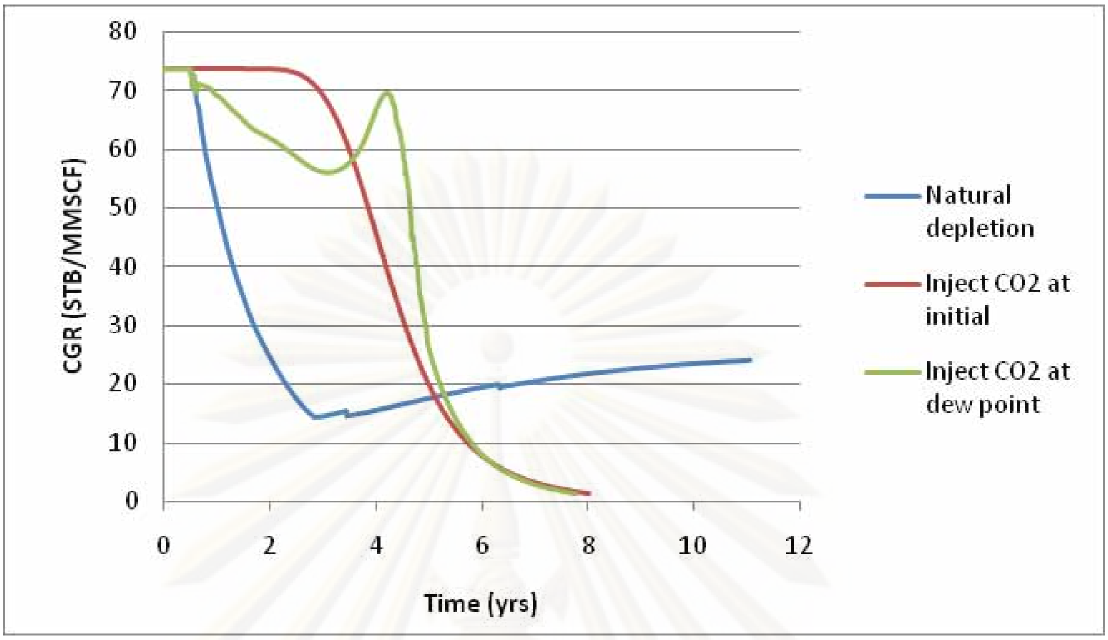

Figure 5.20: Condensate gas ratio for producing with natural depletion, CO_2 injection at the beginning and CO_2 injection at dew point pressure of case 7.

The condensate saturation in the grid blocks for producing with natural depletion, CO_2 injection at the beginning and CO_2 injection at the dew point pressure are shown in Figure 5.21, 5.22 and 5.24, respectively. In Figure 5.21a, the condensate saturation in the grid block at the beginning of simulation is shown. The dark blue in the grid block represents zero condensate saturation. Then, liquid dropout occurs around the wellbore after the bottomhole pressure reach the dew point pressure as shown in Figure 5.21b. In Figure 5.21c, the liquid dropout propagates further until the entire reservoir have the liquid dropout in the pore space. Note that the liquid dropout around the wellbore is mobile since its saturation is higher than the critical condensate saturation. After that, the condensate saturation in the reservoir decreases because the liquid dropout start to revaporize when the bottomhole pressure drop below 1,950 psia as shown in Figure 5.21d.

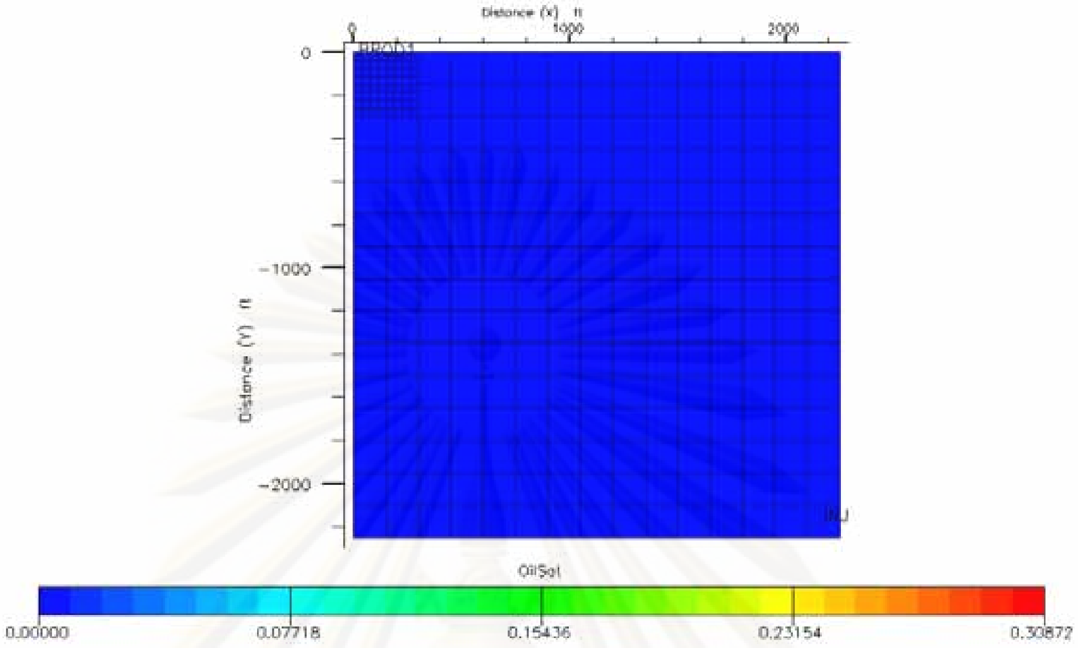

(a) Initial of the production.

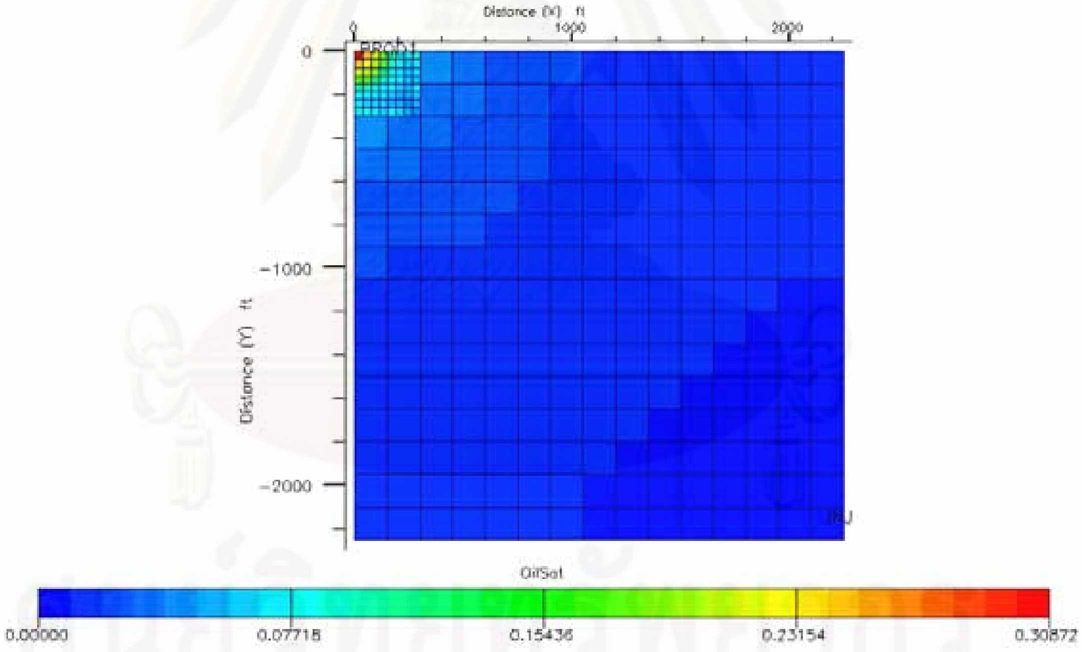

(b) Liquid starts to drop out around the wellbore.

Figure 5.21: Condensate saturation in grid blocks when producing with natural depletion.

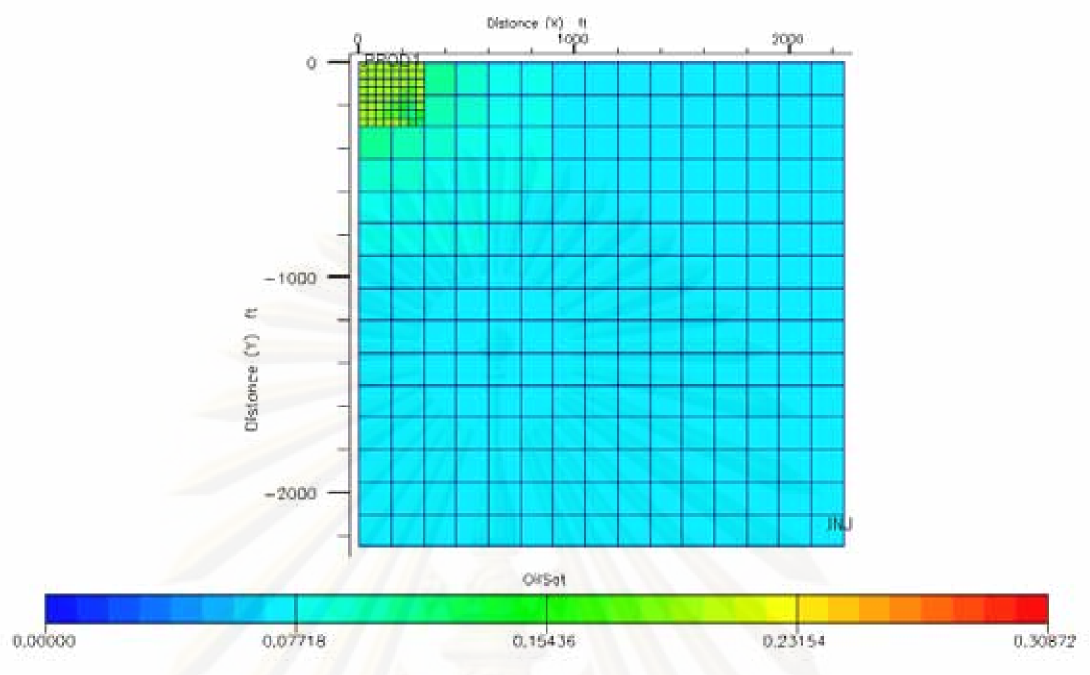

(c) Liquid dropout occurs in the entire of the reservoir.

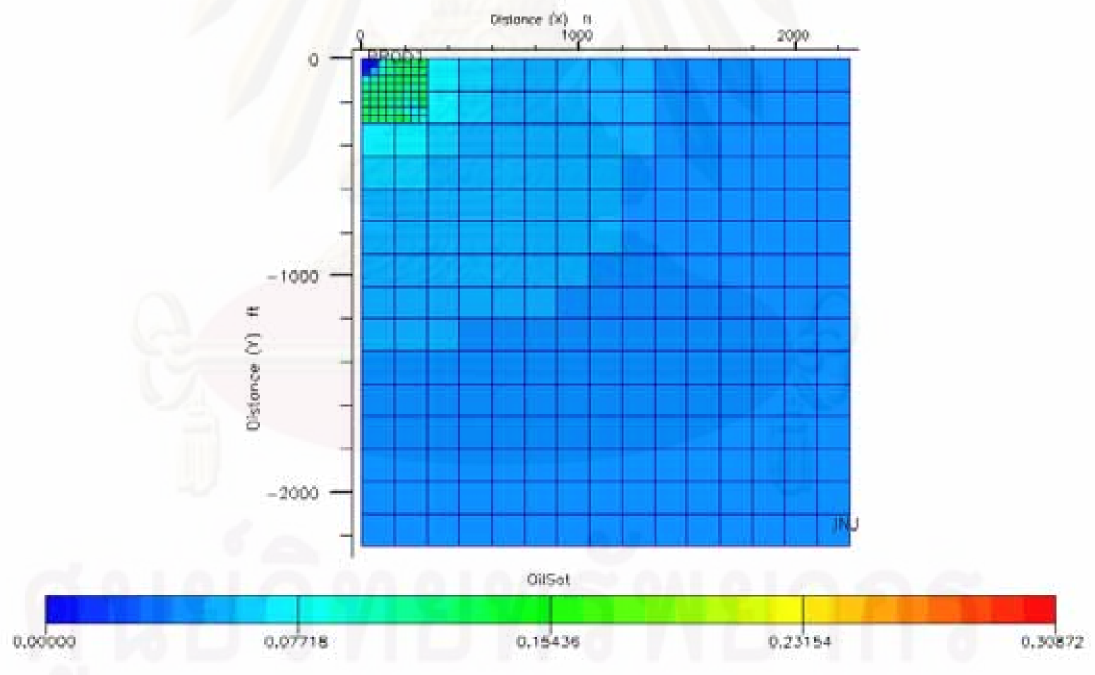

(d) End of the production.

Figure 5.21: Condensate saturation in grid blocks when producing with natural depletion (continued).

For producing with CO_2 injection at the beginning, the CO_2 injection can maintain pressure to be above the dew point pressure and prevent liquid from dropping out. The condensate saturation in the grid blocks at the beginning and the end of simulation when producing with CO_2 injection at the beginning are shown in Figures 5.22a and 5.22b, respectively.

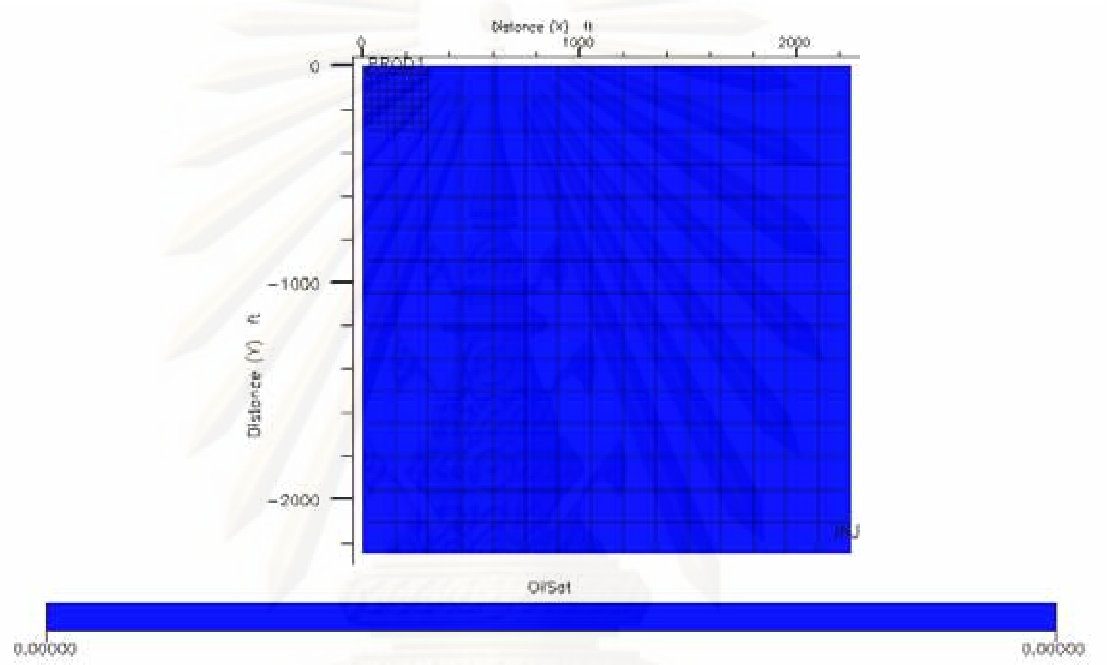

(a) Initial of the production.

Figure 5.22: Condensate saturation in grid blocks when producing with CO_2 injection at the beginning.

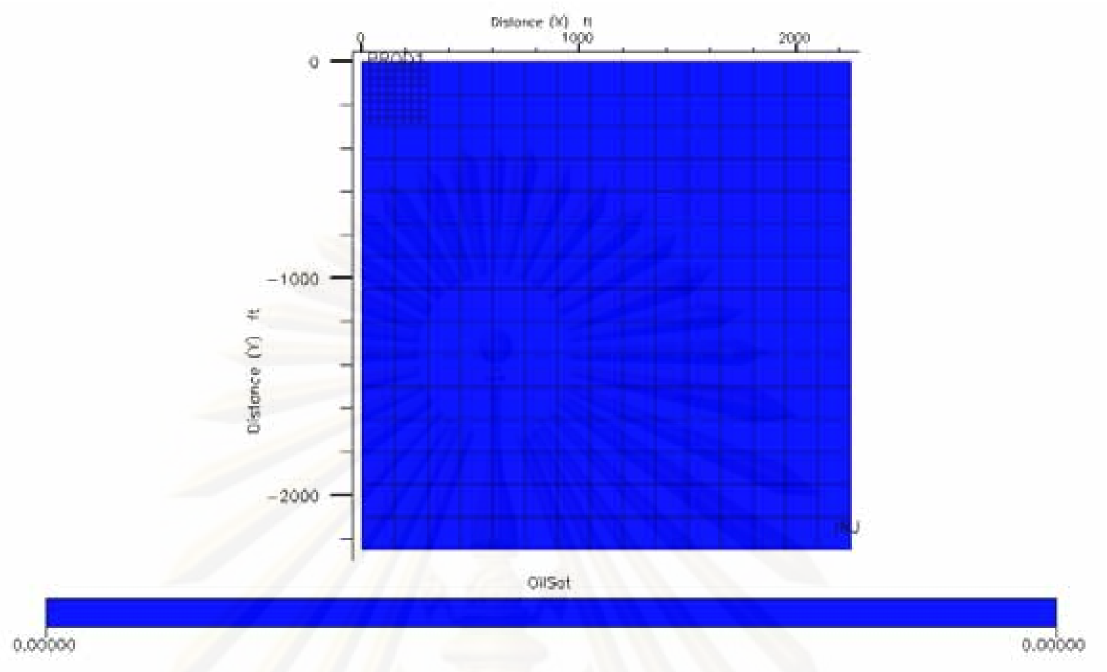

(b) End of the production.

Figure 5.22: Condensate saturation in grid blocks when producing with CO_2 injection at the beginning (continued).

The CO_2 saturation in the grid blocks at the beginning and the end of simulation when producing with CO_2 injection at the beginning are shown in Figures 5.23a and 5.23b, respectively.

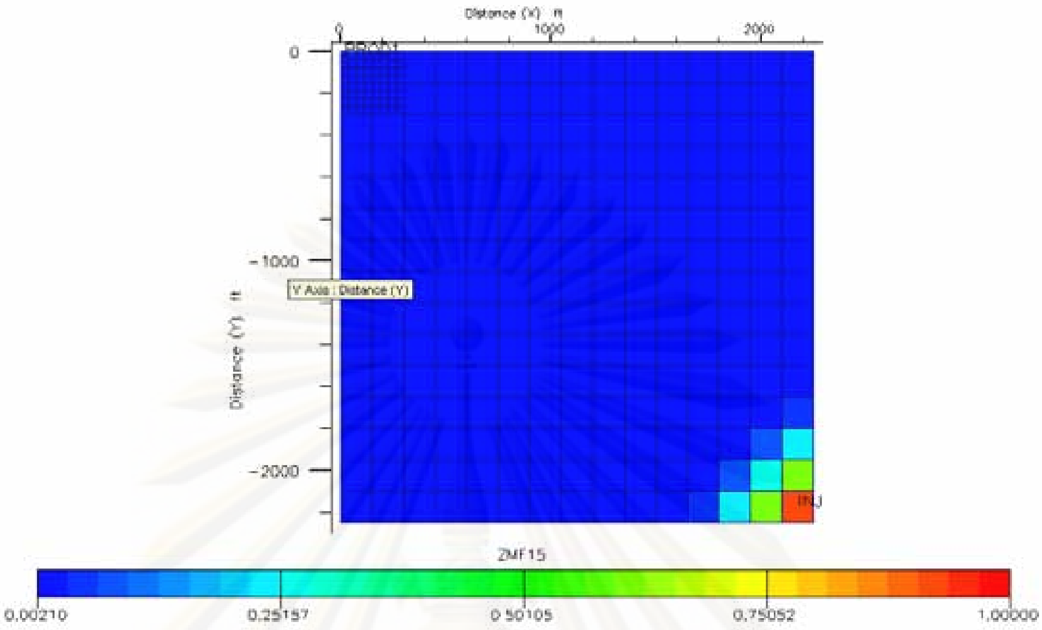

(a) Initial of the production.

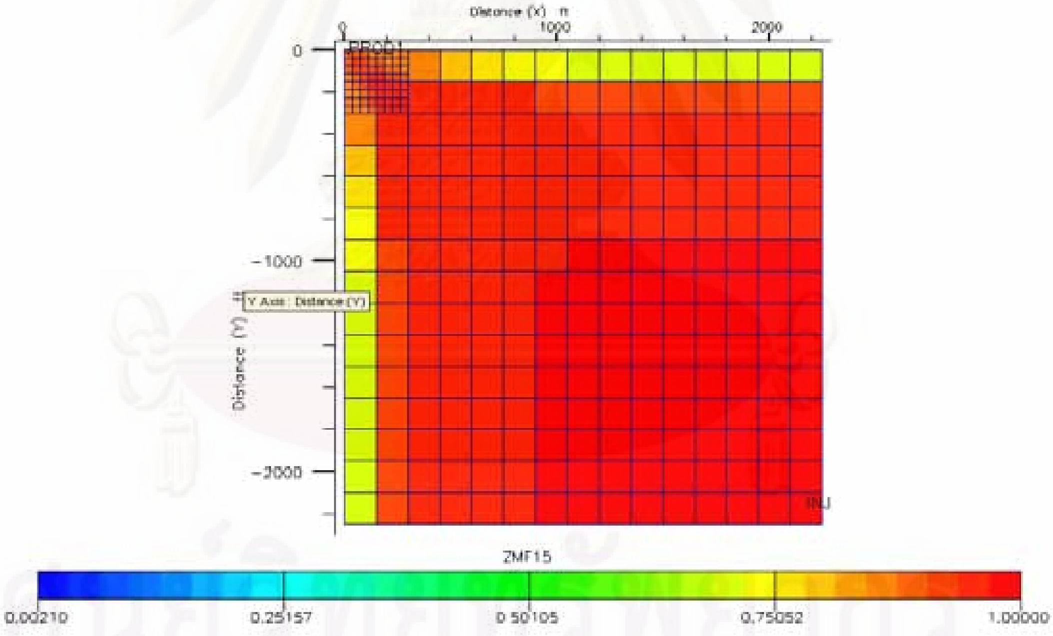

(b) End of the production.

Figure 5.23: CO_2 saturation in grid blocks when producing with CO_2 injection at the beginning.

Figure 5.24a shows condensate saturation in the grid blocks at the beginning of the simulation when producing with CO_2 injection at the dew point pressure. Initially, there is no liquid in each grid block. In Figure 5.24b, the liquid dropout occurs around the wellbore as the pressure in the grid blocks around the wellbore drop below the dew point pressure. Then, the CO_2 starts to invade into the grid blocks around the wellbore as shown in Figure 5.24c. We can see that the condensate saturation in the grid block closer to the producer is around 0.345, and the condensate saturation in the grid block further from the producer is around zero. After continuous injection of CO_2, all liquid around the wellbore is revaporized and condensate saturations in all grid blocks reduce to zero as shown in Figure 5.24d.

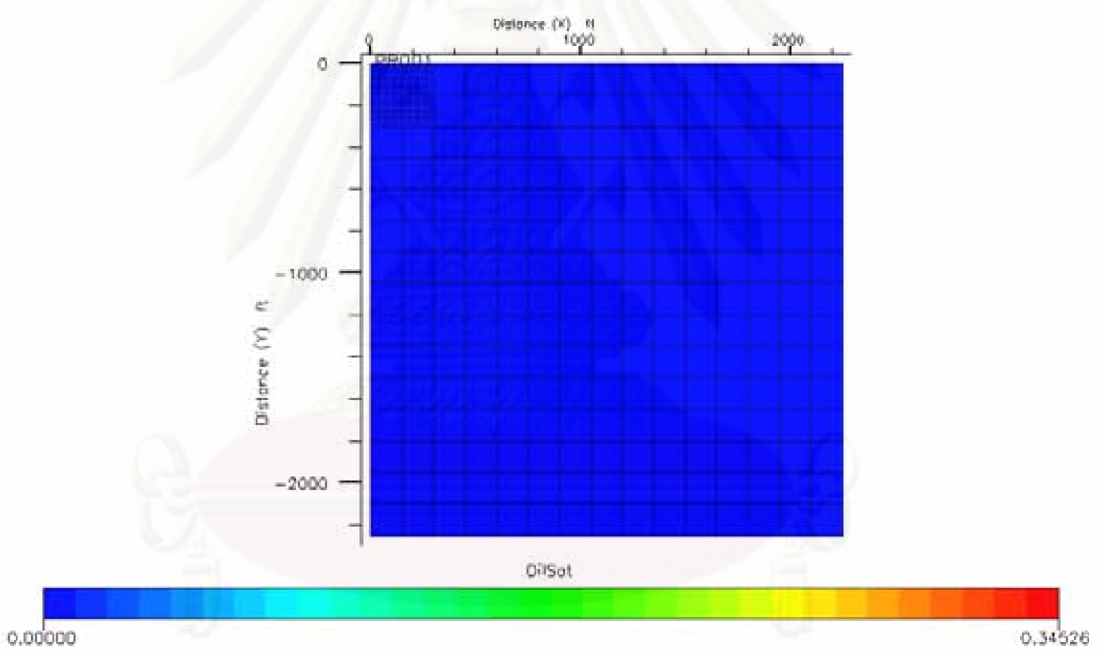

(a) Initial of the production.

Figure 5.24: Condensate saturation in grid blocks when producing with CO_2 injection at the dew point pressure.

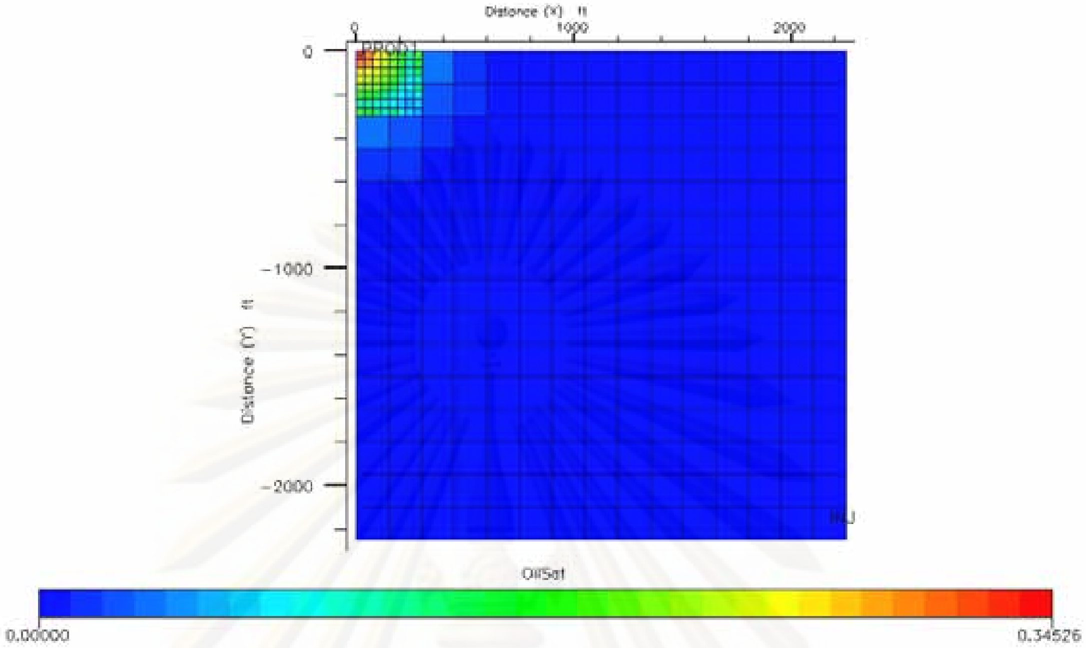

(b) Liquid starts to drop out around the wellbore.

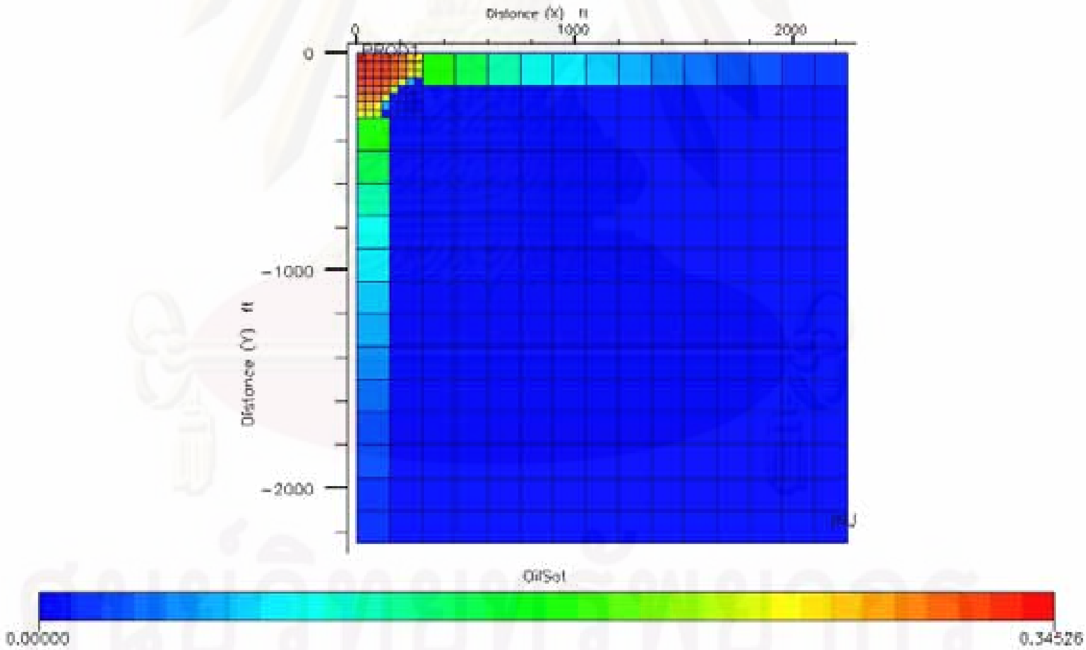

(c) CO_2 starts to revaporize liquid dropout around the wellbore.

Figure 5.24: Condensate saturation in grid blocks when producing with CO_2 injection at the dew point pressure (continued).

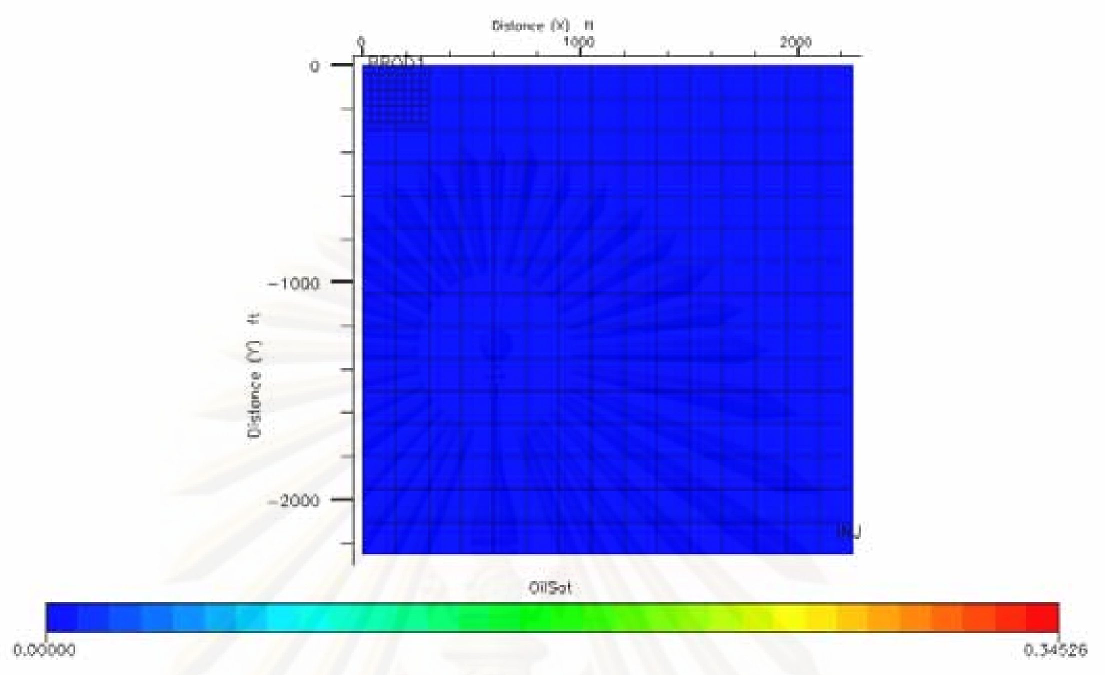

(d) End of the production.

Figure 5.24: Condensate saturation in grid blocks when producing with CO_2 injection at the dew point pressure (continued).

The CO_2 saturation in the grid blocks at the beginning until the end of simulation when producing with CO_2 injection at the dew point pressure are shown in Figures 5.25a to 5.25d.

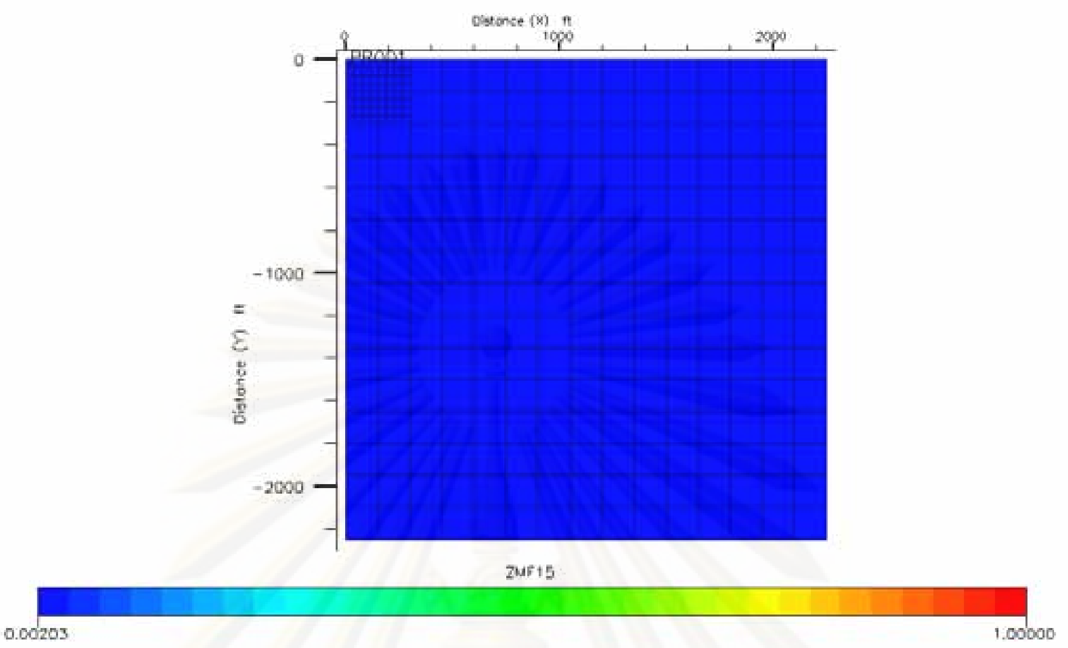

(a) Initial of the production.

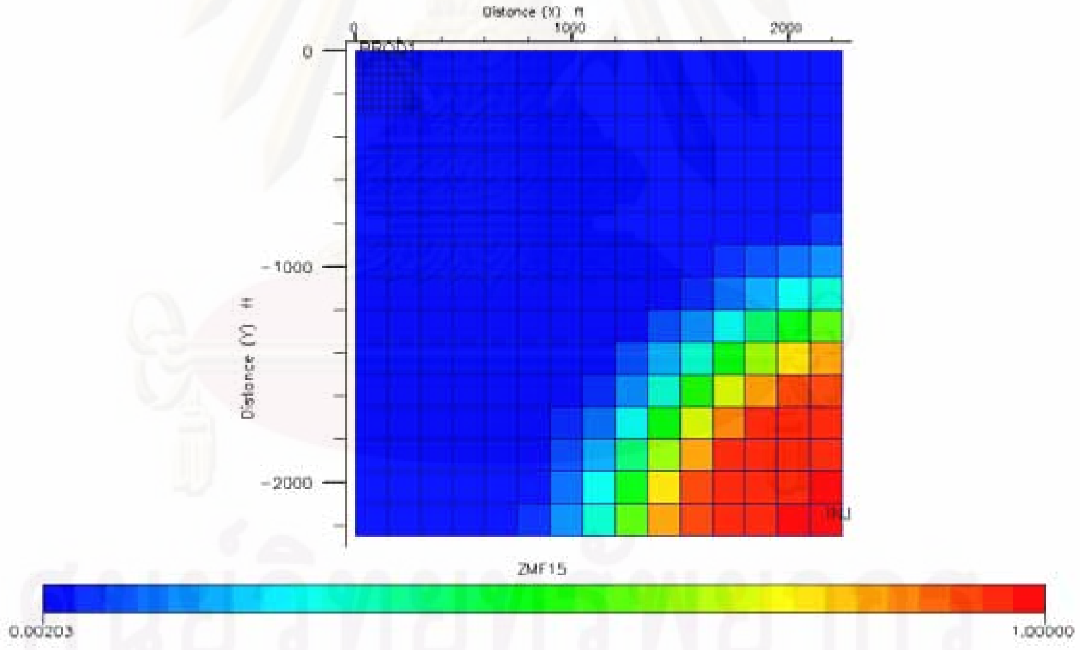

(b) Liquid starts to drop out around the wellbore.

Figure 5.25: CO_2 saturation in grid blocks when producing with CO_2 injection at the dew point pressure.

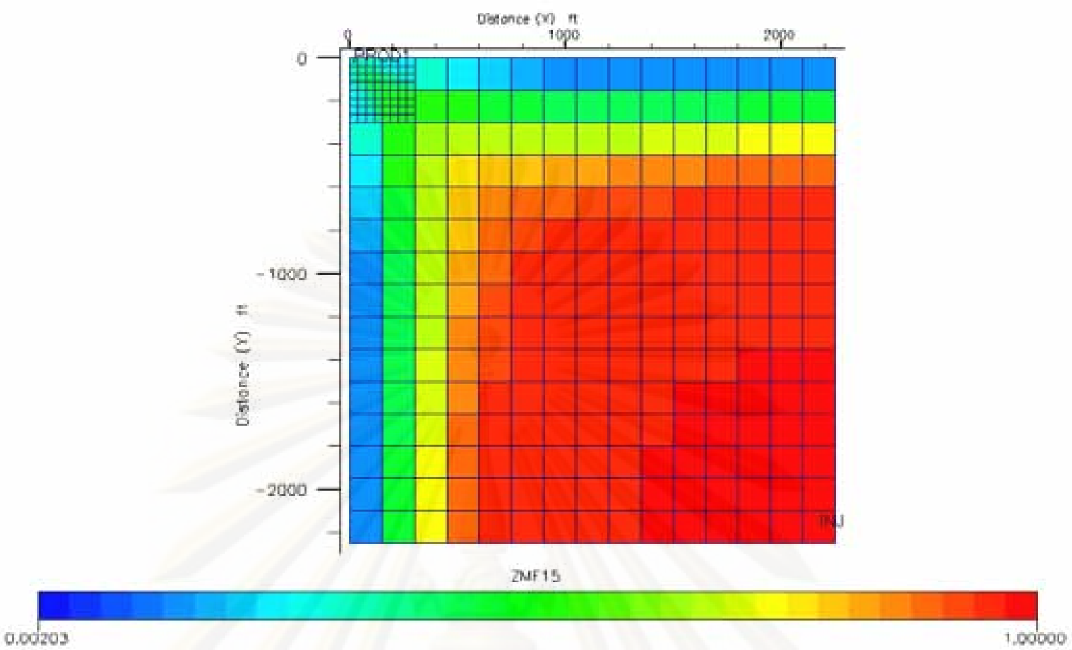

(c) CO_2 starts to invade into grid blocks around the wellbore.

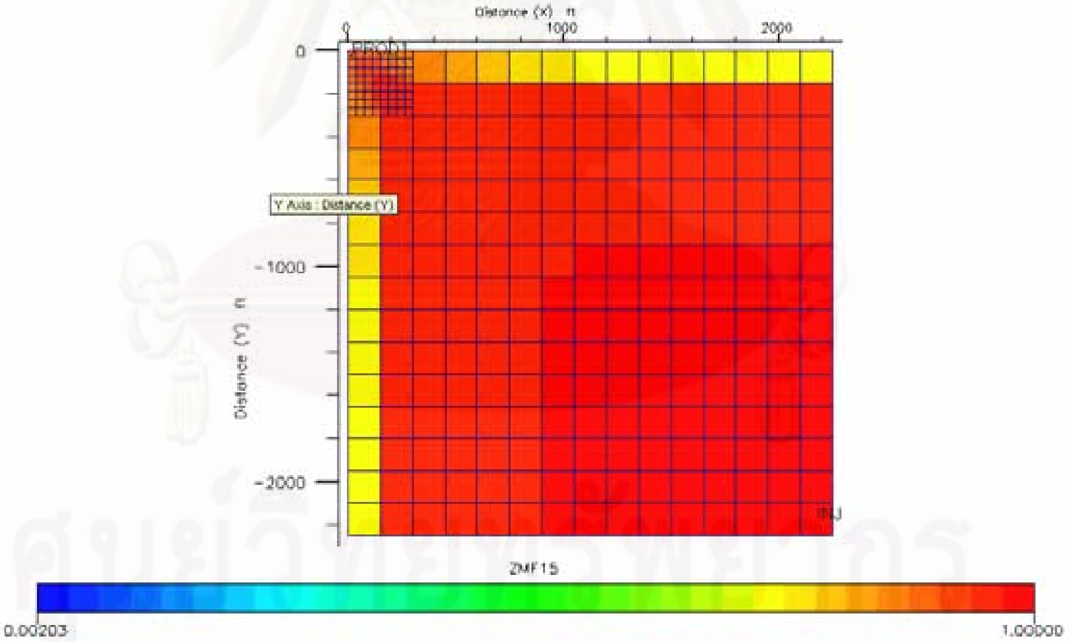

(d) End of the production.

Figure 5.25: CO_2 saturation in grid blocks when producing with CO_2 injection at the dew point pressure (continued).

For injecting CO_2 at the dew point pressure, cases 1, 3, 9 and 10 can obtain maximum condensate recovery, and CO_2 can be completely be revaporized. The condensate saturation and pressure of block (1, 1, 1) which is the well block for cases 1, 3, 9 and 10 are shown in Figure 5.26 to Figure 5.29. We can see from the condensate saturation plot with time that when liquid dropout around the wellbore is revaporized. Condensate saturation decreases from 0.2 – 0.3 to 0 very quick while the pressure in this block slightly changes.

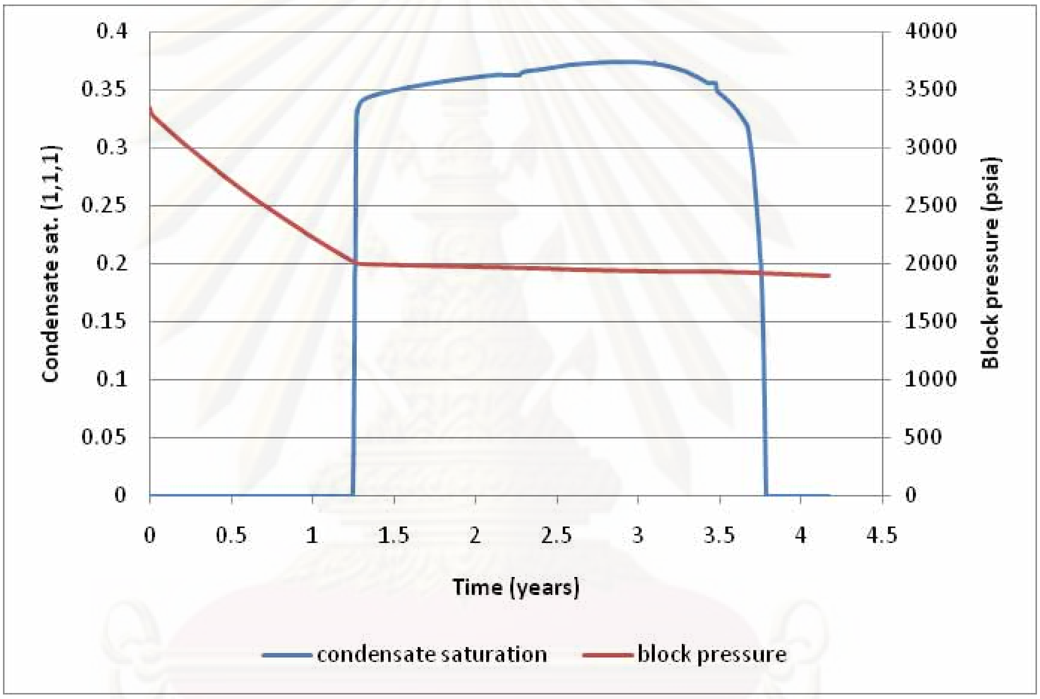

Figure 5.26: Condensate saturation and pressure of block (1, 1, 1) for case 1.

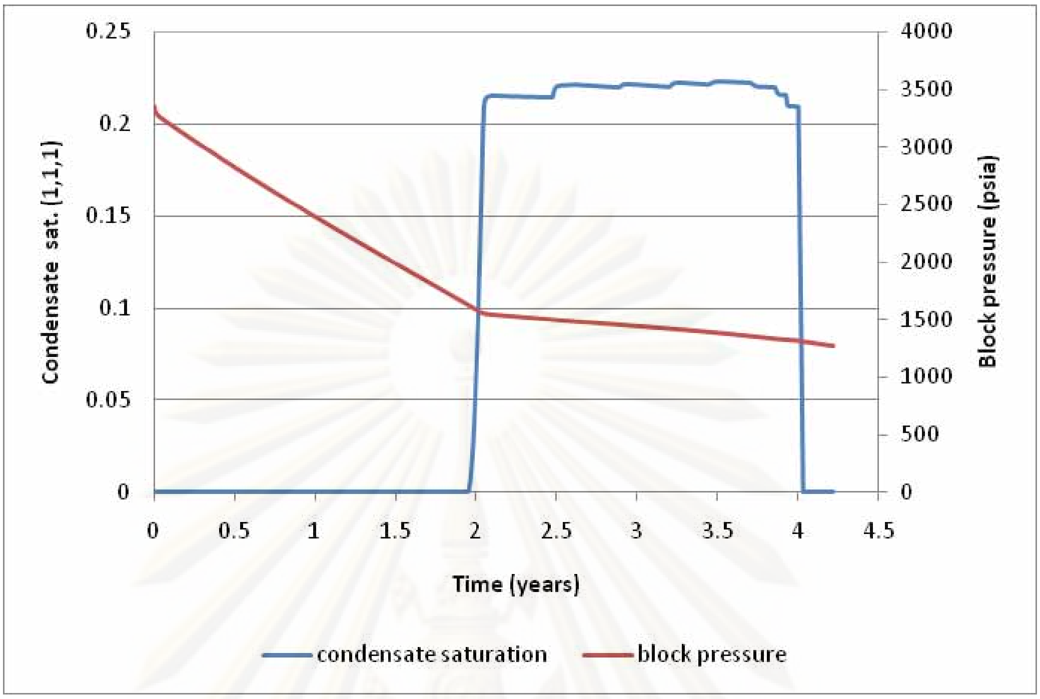

Figure 5.27: Condensate saturation and pressure of block (1, 1, 1) for case 3.

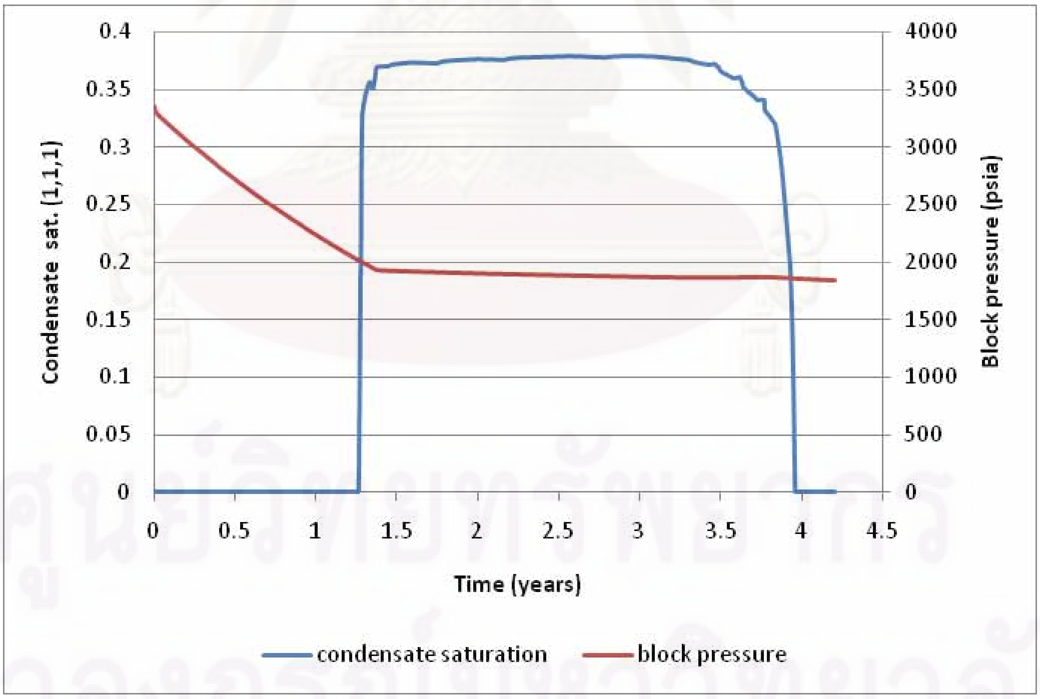

Figure 5.28: Condensate saturation and pressure of block (1, 1, 1) for case 9.

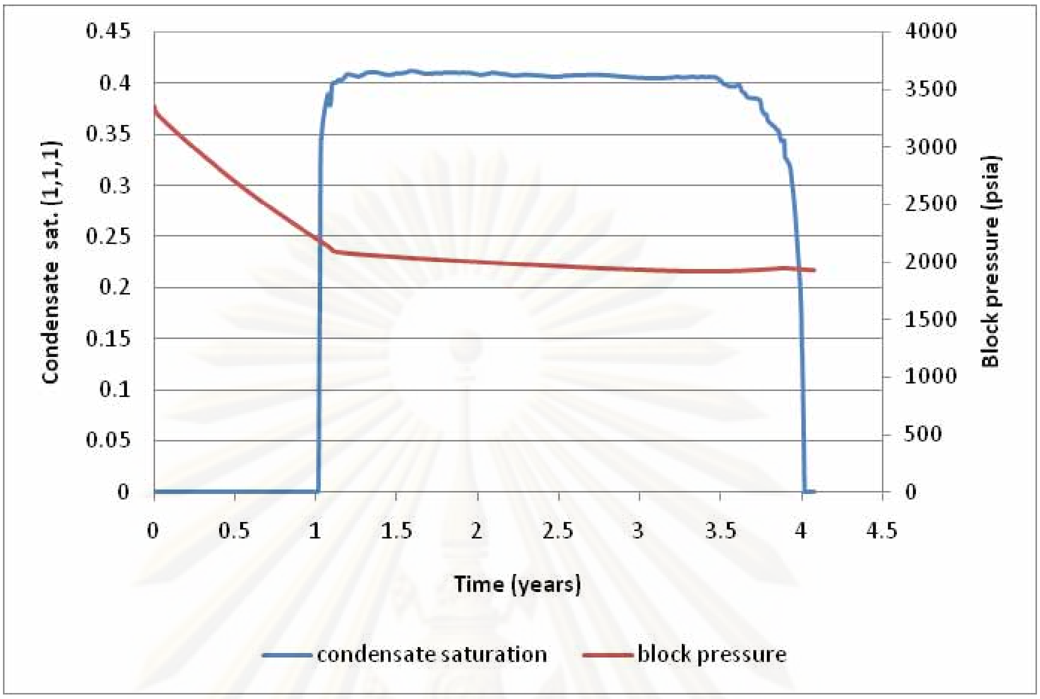

Figure 5.29: Condensate saturation and pressure of block (1, 1, 1) for case 10.

The condensate saturation and block pressure at initial conditions, before liquid dropout is completely revaporized, and after liquid dropout is completely revaporized for cases 1, 3, 9 and 10 is shown in Table 5.15. Initially, the well block pressure is higher than the dew point pressure in all cases. After the producer is put on production, the block pressure declines until it is below the dew point pressure, giving rise to liquid dropout in the block. The condensate saturation in the block increases from 0 to 0.2-0.3. CO_2 injection at the dew point pressure can revaporize the liquid dropout, so the condensate saturation in the block can be decreased to 0.

Table 5.15: Condensate saturation and block pressure at initial conditions, before liquid dropout is completely revaporized, and after liquid dropout is completely revaporized for case 1, 3, 9 and 10.

Case		**Initial conditions**	**Before liquid dropout is completely revaporized**	**After liquid dropout is completely revaporized**
1	**Condensate saturation**	0	0.33	0
	Block pressure (psia)	3350.08	1921.23	1911.88
	Dew point pressure (psia)	2020	2000	1900
3	**Condensate saturation**	0	0.22	0
	Block pressure (psia)	3347.62	1331.29	1314.02
	Dew point pressure (psia)	1680	Not applicable^1	Not applicable^2
9	**Condensate saturation**	0	0.33	0
	Block pressure (psia)	3350.92	1863.35	1851.86
	Dew point pressure (psia)	2010	Not applicable^1	1800
10	**Condensate saturation**	0	0.36	0
	Block pressure (psia)	3347.89	1934.17	1927.03
	Dew point pressure (psia)	2180	Not applicable^1	1900

Not applicable^1 refer the pressure and temperature of the well block falls at the left side of the critical point and inside the phase envelope (two phases).
Not applicable^2 refer the pressure and temperature of the well block falls at the left side of the critical point and outside the phase envelope (one phase).

The mole fraction before and after liquid dropout around wellbore is completely revaporized for case 1, 3, 9, and 10 are shown in Table 5.16 to Table 5.19, respectively. For case 1, the mole fraction of C_1 to C_3 before liquid dropout is completely revaporized decreases while mole fraction of other components increases when compared to the mole fractions at initial conditions. For case 3 and 9, the mole fraction of C_1 to C_3 and N_2 before liquid dropout is completely revaporized decreases while mole fraction of other components increases when compared to the mole fractions at initial conditions. For case 10, the mole fraction of C_1 to i-C_4 and N_2 before liquid dropout is completely revaporized decreases while mole fraction of other components increases when compared to the mole fractions at initial conditions.

Table 5.16: Mole fraction of component at initial conditions, before liquid dropout is completely revaporized, and after liquid dropout is completely revaporized for case 1.

Component	**Fraction of component**		
	Initial conditions	**Before liquid dropout is completely revaporized**	**After liquid dropout is completely revaporized**
C_1	0.5999	0.5110	0.5459
C_2	0.0843	0.0779	0.0766
C_3	0.0640	0.0629	0.0581
i-C_4	0.0341	0.0354	0.0310
n-C_4	0.0390	0.0413	0.0354
i-C_5	0.0143	0.0160	0.0129
n-C_5	0.0140	0.0159	0.0127
C_6	0.0727	0.0884	0.0658
C_7	0.0654	0.0855	0.0590
CO_2	0.0123	0.0659	0.1027

Table 5.17: Mole fraction of component at initial conditions, before liquid dropout is completely revaporized, and after liquid dropout is completely revaporized for case 3.

Component	**Fraction of component**		
	Initial conditions	**Before liquid dropout is completely revaporized**	**After liquid dropout is completely revaporized**
C_1	0.7426	0.5034	0.6549
C_2	0.0818	0.0670	0.0718
C_3	0.0395	0.0393	0.0345
$i\text{-}C_4$	0.0104	0.0126	0.0090
$n\text{-}C_4$	0.0158	0.0206	0.0137
$i\text{-}C_5$	0.0074	0.0121	0.0063
$n\text{-}C_5$	0.0087	0.0153	0.0074
C_6	0.0098	0.0236	0.0082
C_7	0.0656	0.2247	0.0528
CO_2	0.0040	0.0723	0.1286
N_2	0.0144	0.0091	0.0127

Table 5.18: Mole fraction of component at initial conditions, before liquid dropout is completely revaporized, and after liquid dropout is completely revaporized for case 9.

Component	**Fraction of component**		
	Initial conditions	**Before liquid dropout is completely revaporized**	**After liquid dropout is completely revaporized**
C_1	0.6072	0.4916	0.5265
C_2	0.0810	0.0722	0.0702
C_3	0.0637	0.0613	0.0552
$i\text{-}C_4$	0.0398	0.0409	0.0345
$n\text{-}C_4$	0.0445	0.0469	0.0386
$i\text{-}C_5$	0.0291	0.0328	0.0252
$n\text{-}C_5$	0.0252	0.0289	0.0218
C_6	0.0179	0.0224	0.0155
C_7	0.0885	0.1213	0.0767
CO_2	0.0018	0.0807	0.1346
N_2	0.0013	0.0010	0.0011

Table 5.19: Mole fraction of component at initial conditions, before liquid dropout is completely revaporized, and after liquid dropout is completely revaporized for case 10.

Component	**Fraction of component**		
	Initial conditions	**Before liquid dropout is completely revaporized**	**After liquid dropout is completely revaporized**
C_1	0.6372	0.4866	0.5125
C_2	0.0575	0.0486	0.0462
C_3	0.0437	0.0399	0.0351
i-C_4	0.0498	0.0486	0.0400
n-C_4	0.0315	0.0315	0.0253
i-C_5	0.0341	0.0365	0.0274
n-C_5	0.0302	0.0329	0.0242
C_6	0.0109	0.0129	0.0087
C_7	0.1040	0.1345	0.0834
CO_2	0.0008	0.1278	0.1969
N_2	0.0003	0.0002	0.0002

These mole fractions are used to update phase diagram. The phase diagram before and after liquid dropout around wellbore is completely revaporized for case 1, 3, 9, and 10 are shown in Figure 5.30 to Figure 5.33, respectively. The block pressure and temperature before liquid dropout is completely revaporized falls inside the phase envelope. So, the liquid will dropout around the wellbore (Figure 5.30a, Figure 5.31a, Figure 5.32a, and Figure 5.33a). The increasing of CO_2 concentration in the reservoir fluid can shift the phase envelope to the left and decrease the dew point pressure. At some point in time, the dew point pressure will be lower than the block pressure. Since the well block has the lowest pressure and this lowest pressure is higher than the dew point pressure, the entire reservoir is free of liquid (falls outside the phase envelope) (Figure 5.30b, Figure 5.31b, Figure 5.32b, and Figure 5.33b).

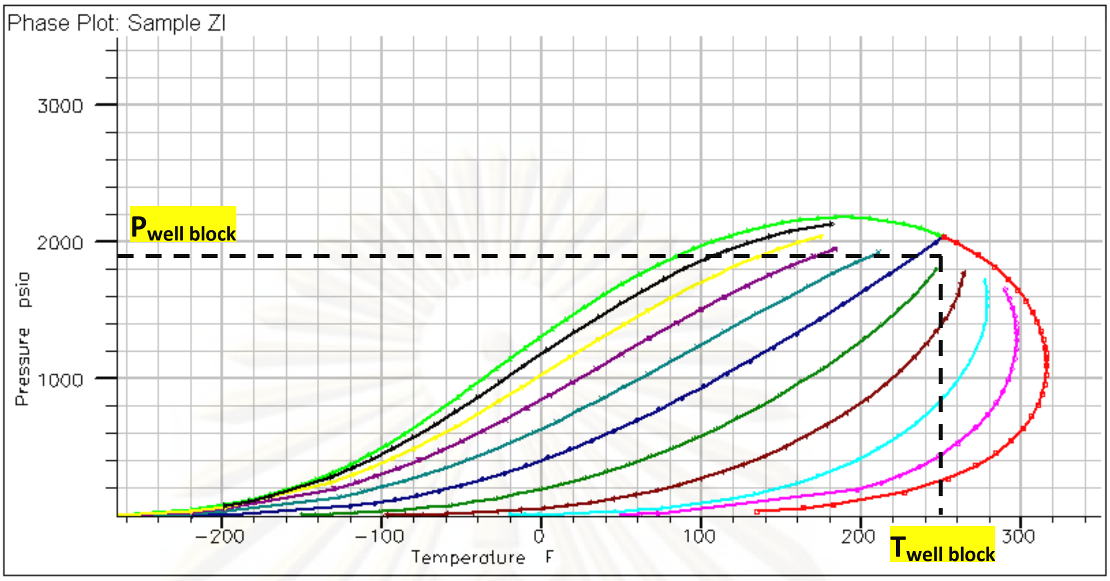

(a) Phase diagram before liquid dropout is completely revaporized.

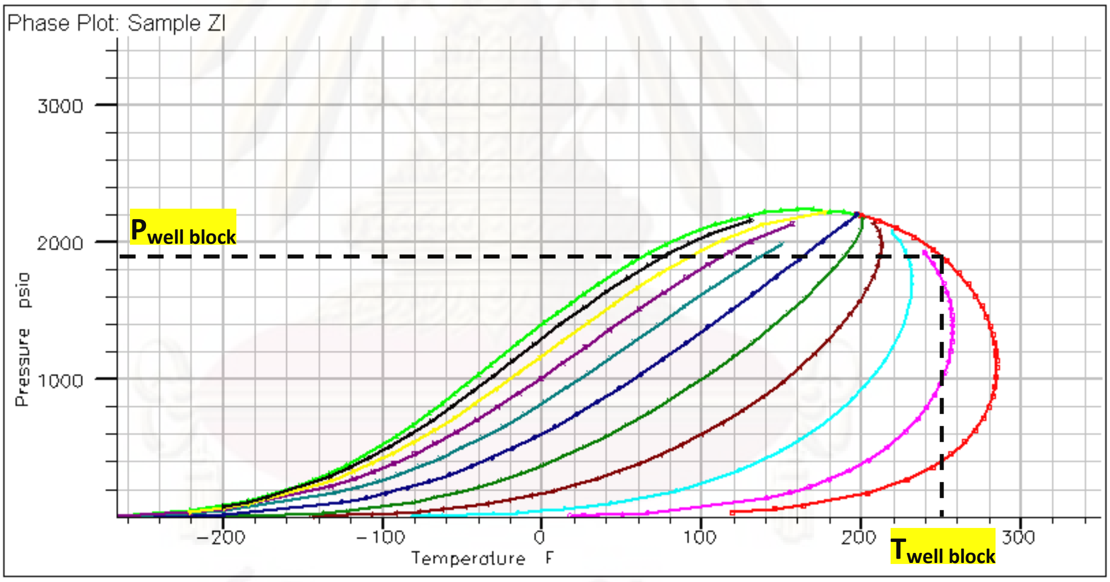

(b) Phase diagram after liquid dropout is completely revaporized.

Figure 5.30: Phase diagram of fluid at the well block before and after liquid dropout is completely revaporized for case 1.

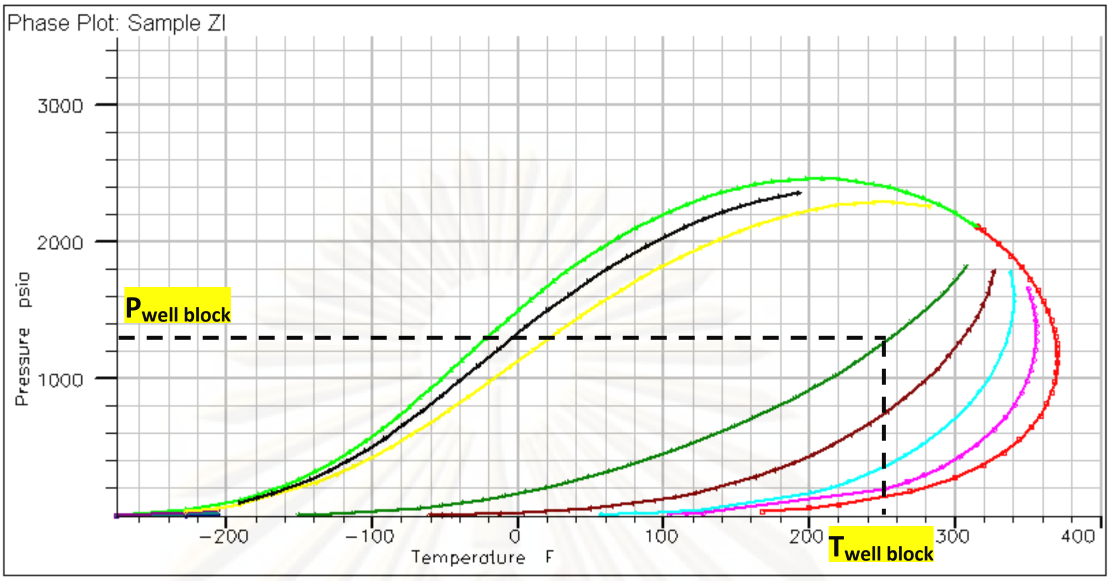

(a) Phase diagram before liquid dropout is completely revaporized.

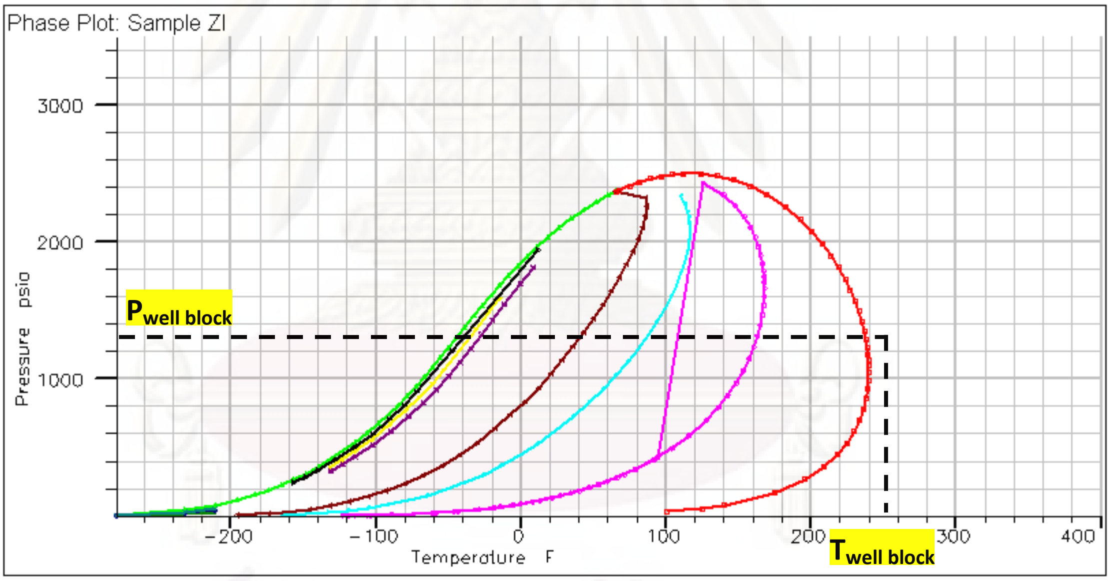

(b) Phase diagram after liquid dropout is completely revaporized.

Figure 5.31: Phase diagram of fluid at the well block before and after liquid dropout is completely revaporized for case 3.

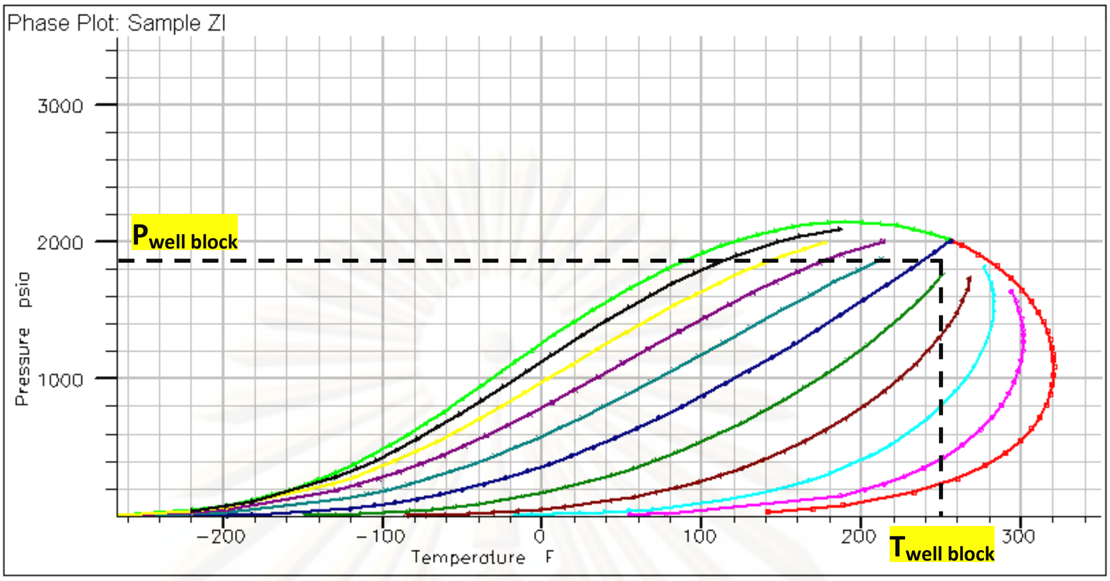

(a) Phase diagram before liquid dropout is completely revaporized.

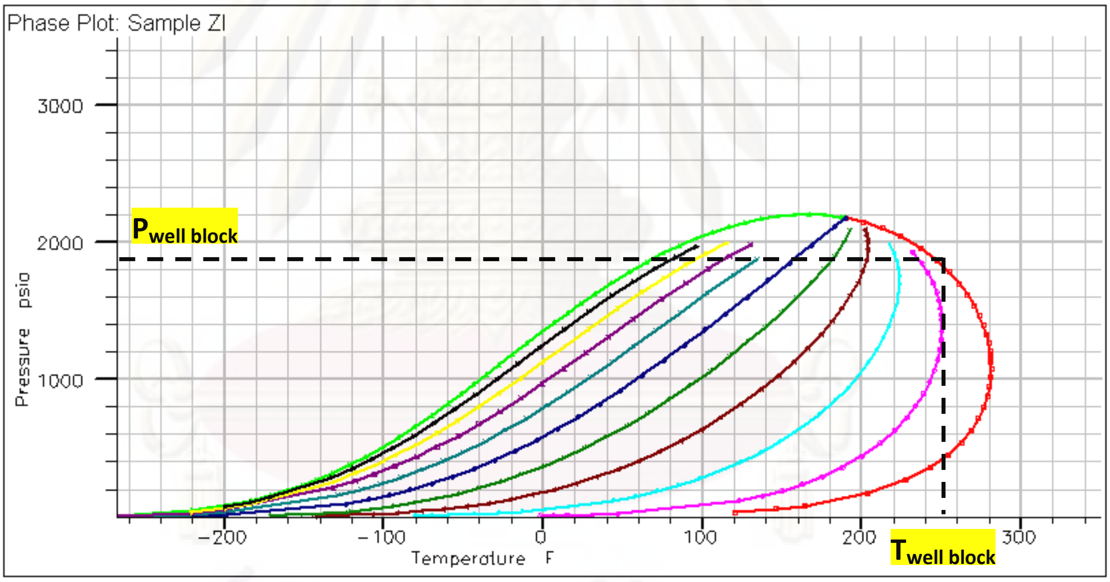

(b) Phase diagram after liquid dropout is completely revaporized.

Figure 5.32: Phase diagram of fluid at the well block before and after liquid dropout is completely revaporized for case 9.

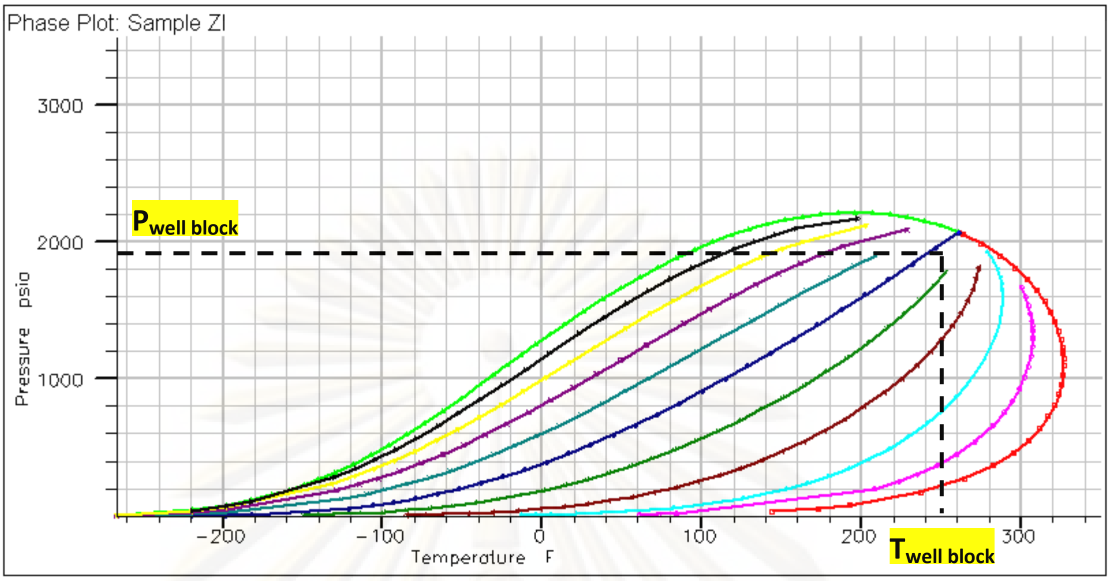

(a) Phase diagram before liquid dropout is completely revaporized.

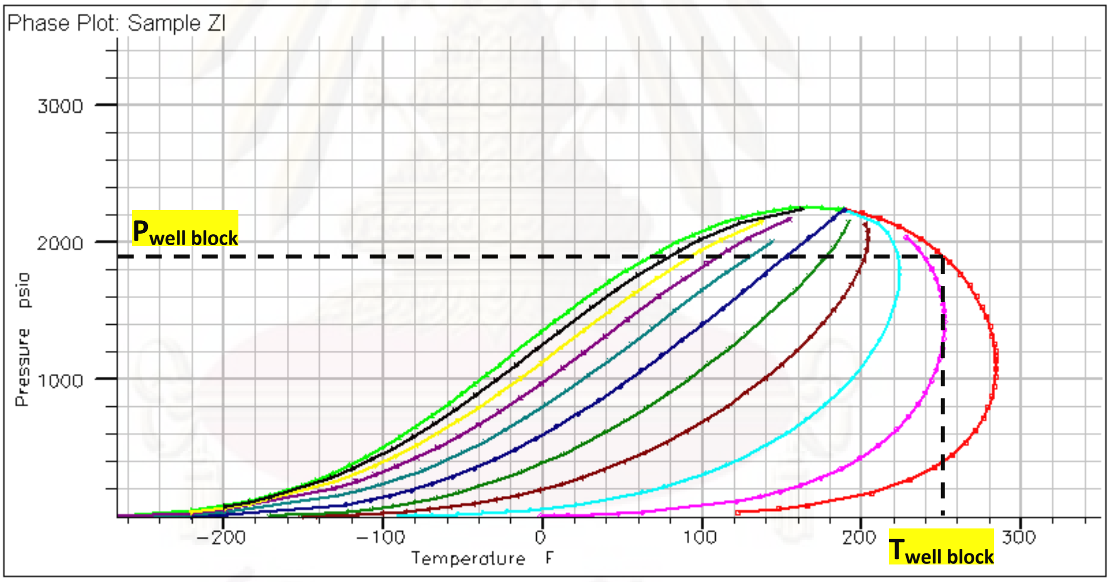

(b) Phase diagram after liquid dropout is completely revaporized.

Figure 5.33: Phase diagram of fluid at the well block before and after liquid dropout is completely revaporized for case 10.

For injecting CO_2 at 200 psia above the dew point pressure, cases 2 and 4 can obtain maximum condensate recovery, and CO_2 can be completely revaporized. The condensate saturation and pressure of block (1, 1, 1) which is the well block for cases 2 and 4 are shown in Figure 5.34 and Figure 5.35, respectively. We can see from the condensate saturation plot with time that when liquid dropout around the wellbore is revaporized. Condensate saturation decreases from 0.2 – 0.3 to 0 very quick while the pressure in this block slightly changes.

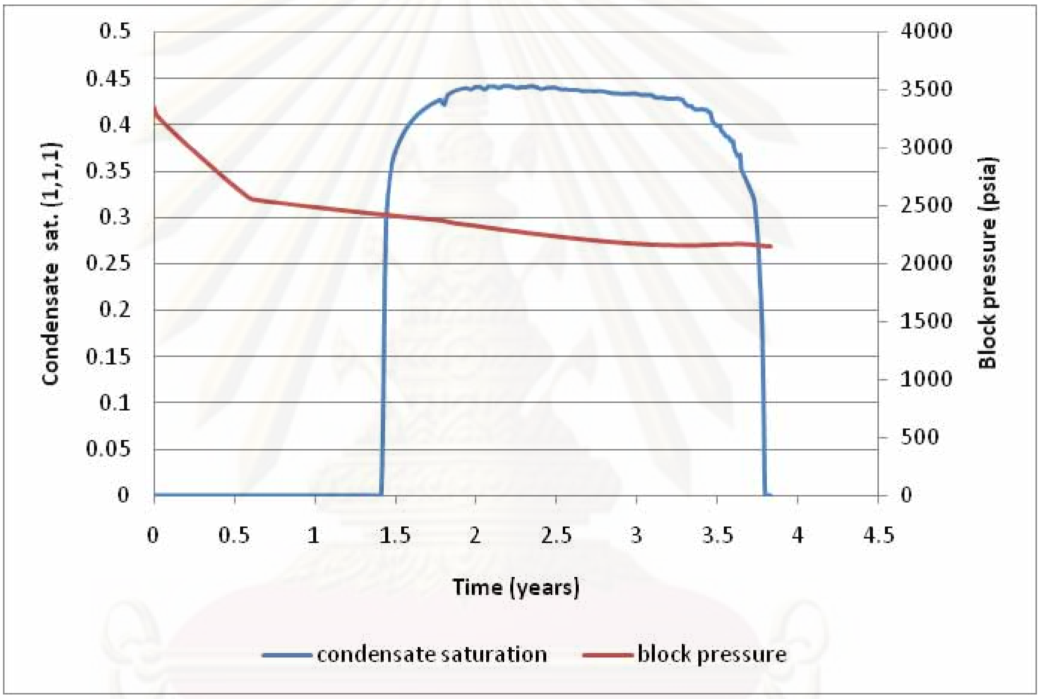

Figure 5.34: Condensate saturation and pressure of block (1, 1, 1) for case 2.

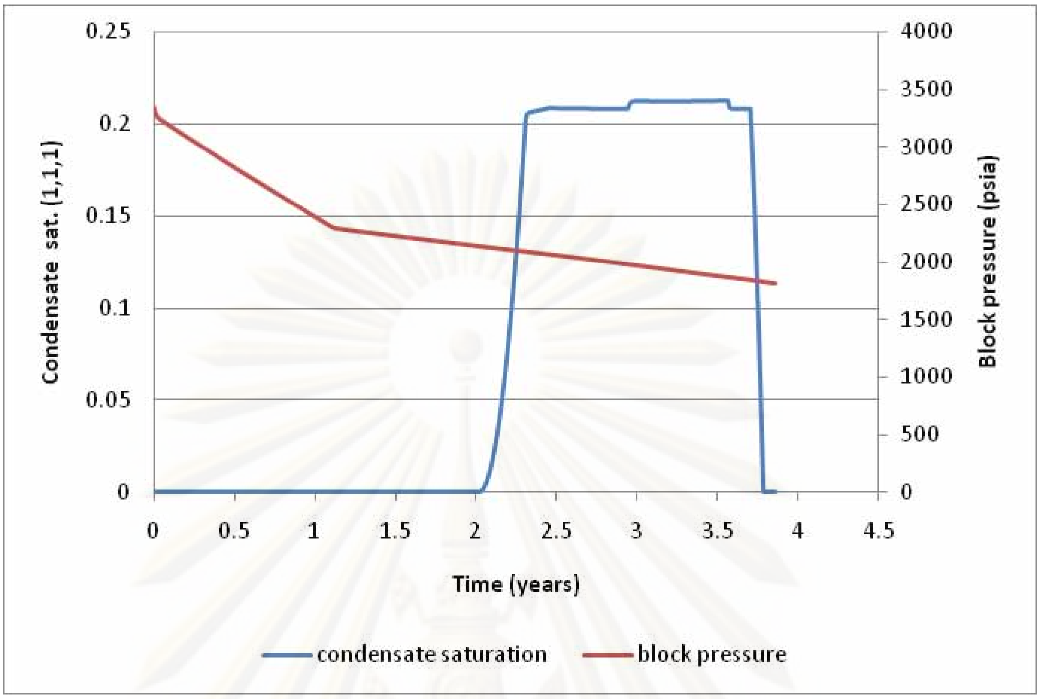

Figure 5.35: Condensate saturation and pressure of block (1, 1, 1) for case 4.

The condensate saturation and block pressure at initial conditions, before liquid dropout is completely revaporized, and after liquid dropout is completely revaporized for cases 2 and 4 is shown in Table 5.20. Initially, the well block pressure is higher than the dew point pressure in all cases. After the producer is put on production, the block pressure declines until it is below the dew point pressure, giving rise to liquid dropout in the block. The condensate saturation in the block increases from 0 to 0.2-0.4. CO_2 injection at 200 psia above the dew point pressure can revaporize the liquid dropout, so the condensate saturation in the block can be decreased to 0.

Table 5.20: Condensate saturation and block pressure at initial conditions, before liquid dropout is completely revaporized, and after liquid dropout is completely revaporized for case 2 and 4.

Case		**Initial conditions**	**Before liquid dropout is completely revaporized**	**After liquid dropout is completely revaporized**
2	**Condensate saturation**	0	0.42	0
	Block pressure (psia)	3341.99	2163.53	2156.56
	Dew point pressure (psia)	2440	Not applicable[1]	2100
4	**Condensate saturation**	0	0.21	0
	Block pressure (psia)	3340.76	1851.17	1824.32
	Dew point pressure (psia)	2150	Not applicable[1]	1500

Not applicable[1] refer the pressure and temperature of the well block falls at the left side of the critical point and inside the phase envelope (two phases).
Not applicable[2] refer the pressure and temperature of the well block falls at the left side of the critical point and outside the phase envelope (one phase).

The mole fraction before and after liquid dropout around wellbore is completely revaporized for case 2 and 4 are shown in Table 5.21 and Table 5.22, respectively. For case 2 and 4, the mole fraction of C_1 to C_3 and N_2 before liquid dropout is completely revaporized decreases while mole fraction of other components increases when compared to the mole fractions at initial conditions.

Table 5.21: Mole fraction of component at initial conditions, before liquid dropout is completely revaporized, and after liquid dropout is completely revaporized for case 2.

Component	**Fraction of component**		
	Initial conditions	**Before liquid dropout is completely revaporized**	**After liquid dropout is completely revaporized**
C_1	0.6481	0.5354	0.5246
C_2	0.0527	0.0475	0.0426
C_3	0.0623	0.0599	0.0502
i-C_4	0.0167	0.0169	0.0134
n-C_4	0.0309	0.0320	0.0249
i-C_5	0.0137	0.0149	0.0110
n-C_5	0.0131	0.0145	0.0105
C_6	0.0159	0.0187	0.0127
C_7	0.1339	0.1673	0.1070
CO_2	0.0106	0.0913	0.2014
N_2	0.0021	0.0017	0.0017

Table 5.22: Mole fraction of component at initial conditions, before liquid dropout is completely revaporized, and after liquid dropout is completely revaporized for case 4.

Component	**Fraction of component**		
	Initial conditions	**Before liquid dropout is completely revaporized**	**After liquid dropout is completely revaporized**
C_1	0.8358	0.6018	0.7008
C_2	0.0595	0.0500	0.0498
C_3	0.0291	0.0285	0.0243
i-C_4	0.0045	0.0052	0.0038
n-C_4	0.0111	0.0137	0.0092
i-C_5	0.0036	0.0054	0.0030
n-C_5	0.0048	0.0076	0.0040
C_6	0.0060	0.0124	0.0049
C_7	0.0080	0.0224	0.0065
C_8	0.0076	0.0297	0.0061
C_9	0.0047	0.0259	0.0037
C_{10}	0.0103	0.0802	0.0078
CO_2	0.0065	0.1116	0.1688
N_2	0.0085	0.0058	0.0071

These mole fractions are used to update phase diagram. The phase diagram before and after liquid dropout around wellbore is completely revaporized for case 2 and case 4 are shown in Figure 5.36 and Figure 5.37, respectively. The block pressure and temperature before liquid dropout is completely revaporized falls inside the phase envelope. So, the liquid will dropout around the wellbore (Figure 5.36a and Figure 5.37a). The increasing of CO_2 concentration in the reservoir fluid can shift the phase envelope to the left and decrease the dew point pressure. At some point in time, the dew point pressure will be lower than the block pressure. Since the well block has the lowest pressure and this lowest pressure is higher than the dew point pressure, the entire reservoir is free of liquid (falls outside the phase envelope) (Figure 5.36b and Figure 5.37b).

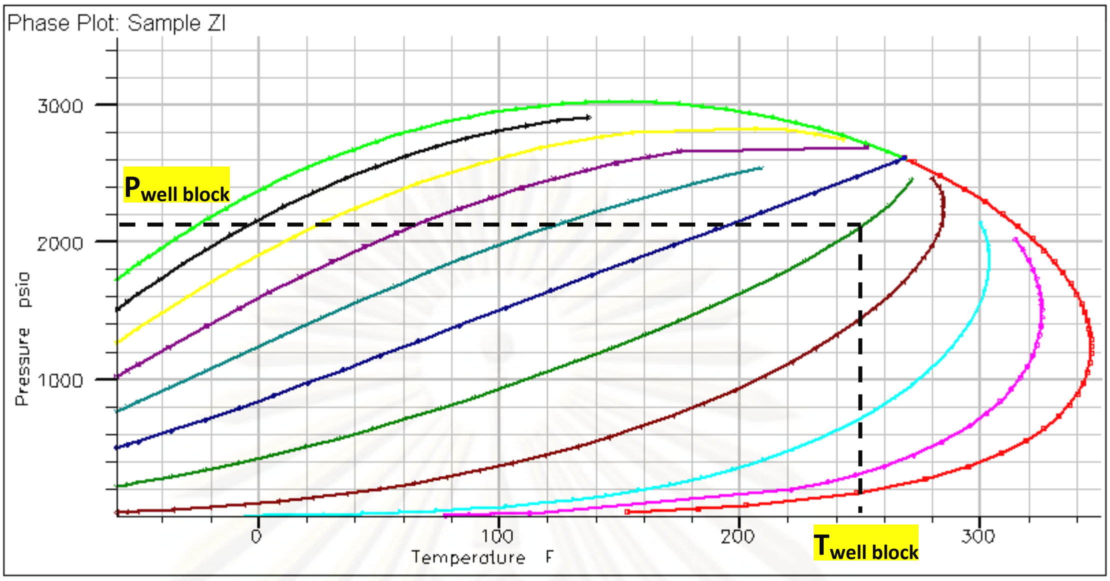

(a) Phase diagram before liquid dropout is completely revaporized.

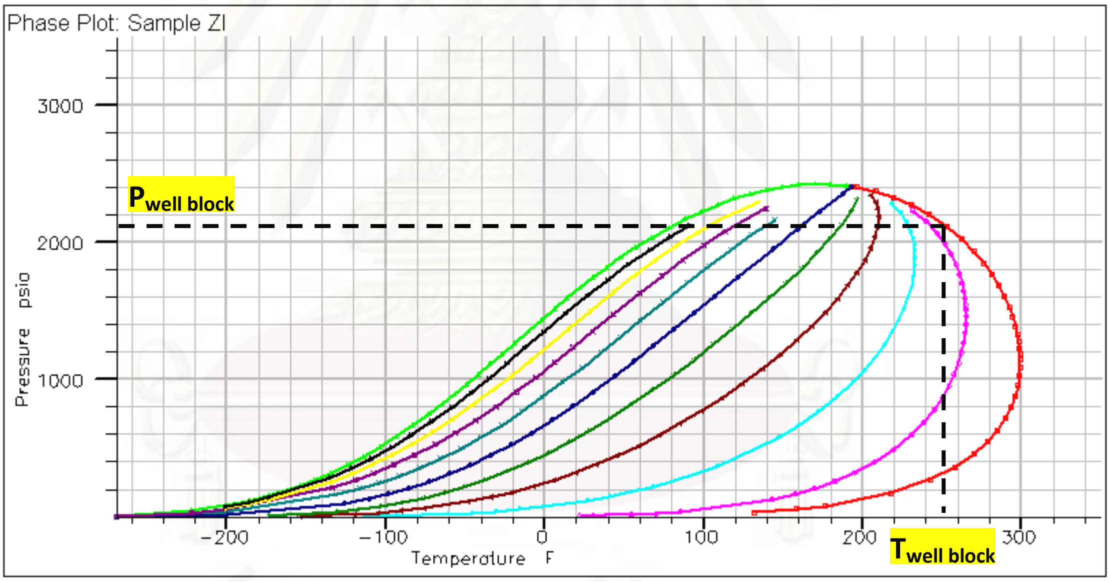

(b) Phase diagram after liquid dropout is completely revaporized.

Figure 5.36: Phase diagram of fluid at the well block before and after liquid dropout is completely revaporized for case 2.

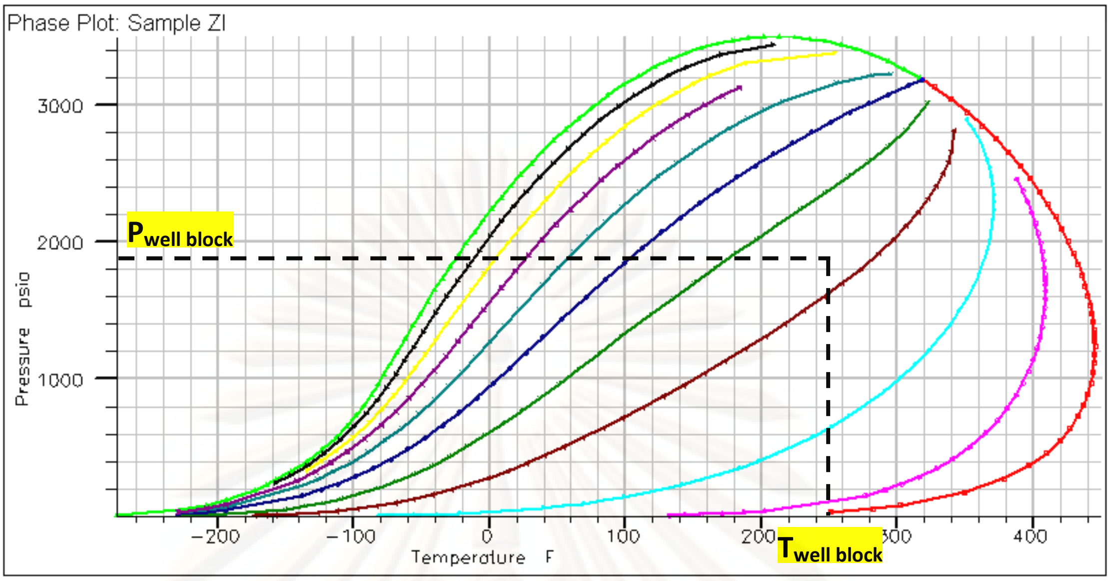

(a) Phase diagram before liquid dropout is completely revaporized.

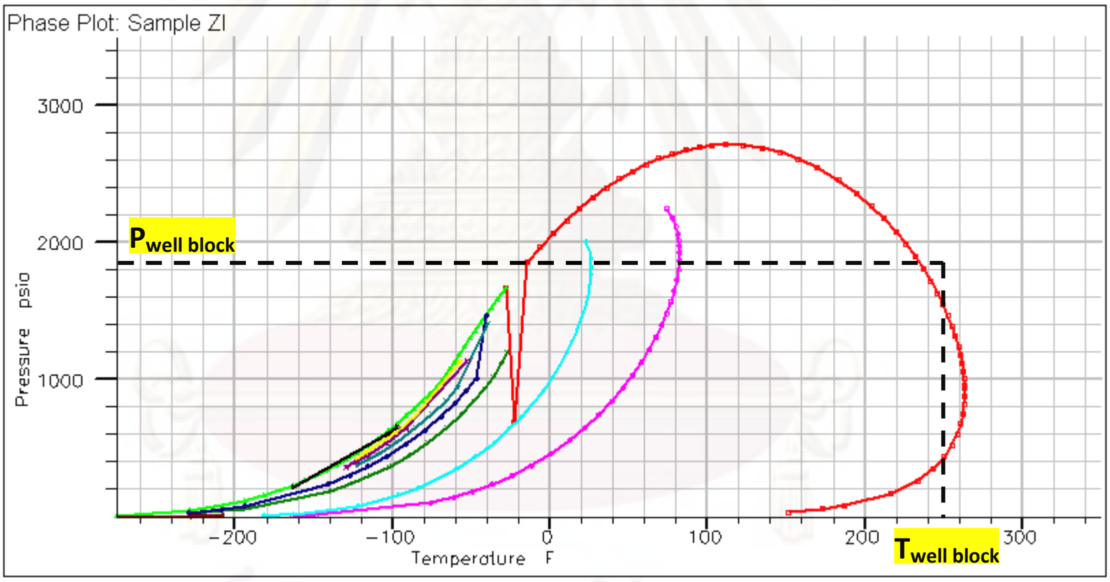

(b) Phase diagram after liquid dropout is completely revaporized.

Figure 5.37: Phase diagram of fluid at the well block before and after liquid dropout is completely revaporized for case 4.

For injecting CO_2 at 300 psia above the dew point pressure, cases 5 and 7 can obtain maximum condensate recovery, and CO_2 can be completely revaporized. The condensate saturation and pressure of block (1, 1, 1) which is the well block for cases 5 and 7 are shown in Figure 5.38 and Figure 5.39, respectively. In case 5, we can see from the condensate saturation plot with time that when liquid dropout around the wellbore is revaporized, condensate saturation decreases from 0.2 – 0.3 to 0 very quick while the pressure in this block slightly changes. In case 7, starting CO_2 injection at 300 psia above the dew point pressure has maximum condensate recovery but the liquid dropout cannot be completely revaporized as shown in Figure 5.39. Therefore, another simulation run was performed to investigate the effect of injecting at a higher pressure, specifically, 400 psia above the dew point pressure. The condensate saturation and pressure of block (1, 1, 1) when injecting at 400 psia above the dew point pressure is shown in Figure 5.40. When start CO_2 injection at 400 psia above the dew point pressure, the condensate saturation decrease from around 0.29 to 0 while the block pressure slightly changes. So, the liquid dropout around the wellbore can be completely revaporized.

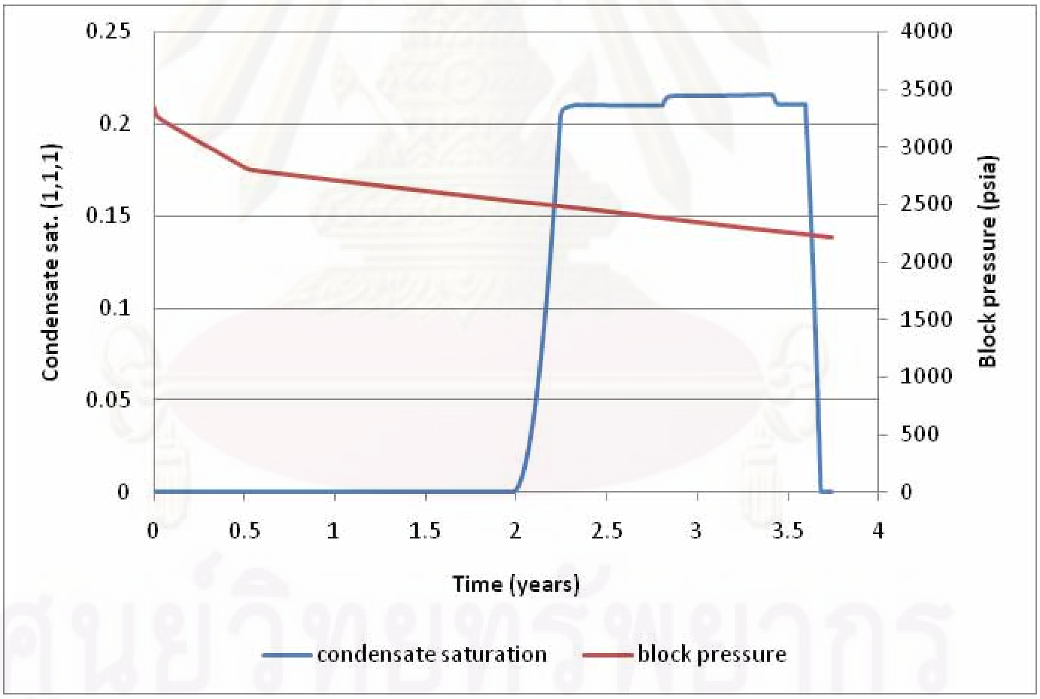

Figure 5.38: Condensate saturation and pressure of block (1, 1, 1) for case 5.

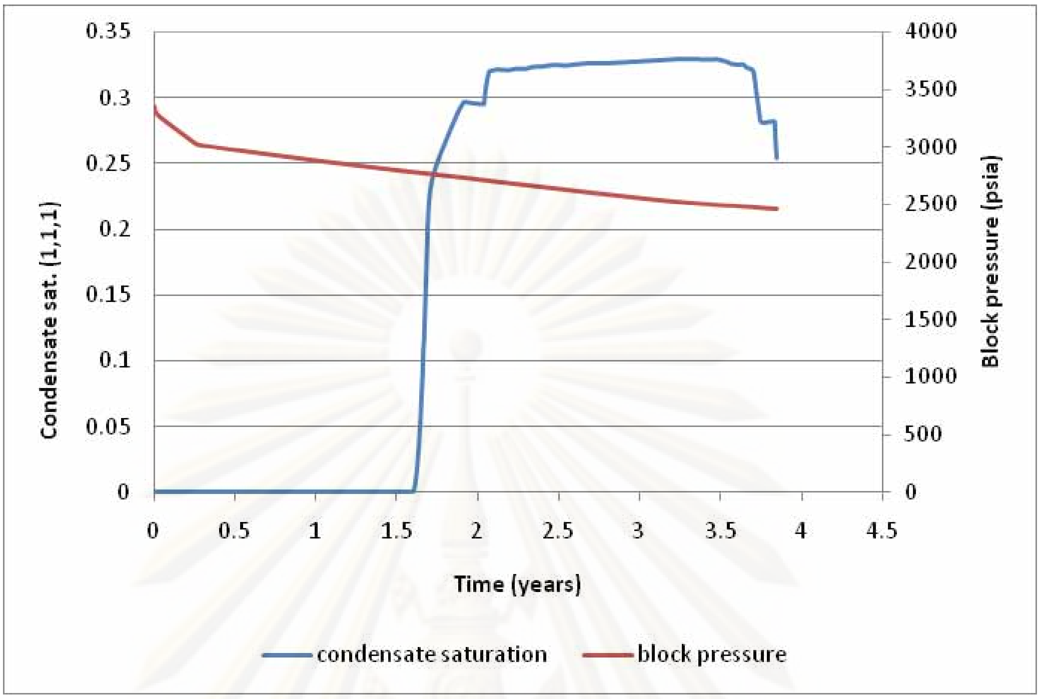

Figure 5.39: Condensate saturation and pressure of block (1, 1, 1) for case 7.

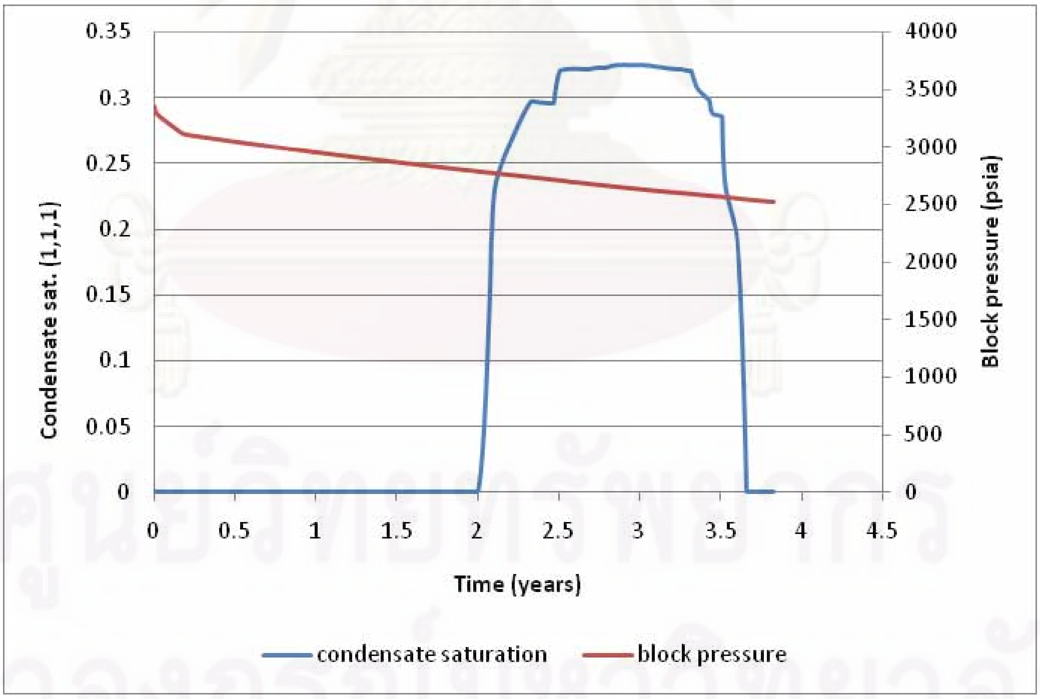

Figure 5.40: Condensate saturation and pressure of block (1, 1, 1) when injecting at 400 psia above the dew point pressure for case 7.

The condensate saturation and block pressure at initial conditions, before liquid dropout is completely revaporized, and after liquid dropout is completely revaporized for cases 5 and 7 is shown in Table 5.23. Initially, the well block pressure is higher than the dew point pressure in all cases. After the producer is put on production, the block pressure declines until it is below the dew point pressure, giving rise to liquid dropout in the block. The condensate saturation in the block increases from 0 to 0.2-0.3. CO_2 injection at 300 psia above the dew point pressure can revaporize the liquid dropout, so the condensate saturation in the block can be decreased to 0.

Table 5.23: Condensate saturation and block pressure at initial conditions, before liquid dropout is completely revaporized, and after liquid dropout is completely revaporized for case 5 and 7.

Case		**Initial conditions**	**Before liquid dropout is completely revaporized**	**After liquid dropout is completely revaporized**
5	**Condensate saturation**	0	0.21	0
	Block pressure (psia)	3342.00	2354.85	2312.16
	Dew point pressure (psia)	2550	Not applicable[1]	2000
7	**Condensate saturation**	0	0.29	0
	Block pressure (psia)	3348.95	2573.37	2542.56
	Dew point pressure (psia)	2800	Not applicable[1]	2500

Not applicable[1] refer the pressure and temperature of the well block falls at the left side of the critical point and inside the phase envelope (two phases).

Not applicable[2] refer the pressure and temperature of the well block falls at the left side of the critical point and outside the phase envelope (one phase).

The mole fraction before and after liquid dropout around wellbore is completely revaporized for case 5 and 7 are shown in Table 5.24 and Table 5.25, respectively. For case 5 and 7, the mole fraction of C_1 to C_3 and N_2 before liquid dropout is completely revaporized decreases while mole fraction of other components increases when compared to the mole fractions at initial conditions.

Table 5.24: Mole fraction of component at initial conditions, before liquid dropout is completely revaporized, and after liquid dropout is completely revaporized for case 5.

Component	**Fraction of component**		
	Initial conditions	**Before liquid dropout is completely revaporized**	**After liquid dropout is completely revaporized**
C_1	0.8320	0.6250	0.6981
C_2	0.0740	0.0634	0.0620
C_3	0.0280	0.0272	0.0234
i-C_4	0.0063	0.0069	0.0053
n-C_4	0.0094	0.0109	0.0078
i-C_5	0.0048	0.0065	0.0040
n-C_5	0.0040	0.0056	0.0033
C_6	0.0064	0.0112	0.0053
C_7	0.0074	0.0164	0.0061
C_8	0.0048	0.0139	0.0039
C_9	0.0036	0.0137	0.0029
C_{10}	0.0026	0.0131	0.0021
C_{11}	0.0099	0.0672	0.0076
CO_2	0.0020	0.1156	0.1642
N_2	0.0048	0.0034	0.0040

Table 5.25: Mole fraction of component at initial conditions, before liquid dropout is completely revaporized, and after liquid dropout is completely revaporized for case 7.

Component	**Fraction of component**		
	Initial conditions	**Before liquid dropout is completely revaporized**	**After liquid dropout is completely revaporized**
C_1	0.7351	0.5948	0.6325
C_2	0.0623	0.0558	0.0534
C_3	0.0301	0.0292	0.0257
i-C_4	0.0289	0.0302	0.0246
n-C_4	0.0365	0.0393	0.0311
i-C_5	0.0240	0.0279	0.0204
n-C_5	0.0111	0.0132	0.0094
C_6	0.0174	0.0228	0.0147
C_7	0.0138	0.0202	0.0116
C_8	0.0097	0.0159	0.0081
C_9	0.0077	0.0142	0.0063
C_{10}	0.0048	0.0099	0.0039
C_{11}	0.0143	0.0336	0.0115
CO_2	0.0021	0.0912	0.1449
N_2	0.0022	0.0017	0.0019

These mole fractions are used to update phase diagram. The phase diagram before and after liquid dropout around wellbore is completely revaporized for case 5 and case 7 are shown in Figure 5.41 and Figure 5.42, respectively. The block pressure and temperature before liquid dropout is completely revaporized falls inside the phase envelope. So, the liquid will dropout around the wellbore (Figure 5.41a and Figure 5.42a). The increasing of CO_2 concentration in the reservoir fluid can shift the phase envelope to the left and decrease the dew point pressure. At some point in time, the dew point pressure will be lower than the block pressure. Since the well block has the lowest pressure and this lowest pressure is higher than the dew point pressure, the entire reservoir is free of liquid (falls outside the phase envelope) (Figure 5.41b and Figure 5.42b).

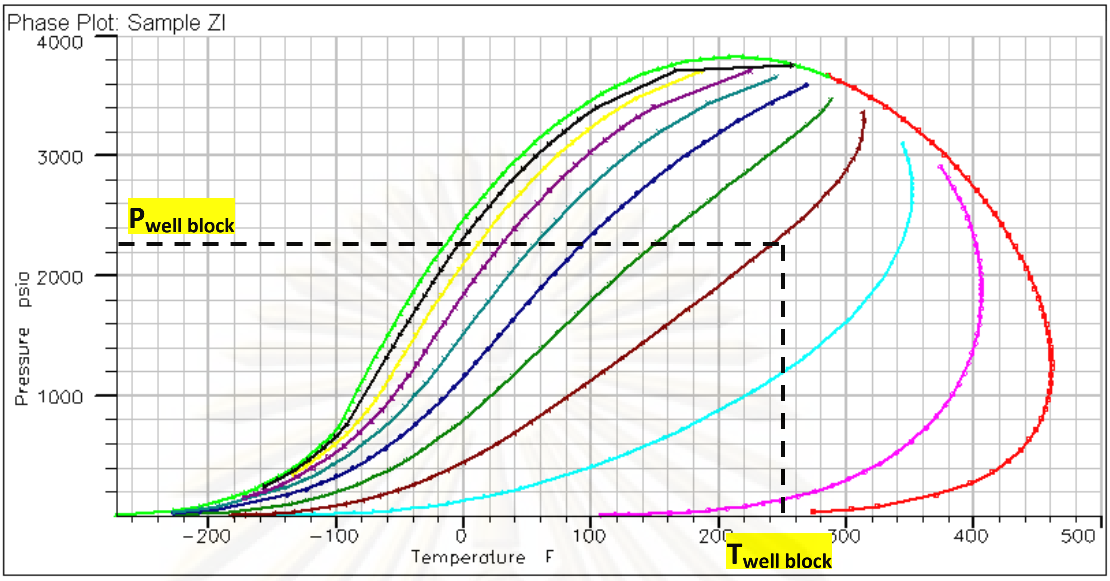

(a) Phase diagram before liquid dropout is completely revaporized.

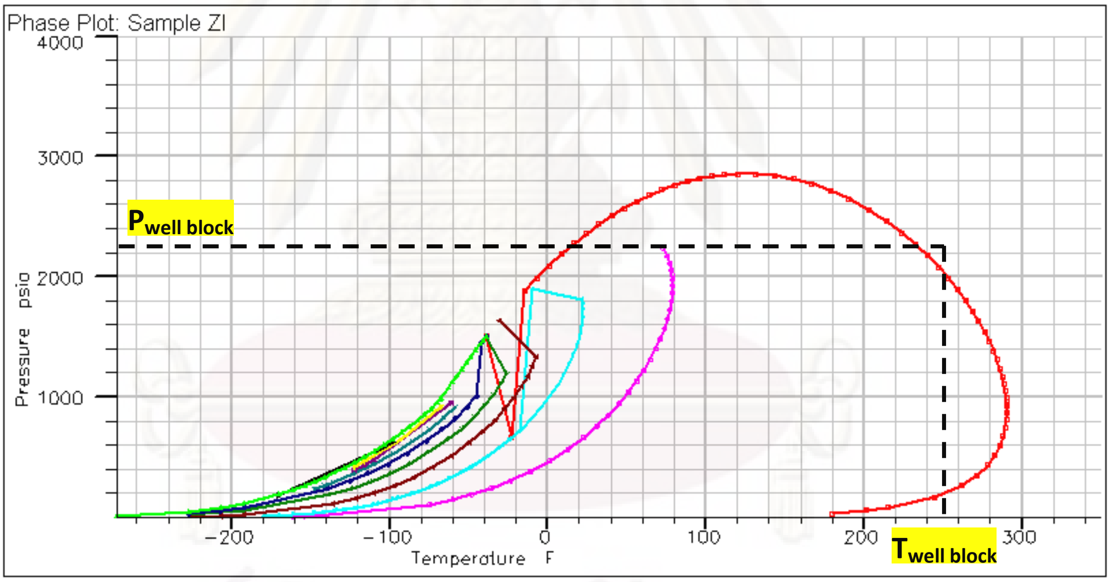

(b) Phase diagram after liquid dropout is completely revaporized.

Figure 5.41: Phase diagram of fluid at the well block before and after liquid dropout is completely revaporized for case 5.

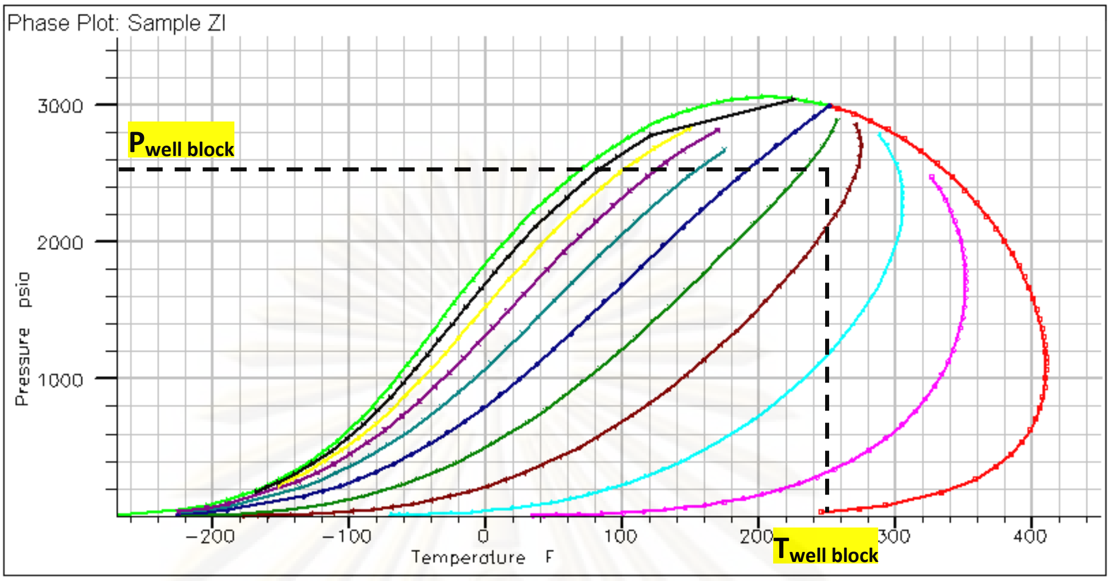

(a) Phase diagram before liquid dropout is completely revaporized.

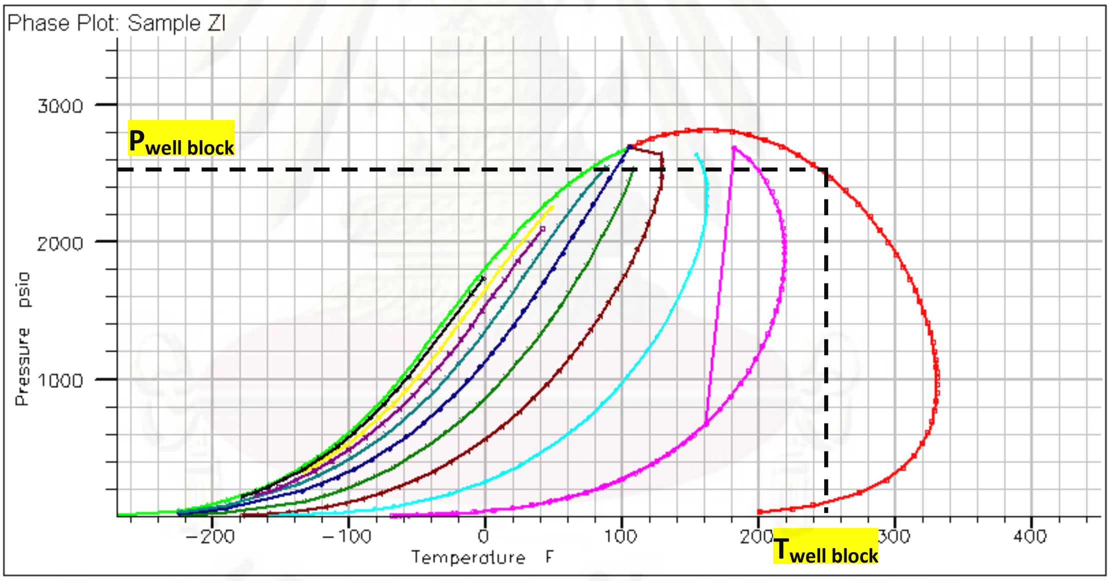

(b) Phase diagram after liquid dropout is completely revaporized.

Figure 5.42: Phase diagram of fluid at the well block before and after liquid dropout is completely revaporized for case 7.

In the first scenario, we can observe that CO_2 injection does effectively enhance condensate recovery. The amount of condensate recovery depends on the time to start CO_2 injection. Starting CO_2 injection too early will cause CO_2 to break through the producer too fast, resulting in reduction in condensate recovery. Starting

CO_2 injection too late will cause liquid to drop around the wellbore and cannot be recovered at surface. By studying different reservoir fluid compositions and times to start CO_2 injection, we found that maximum liquid dropout and dew point pressure has an effect on the best time to start CO_2 injection and the condensate recovery. The best time to start injection is the latest time which the liquid dropout around the wellbore can be completely revaporized. And, when the maximum liquid dropout is very low (around 1%), the condensate in the reservoir will be difficult to be revaporized and require the earlier injection.

5.2 Scenario 2: Initial reservoir pressure is equal to the dew point pressure

In this scenario, the initial reservoir pressure is equal to the dew point pressure which is commonly seen in Gulf of Thailand. The liquid dropout around the wellbore will occur at the beginning of the production. Two types of production and injection scenarios: natural depletion and CO_2 injection at the beginning were simulated. The initial reservoir pressure is shown in Table 5.26.

Table 5.26: Initial reservoir pressure of each case

Case	Initial reservoir pressure (psia)	Case	Initial reservoir pressure (psia)
1	2020	**6**	2990
2	2440	**7**	2800
3	1680	**8**	3500
4	2150	**9**	2010
5	2550	**10**	2180

From Table 5.26, the initial reservoir pressure ranges from 1680 psia to 3500 psia. The lowest initial reservoir pressure is 1680 psia in case 3 and the highest initial reservoir pressure is 3500 psia in case 8.

5.2.1 Production with Natural Depletion

In this scenario, gas condensate reservoirs having different compositions were simulated by natural depletion strategy. The maximum gas production rate is set at 10,000 MSCF/D. And, the economic limit for condensate production rate is 5 STB/D.

The gas production rate and the tubing head pressure (THP) are shown in Figures 5.43 and 5.44, respectively. In all cases, the gas production rate is constant at the beginning. The gas production rate starts to decline when the tubing head pressure reaches its limit at 200 psia. The simulation stops when the gas or condensate production rate reaches the economic limit.

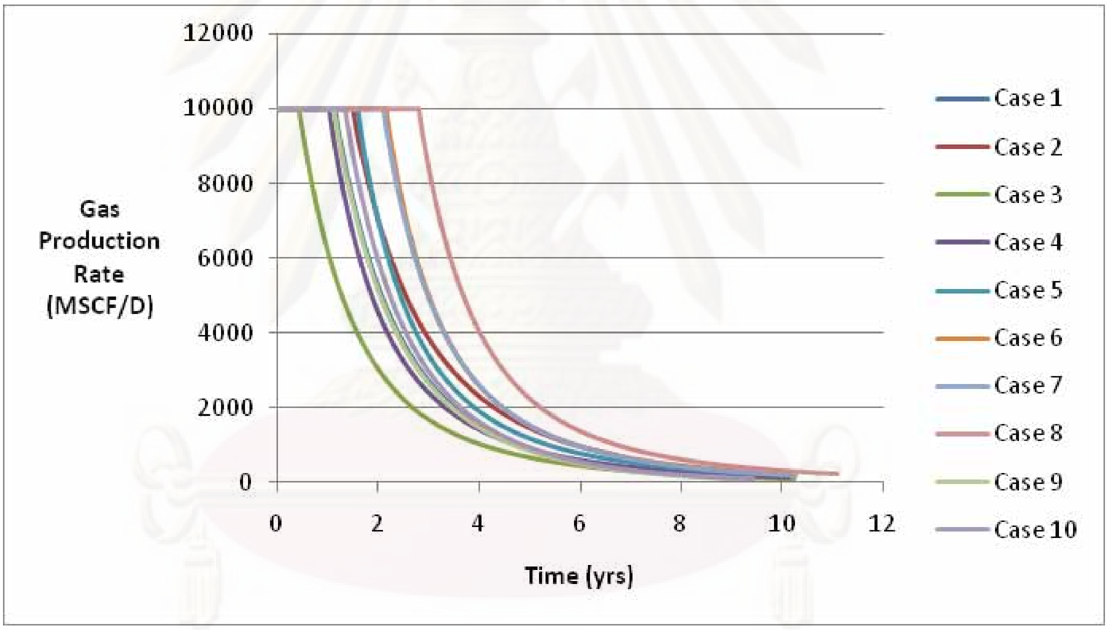

Figure 5.43: Gas production rate for producing with natural depletion with initial reservoir pressure equal to the dew point pressure.

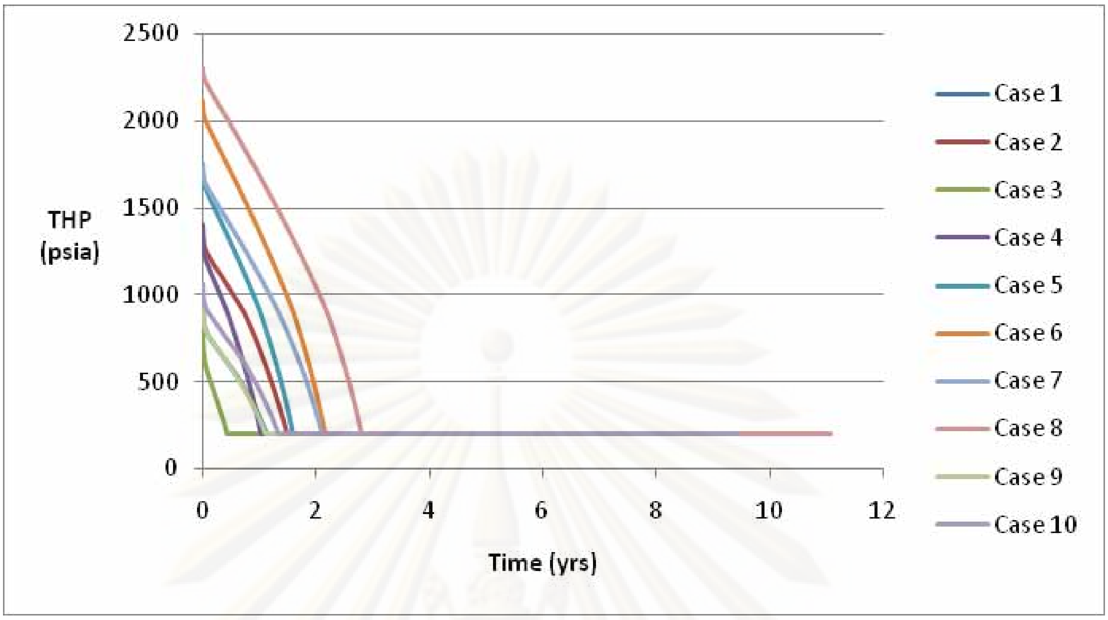

Figure 5.44: Tubing head pressure for producing with natural depletion with initial reservoir pressure equal to the dew point pressure.

The producing time before reaching the tubing head pressure limit, cumulative production of gas, recovery factor, and the production life of natural depletion are summarized in Table 5.27. The producing time before reaching THP limit ranges from 0.43 to 2.80 years. The production life ranges from 6.7 to 11.1 years. Case 3 reaches THP limit faster than the other cases, so the total gas production of this case is the lowest. Case 8 reaches THP limit slower than other cases, so the total gas production of this case is the highest. The gas production rate drops after the THP reaches the THP limit. Therefore, the case that THP reaches the THP limit faster will have less total gas production.

Table 5.27: Producing time before reaching THP limit, cumulative production of gas, recovery factor, and production life for producing with natural depletion with initial reservoir pressure equal to the dew point pressure.

Case	Producing time before reaching THP limit (years)	Total gas production (BCF)	Gas recovery factor (%)	Production life (years)
1	1.13	9.54	76%	9.0
2	1.49	11.30	82%	6.7
3	0.43	6.97	78%	10.3
4	1.03	9.26	85%	10.2
5	1.59	11.30	88%	9.7
6	2.16	13.35	89%	10.2
7	2.11	13.26	88%	10.3
8	2.80	15.92	91%	11.1
9	1.11	9.49	77%	9.1
10	1.34	10.19	78%	9.4

From the simulation results, we can see that the gas recovery factor depend on dew point pressure and maximum liquid dropout. From Table 4.4 we separate the reservoir fluids into two main categories which are moderate-high maximum liquid dropout and low maximum liquid dropout. Cases 1, 2, 7, 8, 9, and 10 are moderate-high maximum liquid dropout case and case 3, 4, 5, and 6 are low maximum liquid dropout case. The gas recovery factor as a function of dew point pressure for moderate-high maximum liquid dropout and low maximum liquid dropout are shown in Figure 5.45 and 5.46, respectively. The gas recovery factor increase when the dew point pressure increase.

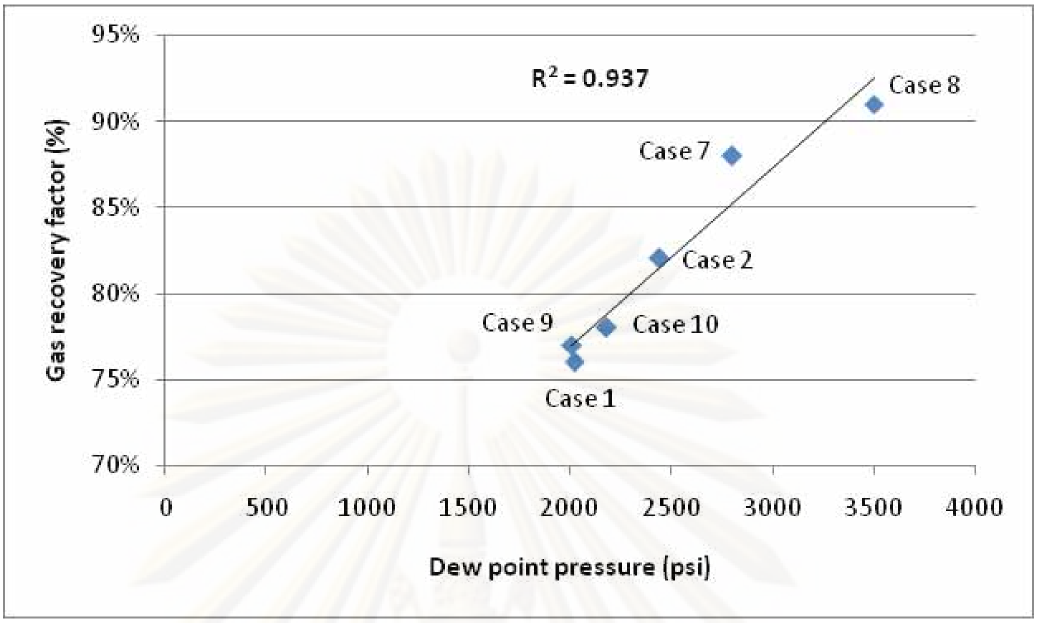

Figure 5.45: Gas recovery factor as a function of dew point pressure for producing with natural depletion with initial reservoir pressure equal to the dew point pressure (moderate-high maximum liquid dropout).

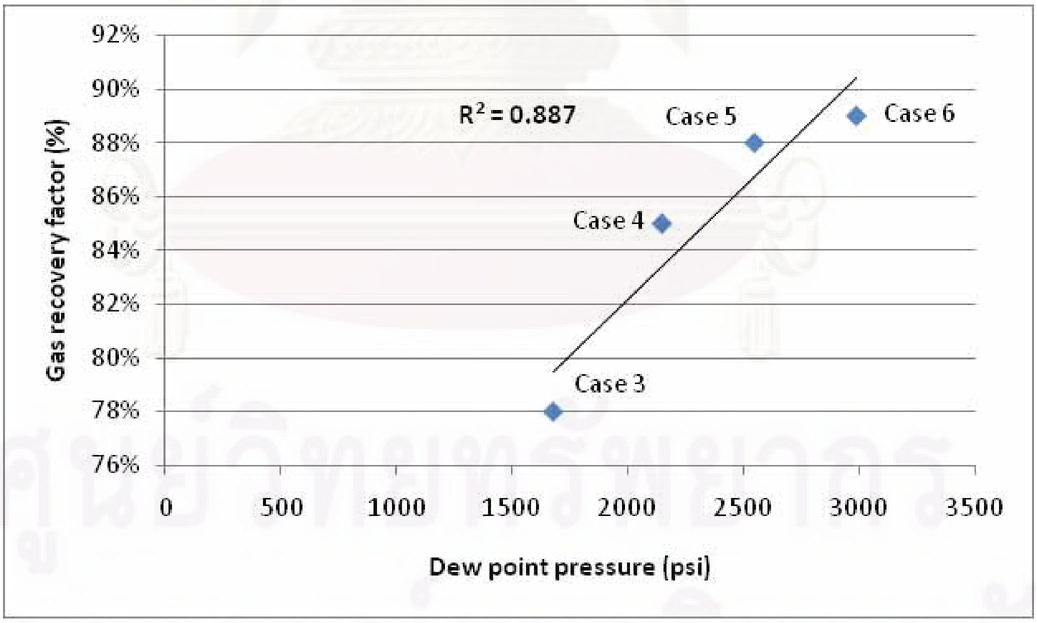

Figure 5.46: Gas recovery factor as a function of dew point pressure for producing with natural depletion with initial reservoir pressure equal to the dew point pressure (low maximum liquid dropout).

The condensate production rate and the bottomhole pressure (BHP) are shown in Figures 5.47 and 5.48, respectively. The condensate production rates for the ten cases are different because the condensate-gas ratios (CGR) are different. The condensate production rates starts to decline at the beginning. In general, the condensate production rate declines because the bottomhole pressure drops below the dew point pressure and liquid starts to condense in the pore space.

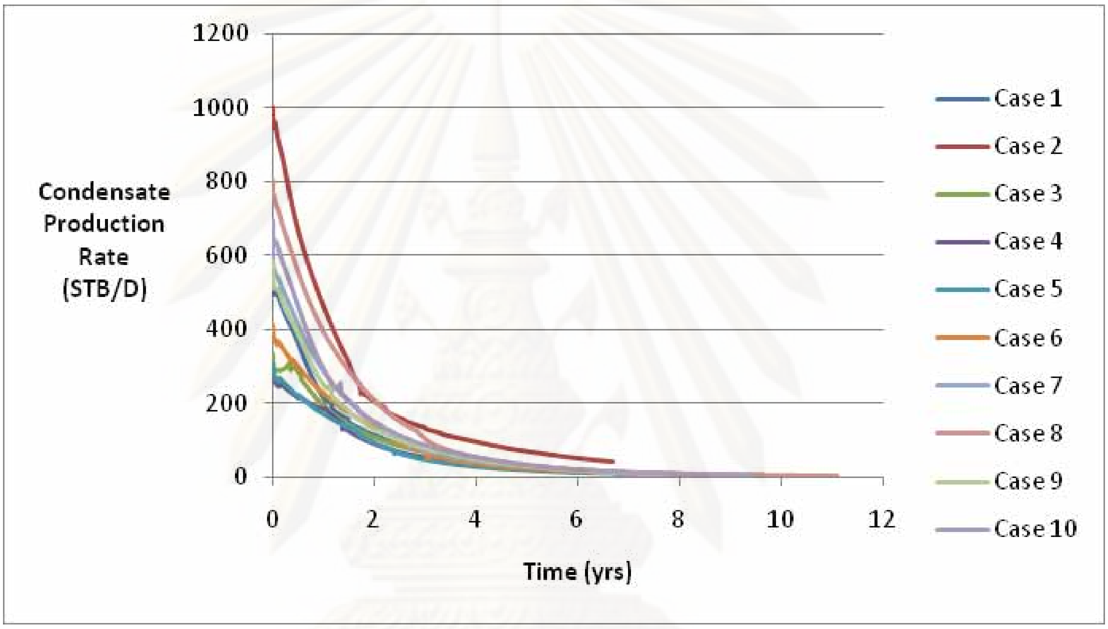

Figure 5.47: Condensate production rate for producing with natural depletion with initial reservoir pressure equal to the dew point pressure.

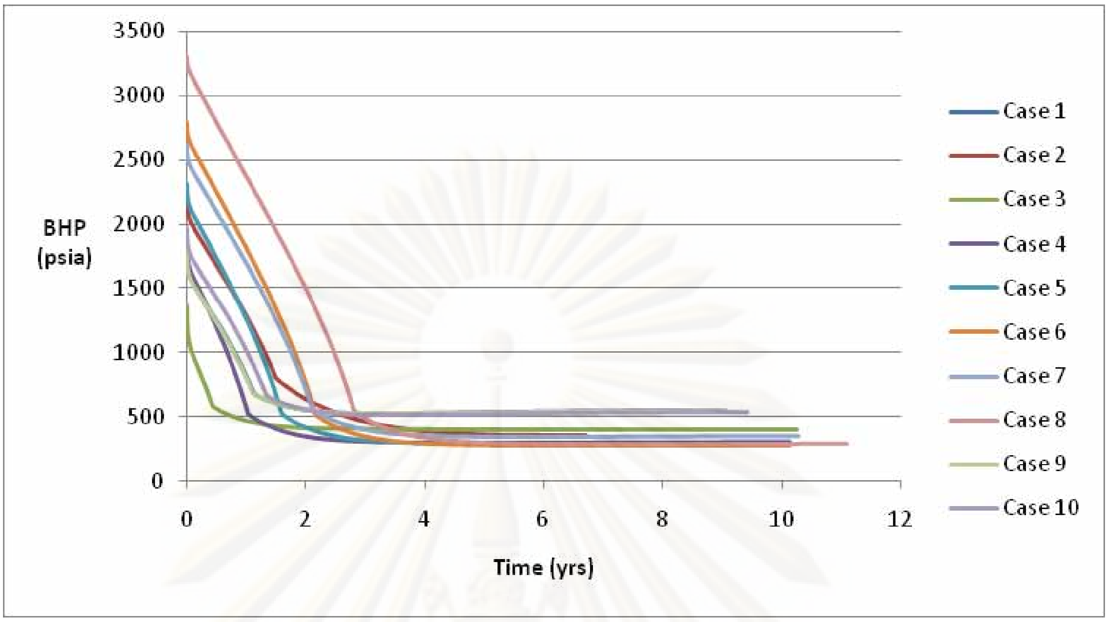

Figure 5.48: Bottomhole pressure for producing with natural depletion with initial reservoir pressure equal to the dew point pressure.

The condensate-gas ratio (CGR), mole fraction of heptanes plus, cumulative production of condensate, and recovery factor of natural depletion are summarized in Table 5.28. The condensate-gas ratio ranges from 30 to 100 STB/MMSCF. The highest condensate-gas ratio is obtained in case 2 because this case has highest mole fraction of heptanes plus. Case 4 and case 5 have almost equal condensate-gas ratio and can be considered as the lowest compared to the other cases because these cases have highest mole fraction of methane and lowest mole fraction of heptanes plus.

Table 5.28: Condensate-gas ratio, mole fraction of heptanes plus, cumulative production of condensate, and recovery factor for producing with natural depletion with initial reservoir pressure equal to the dew point pressure.

Case	CGR (STB/MMSCF)	Mole fraction of heptanes plus	Total condensate Production (STB)	Condensate recovery factor (%)
1	57	0.0654	278,867	25%
2	100	0.1339	536,591	26%
3	33	0.0656	243,921	71%
4	30	0.0306	201,693	56%
5	31	0.0283	195,492	44%
6	41	0.0326	261,062	38%
7	62	0.0503	330,475	30%
8	80	0.0633	442,274	26%
9	59	0.0885	306,234	28%
10	70	0.1040	356,882	26%

The performance of gas condensate reservoirs with natural depletion can be summarized as follows:

(a) The total gas production ranges from 6.97 to 15.92 BCF. The gas recovery factor ranges from 76 to 91%.

(b) The total condensate production ranges from 195,492 to 536,591 STB. The condensate recovery factor ranges from 25 to 71%. The highest recovery factor of condensate is 71% and is obtained in case 3.

(c) The highest recovery factor of total gas production is 91% and is obtained in case 8. This case has longest producing time before reaching the tubing head pressure limit. From the simulation results, the gas recovery factor is a function of dew point pressure and maximum liquid dropout. The gas recovery factor is higher, when the dew point pressure is higher. And, the gas recovery factor is lower, when the maximum liquid dropout is higher.

5.2.2 Production of gas condensate reservoir with CO_2 injection at the beginning

In this scenario, the gas-condensate reservoirs are produced together with CO_2 injection at the beginning in order to minimize the reservoir pressure drop and liquid dropout around the wellbore.

The gas production rate and the tubing head pressure (THP) for production with CO_2 injection at the beginning are shown in Figures 5.49 and 5.50, respectively. In all cases, the gas production rate is constant at the initial period. The gas production rate starts to decline when CO_2 breaks through the producer. The simulation stops when CO_2 concentration reaches the economic limit of 23%. The production with CO_2 injection can keep the reservoir pressure to be high, so the tubing head pressure (THP) does not reach the limit of 200 psia.

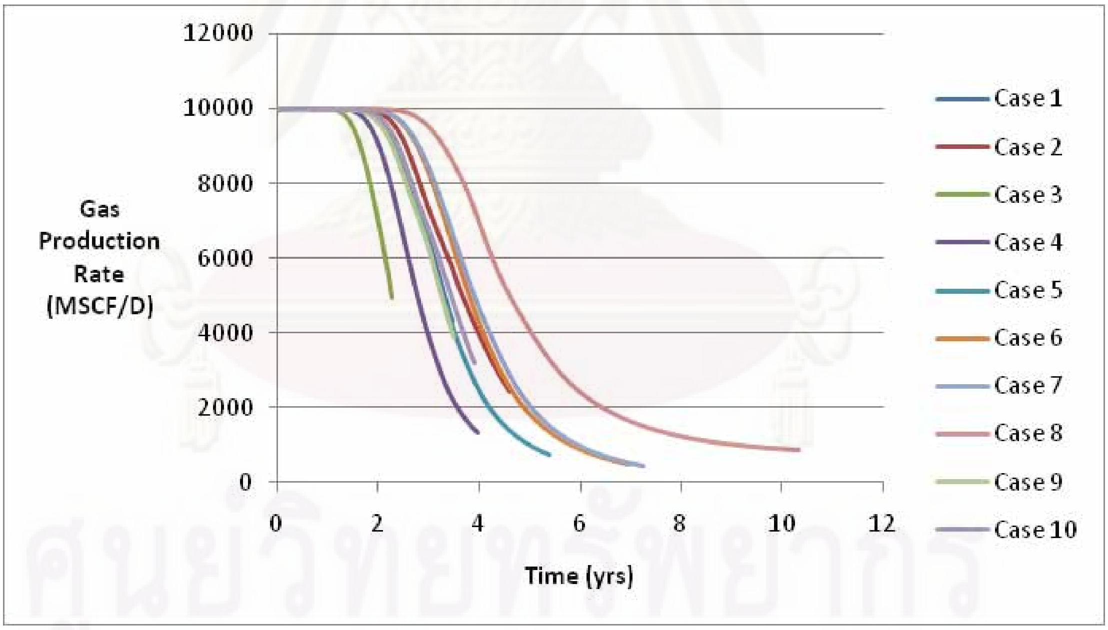

Figure 5.49: Gas production rate for producing with CO_2 injection at the beginning with initial reservoir pressure equal to the dew point pressure.

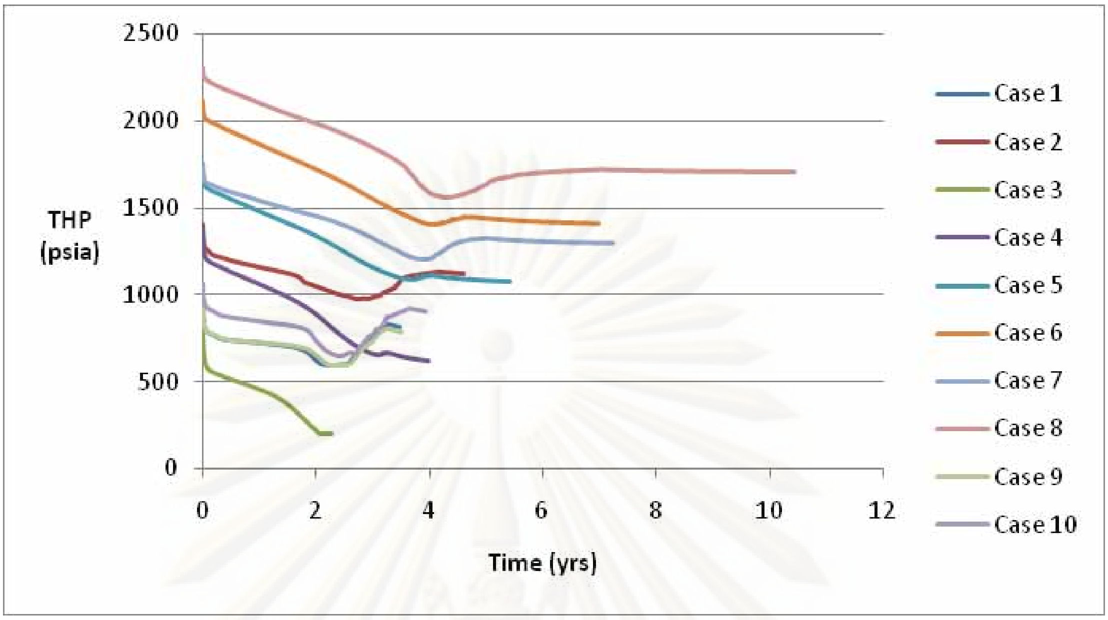

Figure 5.50: Tubing head pressure for producing with CO_2 injection at the beginning with initial reservoir pressure equal to the dew point pressure.

The production life between no CO_2 concentration limit and 23% CO_2 concentration limit of injecting CO_2 at the beginning are summarized in Table 5.29. The highest and lowest production life of no CO_2 concentration limit is obtained in case 8 and case 3, respectively.

Table 5.29: Production life for producing with CO_2 injection at the beginning with initial reservoir pressure equal to the dew point pressure.

Case	**Production life (years)**	
	No limit	**23% CO_2 limit**
1	3.5	2.6
2	4.7	2.9
3	2.3	1.9
4	4.0	2.3
5	5.4	2.7
6	7.0	3.2
7	7.3	3.2
8	10.5	3.6
9	3.6	2.6
10	4.0	2.8

The total gas production and the gas recovery factor for the case with no CO_2 concentration limit and 23% CO_2 concentration limit for CO_2 injection at the beginning are summarized in Table 5.30.

Table 5.30: Total gas production and recovery factor for producing with CO_2 injection at the beginning with initial reservoir pressure equal to the dew point pressure.

Case	**Total gas production (BCF)**		**Gas recovery factor (%)**	
	No limit	**23% CO_2 limit**	**No limit**	**23% CO_2 limit**
1	11.19	9.33	89%	75%
2	13.29	10.21	96%	74%
3	7.60	6.69	85%	75%
4	10.43	8.11	96%	75%
5	12.63	9.67	98%	75%
6	14.81	11.21	99%	75%
7	15.09	11.36	100%	75%
8	16.56	11.82	94%	67%
9	11.18	9.30	90%	75%
10	12.09	9.75	93%	75%

The condensate production rate and the bottomhole pressure (BHP) for production with CO_2 injection at the beginning are shown in Figures 5.51 and 5.52, respectively. The condensate production rates for different cases are different because the condensate-gas ratios (CGR) are different. The condensate production rate slowly declines after CO_2 injection starts and then shoots up when CO_2 breaks through the producer. Injecting CO_2 at the beginning cannot maintain the bottomhole pressure above the dew point pressure of the original reservoir fluid. So, liquid dropout occurs in the reservoir. As already mention in previous section, the condensate production rate increase because the condensate around the well bore is revaporized by CO_2 and swept to the producer.

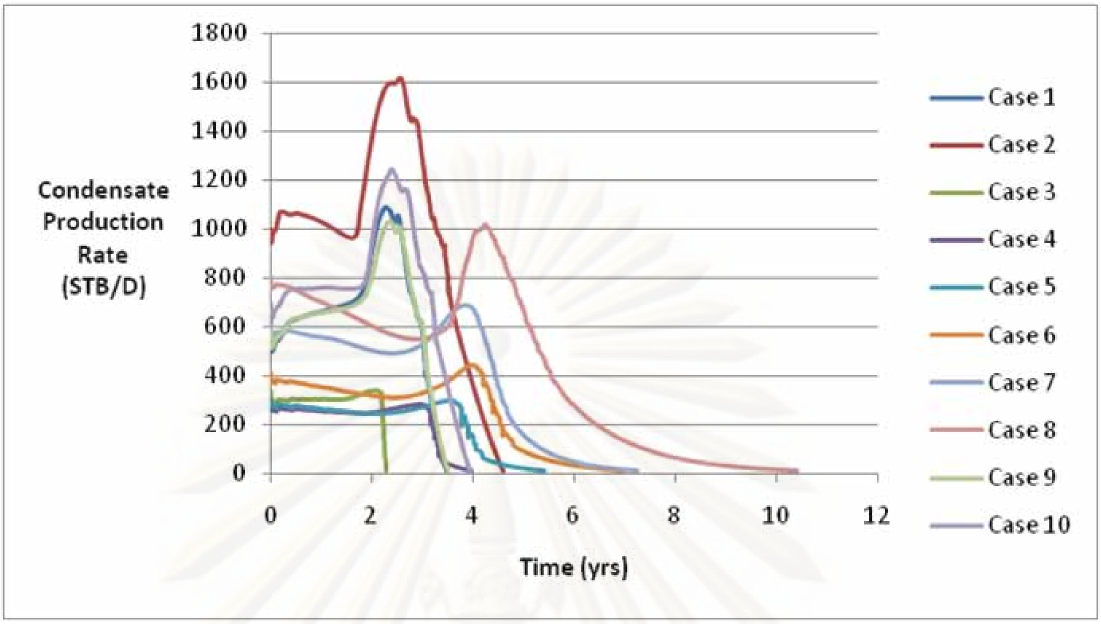

Figure 5.51: Condensate production rate for producing with CO_2 injection at the beginning with initial reservoir pressure equal to the dew point pressure.

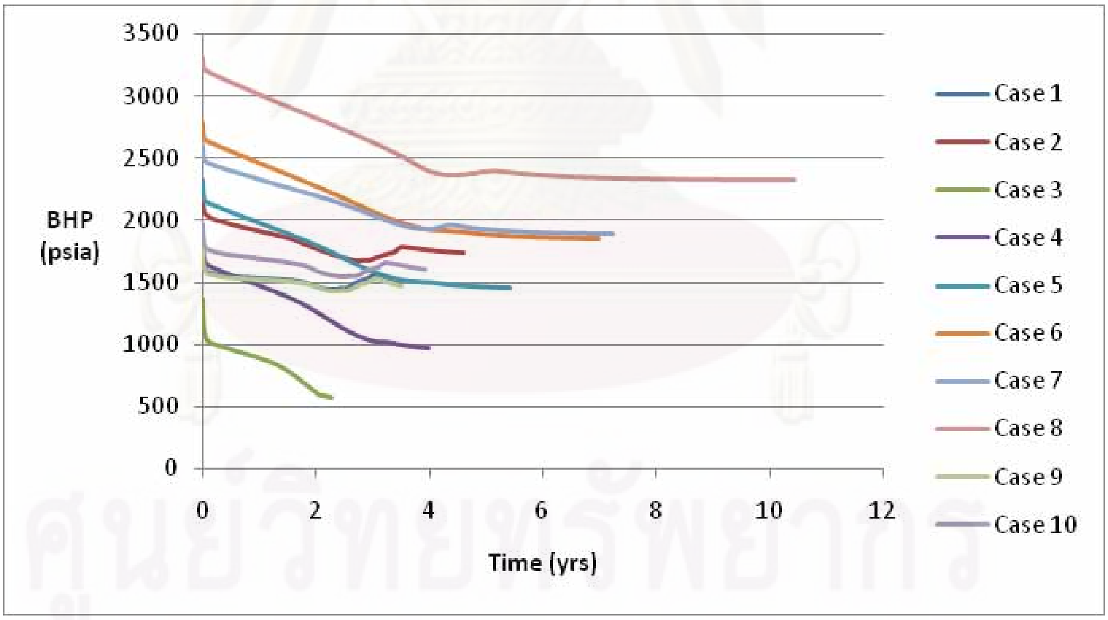

Figure 5.52: Bottomhole pressure for producing with CO_2 injection at the beginning with initial reservoir pressure equal to the dew point pressure.

The condensate saturation at local grid block (1, 1, 1), which is the producer for the case with 23% CO_2 concentration limit and no CO_2 concentration limit is shown in Figures 5.53 and 5.54, respectively. In the case of 23% CO_2 concentration limit, the liquid dropout cannot be completely revaporized in all cases as depicted in Figure 5.53. In the case of no CO_2 concentration limit, the liquid dropout can be completely revaporized in all cases.

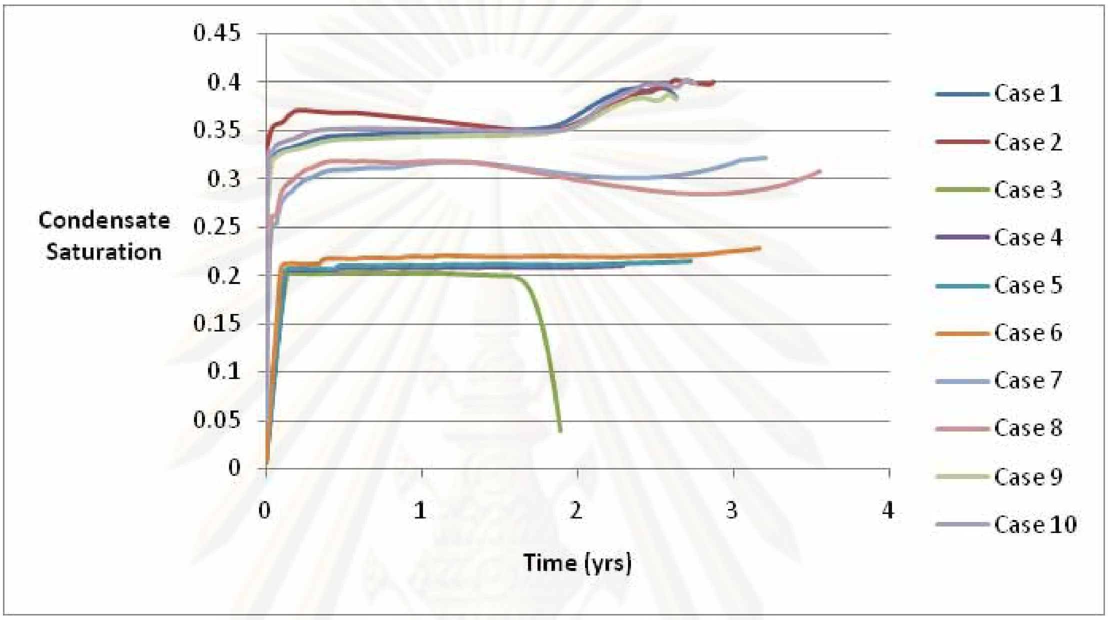

Figure 5.53: Condensate saturation for producing with CO_2 injection at the beginning with initial reservoir pressure equal to 3,500 psia (23% CO_2 concentration limit).

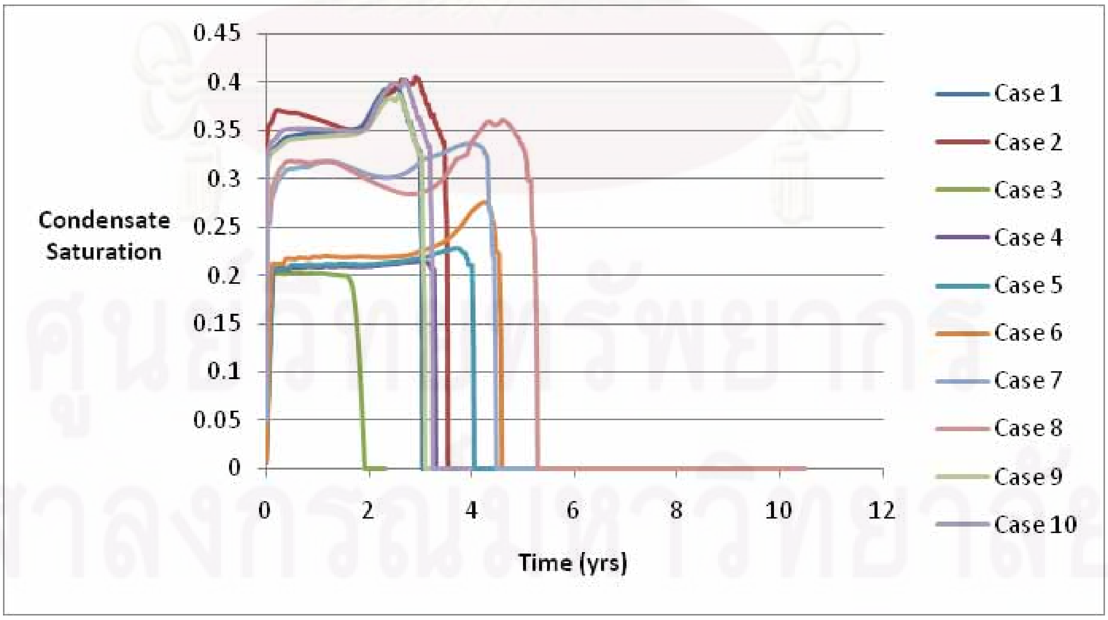

Figure 5.54: Condensate saturation for producing with CO_2 injection at the beginning with initial reservoir pressure equal to 3,500 psia (no CO_2 concentration limit).

The total condensate production and the condensate recovery factor for the case with no CO_2 concentration limit and 23% CO_2 concentration limit for CO_2 injection at the beginning are summarized in Table 5.31.

Table 5.31: Total condensate production and recovery factor for producing with CO_2 injection at the beginning with initial reservoir pressure equal to the dew point pressure.

Case	**Total condensate production (STB)**		**Condensate recovery factor (%)**	
	No limit	**23% CO_2 limit**	**No limit**	**23% CO_2 limit**
1	858,750	724,237	77%	65%
2	1,647,563	1,254,617	81%	61%
3	250,265	208,635	73%	61%
4	317,706	213,079	88%	59%
5	402,470	257,918	91%	58%
6	633,755	392,336	93%	57%
7	998,481	625,745	90%	56%
8	1,582,471	833,376	93%	49%
9	846,110	699,421	78%	65%
10	1,089,134	871,761	79%	63%

From the simulation results, we can see that the condensate recovery factor depend on dew point pressure and maximum liquid dropout. From Table 4.4 we separate the reservoir fluids into two main categories which are moderate-high maximum liquid dropout and low maximum liquid dropout. Cases 1, 2, 7, 8, 9, and 10 are moderate-high maximum liquid dropout case and case 3, 4, 5, and 6 are low maximum liquid dropout case. The condensate recovery factor as a function of dew point pressure for moderate-high maximum liquid dropout and low maximum liquid dropout are shown in Figure 5.55 and 5.56, respectively. The condensate recovery factor decrease when the dew point pressure increase.

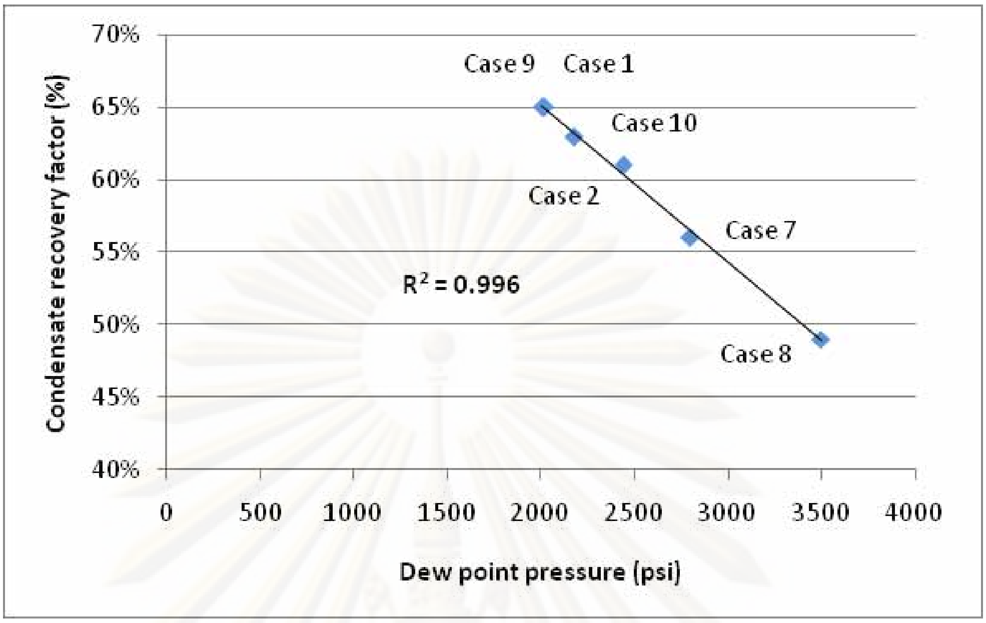

Figure 5.55: Condensate recovery factor as a function of dew point pressure for producing with CO_2 injection at the beginning with initial reservoir pressure equal to the dew point pressure (moderate-high maximum liquid dropout).

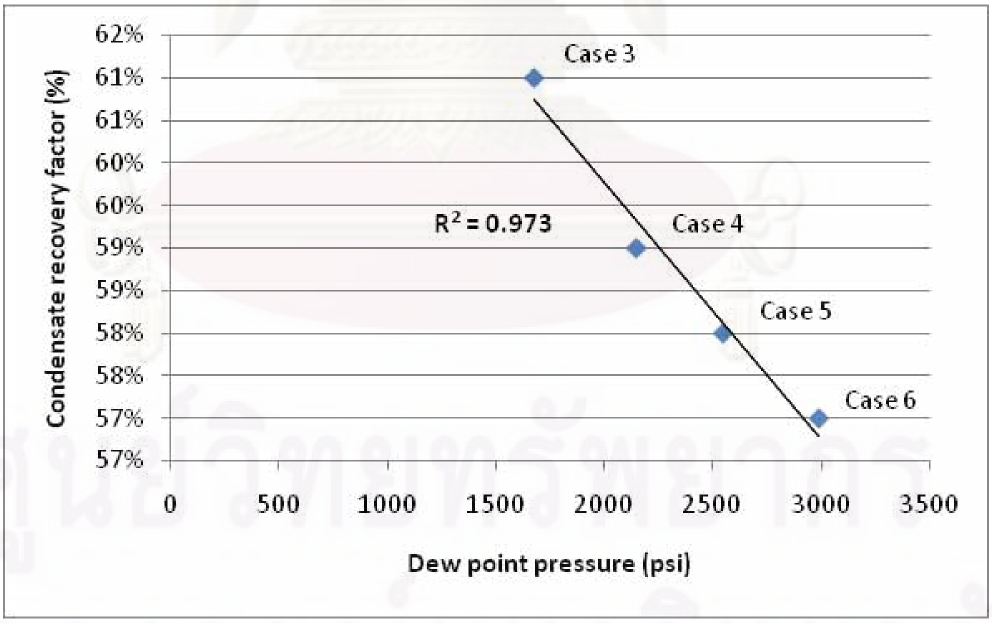

Figure 5.56: Condensate recovery factor as a function of dew point pressure for producing with CO_2 injection at the beginning with initial reservoir pressure equal to the dew point pressure (low maximum liquid dropout).

The performance of gas condensate reservoirs with CO_2 injection at the beginning can be summarized as follows:

(a) In the case of 23% CO_2 concentration limit, the total gas production ranges from 6.69 to 11.82 BCF, yielding gas recovery factor between 67 to 75%.

(b) In the case of 23% CO_2 concentration limit, the total condensate production ranges from 208,635 to 1,254,617 STB, yielding condensate recovery factor between 49 to 65%. . For 23% CO_2 concentration limit, the condensate recovery factor is a function of dew point pressure and maximum liquid dropout. The condensate recovery factor is higher, when the dew point pressure is lower. And, the condensate recovery factor is lower, when the maximum liquid dropout is lower.

(c) The lowest recovery factor of total condensate production and total gas production are 49% and 67%, respectively in case 8.

The comparisons of the simulation results between production with natural depletion and production with CO_2 injection at the beginning are reported. The difference in cumulative gas production and cumulative condensate production, and recovery factors of 23% CO_2 concentration limit are summarized in Table 5.32.

Table 5.32: The difference in cumulative gas production, cumulative condensate production, and recovery factors of 23% CO_2 concentration limit between natural depletion and CO_2 injection at the beginning with initial reservoir pressure equal to the dew point pressure.

Case	ΔGp (MSCF)	ΔRF for gas (%)	ΔNp (STB)	ΔRF for condensate (%)
1	-0.21	-1%	445,370	40%
2	-1.09	-8%	718,026	35%
3	-0.28	-3%	-35,286	-10%
4	-1.15	-10%	11,386	3%
5	-1.63	-13%	62,426	14%
6	-2.14	-14%	131,274	19%
7	-1.90	-13%	295,270	26%
8	-4.10	-24%	391,102	23%
9	-0.19	-2%	393,187	36%
10	-0.44	-3%	514,879	37%

The performance of gas condensate reservoirs with CO_2 injection at the beginning compared with production by natural depletion can be summarized as follows:

(a) In all cases, injecting CO_2 at the beginning of the production decreases the total gas production compared with production by natural depletion. When producing with natural depletion, most of the reservoir fluid is produced as gas but the produced reservoir fluid is changed from gas to condensate when producing with CO_2 injection at the beginning. When injection CO_2 at the beginning, the reservoir can be produced until reaching the economic limit of CO_2 concentration even though the economic limit of gas production may not be reached yet. But in the natural depletion case, the reservoir can be produced until reaching the economic limit of condensate and gas production rates.

(b) Injecting CO_2 at the beginning of the production increases the total condensate production compared with production by natural depletion in all cases except case 3.

(c) In case 3, the total condensate production with production by CO_2 injection at the beginning is lower than production by natural depletion. From the phase diagram in Figure 5.13, the reservoir fluid in this case has a dew point pressure of 1680 psia which is the lowest among the 10 cases in this study. The maximum liquid dropout is only 1%. The liquid dropout can be completely revaporized even in natural depletion case when the reservoir pressure drops below 620 psia. CO_2 injection will cause an early termination of gas production due to high CO_2 concentration at the producer (CO_2 limit = 23%), resulting in lower recovery factor.

5.2.3 Production of gas condensate reservoir with CO_2 injection at the beginning with injection rate higher than production rate

From the previous result, CO_2 injection rate equal to the production rate cannot completely revaporize the liquid dropout around the wellbore when 23% CO_2 concentration limit is reached. The objective of this scenario is to find the optimum injection rate which the liquid dropout can be completely revaporized and the maximum condensate recovery can be obtained. Three different injection rates, which are (1) injection rate is 1.25 times the production rate (2) injection rate is 1.5 times the production rate and (3) injection rate is 1.75 times the production rate, are used.

The maximum liquid dropout, total gas production, and total condensate production for producing with CO_2 injection at the beginning which injection rate higher than production rate are summarized in Tables 5.33 and 5.34, respectively.

Table 5.33: Maximum liquid dropout, total gas production for producing with CO_2 injection at the beginning with injection rate higher than production rate for initial reservoir pressure equal to the dew point pressure.

Case	**Maximum liquid dropout (%)**	**Gas production total (BCF)**			
		Injection rate is 1.0 times the production rate	**Injection rate is 1.25 times the production rate**	**Injection rate is 1.5 times the production rate**	**Injection rate is 1.75 times the production rate**
1	19	9.33	9.05	8.79	8.56
2	25	10.21	10.11	9.82	9.58
3	1	6.69	6.46	6.24	6.07
4	1	8.11	7.83	7.59	7.38
5	2	9.67	9.35	9.05	8.81
6	2	11.21	10.83	10.48	10.20
7	10	11.36	10.99	10.66	10.37
8	12	12.73	12.19	11.81	11.46
9	15	9.30	9.02	8.76	8.54
10	20	9.75	9.54	9.27	9.04

Table 5.34: Maximum liquid dropout, total condensate production for producing with CO_2 injection at the beginning with injection rate higher than production rate for initial reservoir pressure equal to the dew point pressure.

Case	**Maximum liquid dropout (%)**	**Condensate production total (STB)**			
		Injection rate is 1.0 times the production rate	**Injection rate is 1.25 times the production rate**	**Injection rate is 1.5 times the production rate**	**Injection rate is 1.75 times the production rate**
1	19	724,237	781,188	756,925	736,270
2	25	1,254,617	1,464,636	1,422,598	1,387,162
3	1	208,635	223,346	227,378	221,060
4	1	213,079	231,842	250,764	244,117
5	2	257,918	291,399	309,332	301,057
6	2	392,336	456,632	477,293	464,130
7	10	625,745	801,121	778,019	756,494
8	12	833,376	1,087,629	1,133,342	1,099,643
9	15	699,421	760,861	737,300	718,072
10	20	871,761	981,357	951,890	927,455

The production life for producing with CO_2 injection at the beginning with injection rate higher than production rate is summarized in Table 5.35.

Table 5.35: Production life for producing with CO_2 injection at the beginning with injection rate higher than production rate for initial reservoir pressure equal to the dew point pressure.

Case	**Production life (years)**		
	Injection rate is 1.25 times the production rate	**Injection rate is 1.5 times the production rate**	**Injection rate is 1.75 times the production rate**
1	2.6	2.5	2.4
2	2.9	2.8	2.7
3	1.8	1.8	1.7
4	2.2	2.1	2.1
5	2.6	2.6	2.5
6	3.1	3.0	2.9
7	3.1	3.0	2.9
8	3.4	3.3	3.2
9	2.6	2.5	2.4
10	2.7	2.6	2.6

The performance of gas condensate reservoirs for producing with CO_2 injection at the beginning with injection rate higher than production rate can be summarized as follows:

(a) Injecting CO_2 at a rate higher than the production rate decreases the total gas production because the CO_2 concentration reaches the economic limit faster than injecting CO_2 at a lower rate. Increasing the CO_2 injection rate shortens the production life.

(b) Increasing the injection rate does not always increase the total condensate production. There is an optimum point which the maximum condensate production can be obtained.

(c) In cases 1, 2, 7, 9 and 10, the highest total condensate production can be obtained when the injection rate is between 1.0 to 1.25 times the production rate. These cases have relatively moderate-high maximum liquid dropout. If the injection rate is more than this, the total condensate production will decrease.

(d) In cases 3, 4, 5, 6 and 8 the highest total condensate production can be obtained when the injection rate is between 1.25 to 1.75 times the production rate. These cases have relatively low maximum liquid dropout except case 8. If the injection rate is more than this, the total condensate production will decrease.

From the observation, the optimum rate which maximizes the condensate recovery is the rate that the liquid around wellbore can be completely revaporized. In this section, the condensate saturation in grid block 1, 1, 1 for the case that maximizes total condensate production total is discussed:

Injection rate of CO_2 is 1.25 times production rate

Cases 1, 2, 7, 9 and 10 have maximum condensate recovery when injecting at 1.25 times the production rate. The condensate saturation of grid block 1, 1, 1 is shown in Figure 5.57. From Figure 5.57, the condensate saturation can be completely revaporized in case 1, 2, 7, 9 and 10. The optimum rate of CO_2 injection of case 1, 2, 7, 9 and 10 is between 1.0 to 1.25 times the higher than the production rate because the liquid dropout can be completely revaporized and maximum condensate recovery can be obtained.

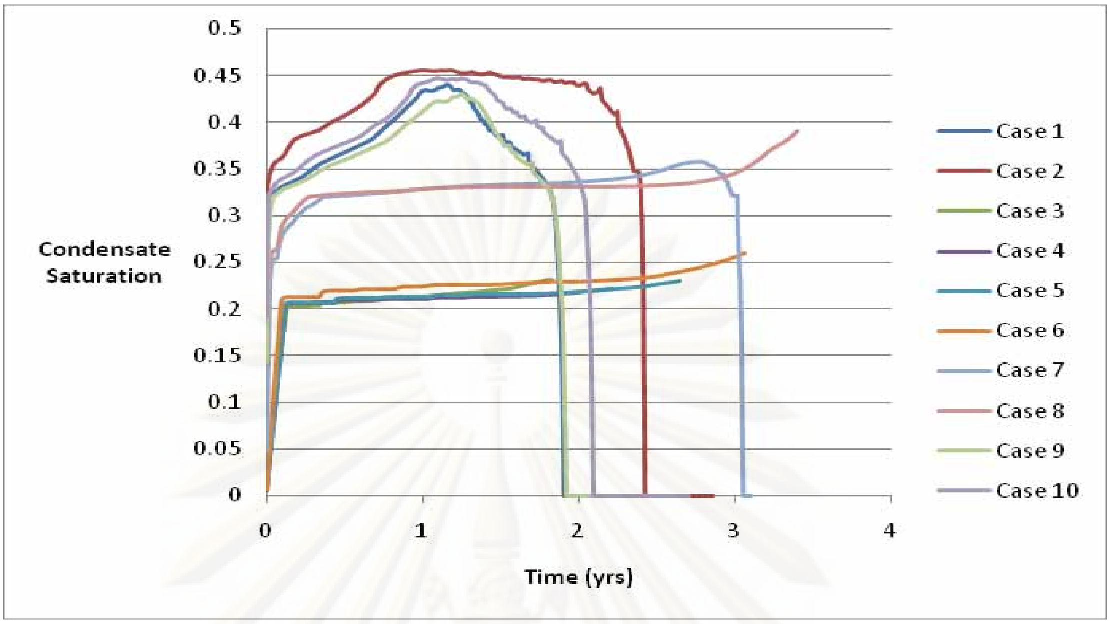

Figure 5.57: Condensate saturation of injection rate of CO_2 equal to 1.25 times the production rate for initial reservoir pressure equal to the dew point pressure.

<u>**Injection rate of CO_2 is 1.5 times production rate**</u>

Cases 3, 4, 5, 6 and 8 have maximum condensate recovery when injecting at 1.5 times the production rate. The condensate saturation of grid block 1, 1, 1 is shown in Figure 5.58. From Figure 5.58, the condensate saturation can be completely revaporized in cases 3, 5, 6 and 8 except case 4. In case 4, the condensate saturation starts to decrease but the liquid dropout cannot be completely revaporized because it reaches the CO_2 concentration limit before.

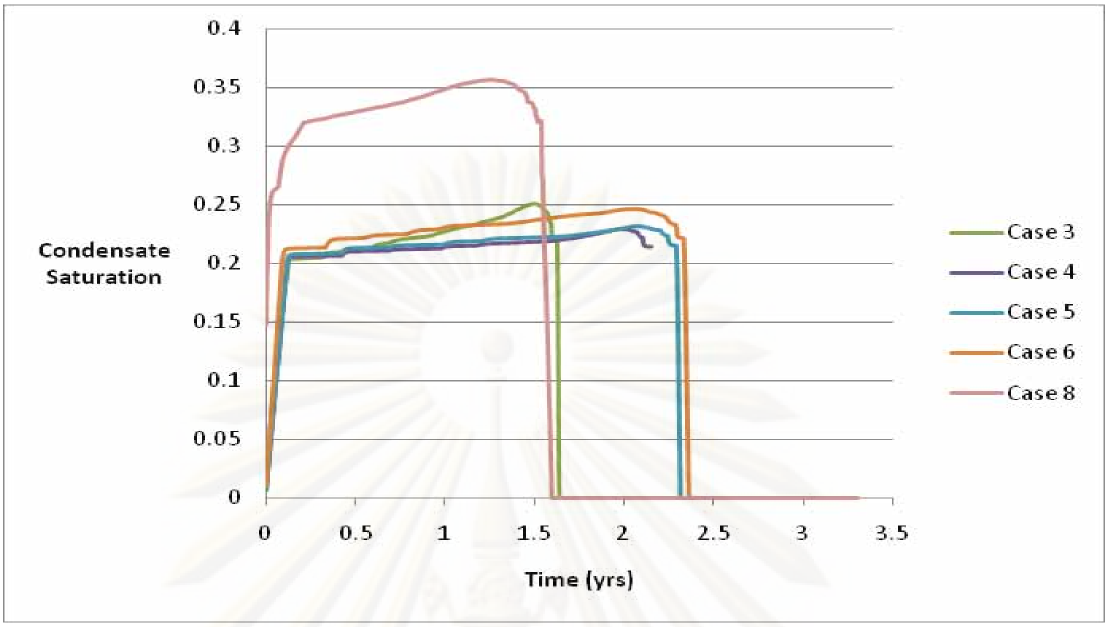

Figure 5.58: Condensate saturation of injection rate of CO_2 equal to 1.5 times the production rate for initial reservoir pressure equal to the dew point pressure.

In case 4, another simulation with the injection rate equal to 1.75 times the production rate was run. The condensate saturation of injection rate of CO_2 equal to 1.75 times the production rate of case 4 is shown in Figure 5.59.

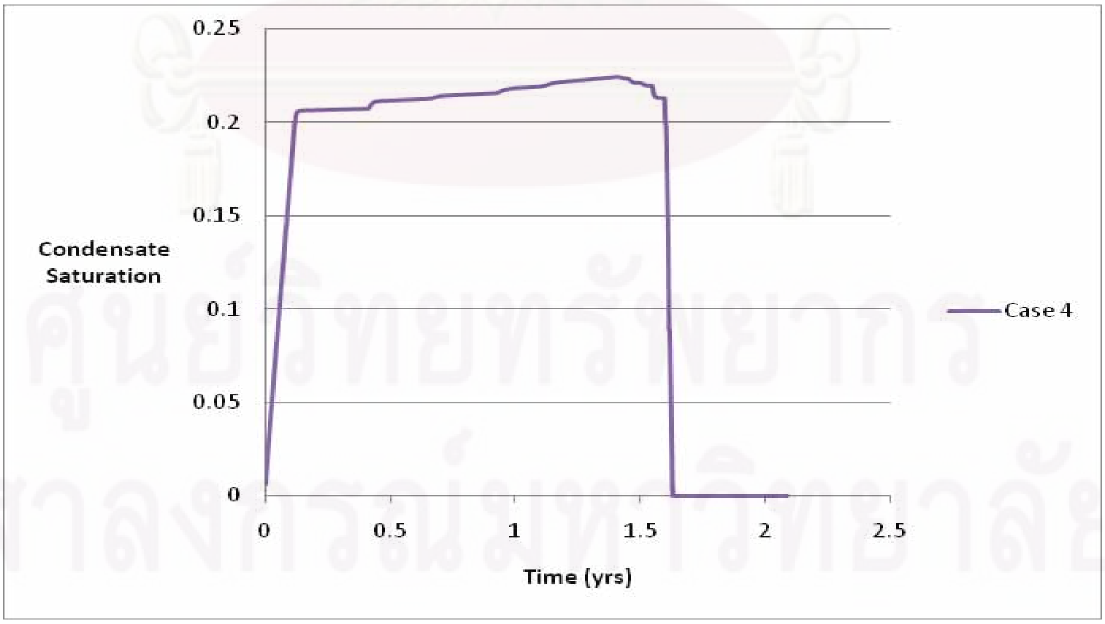

Figure 5.59: Condensate saturation of injection rate of CO_2 equal to 1.75 times the production rate for initial reservoir pressure equal to the dew point pressure.

When the injection rate of CO_2 is 1.75 times the production rate, the liquid dropout can be completely revaporized but the total condensate recovery decreases. Because when the injection rate is 1.5 times the production rate in case 4, the liquid dropout around the wellbore is almost completely revaporized. But when the injection rate increases to 1.75 times the production rate, CO_2 will breakthrough too fast. After performing a detailed study, it was found that the best CO_2 injection rate of this case is 1.51 times the production rate, in which the total condensate recovery is 250,772 STB, and liquid dropout can be completely revaporized.

In the second scenario, we can observe that CO_2 injection does effectively enhance condensate recovery. The amount of condensate recovery depends on the CO_2 injection rate. When the injection rate is higher than the optimum rate, CO_2 breaks through the producer too fast, reducing the amount of condensate recovery. When the injection rate is lower than the optimum rate, liquid drops out in the reservoir and cannot be fully recovered at surface. By varying reservoir fluid composition and injection rate of CO_2, we found that the maximum liquid dropout has significant correlation on the optimum injection rate of CO_2 and the condensate recovery. The injection rate of reservoir fluid having moderate-high maximum liquid dropout is lower than low maximum liquid dropout.

5.3 Economic Analysis

The financial aspect of selected production profile of condensate reservoir is evaluated using net present value (NPV). The capital cost is invested since starting the project. The assumptions for this economic evaluation base on Tangkaprasert' study which are:

a) Oil price equal to 77.5 US$/bbl
b) Gas price equal to 3.5 US$/MMBTU
c) Constant discount rate at 10 %
d) Total fixed cost/investment cost of production well and injection well equal to 1,800,000 US$.
e) Total cost of compressor is 2,725,000 US$. (The calculation method is shown in Appendix D-1)

f) Apply linear depreciation for salvage cost of compressor, and compressor life time is defined at 5 years.
g) Operating cost varies only on electricity consumption. (The calculation method is shown in Appendix D-2)
h) The gas processing cost is not accounted in the economic evaluation.
i) The composition of injection gas is constant throughout the entire production period.

Cases selected for economic analysis are case 6 and case 9 when the initial reservoir pressure is at 3,500 psia. Case 6 has low maximum liquid dropout (2%) with a high dew point pressure (2,990 psia). The CO_2 injection time which maximizes condensate recovery is injecting CO_2 at the beginning of the production. Case 9 has moderate-high maximum liquid dropout (15%) with a low dew point pressure (2,010 psia). The CO_2 injection time which maximizes condensate recovery is injecting CO_2 at the dew point pressure. Economics analysis will be used to compare between the cases of 23% CO_2 limit and production with natural depletion. NPV and annual cash flow of these selected cases are illustrated in Figures 5.60 and 5.61, respectively. The cash flow table of each case is shown in Appendix E.

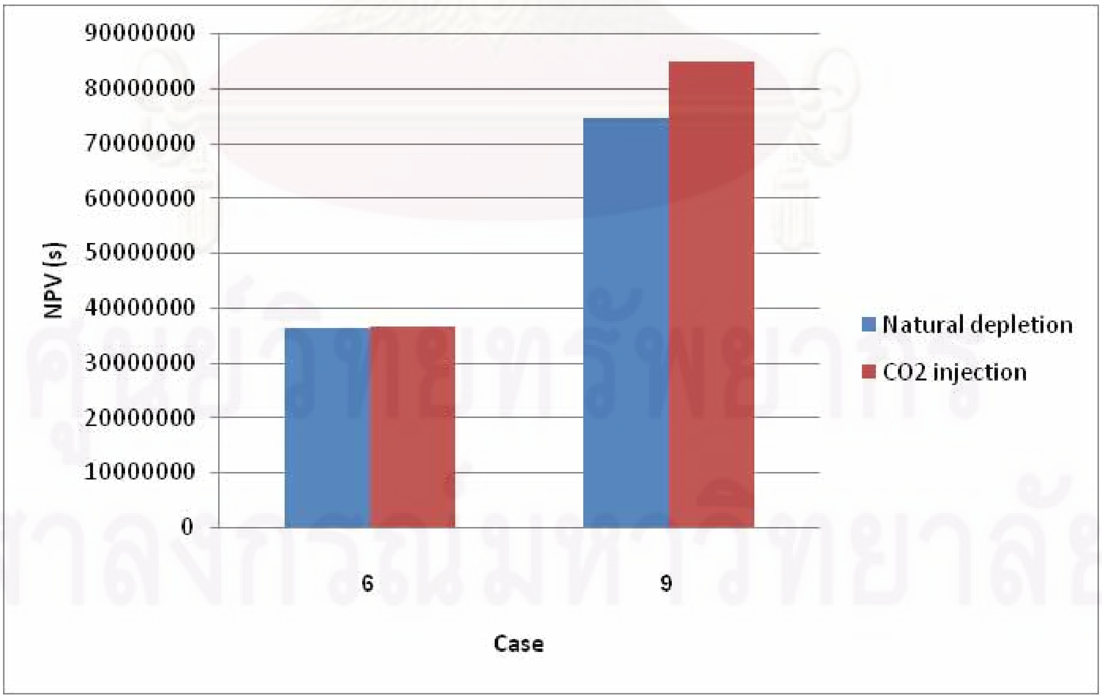

Figure 5.60: Net present value (NPV) for selected cases.

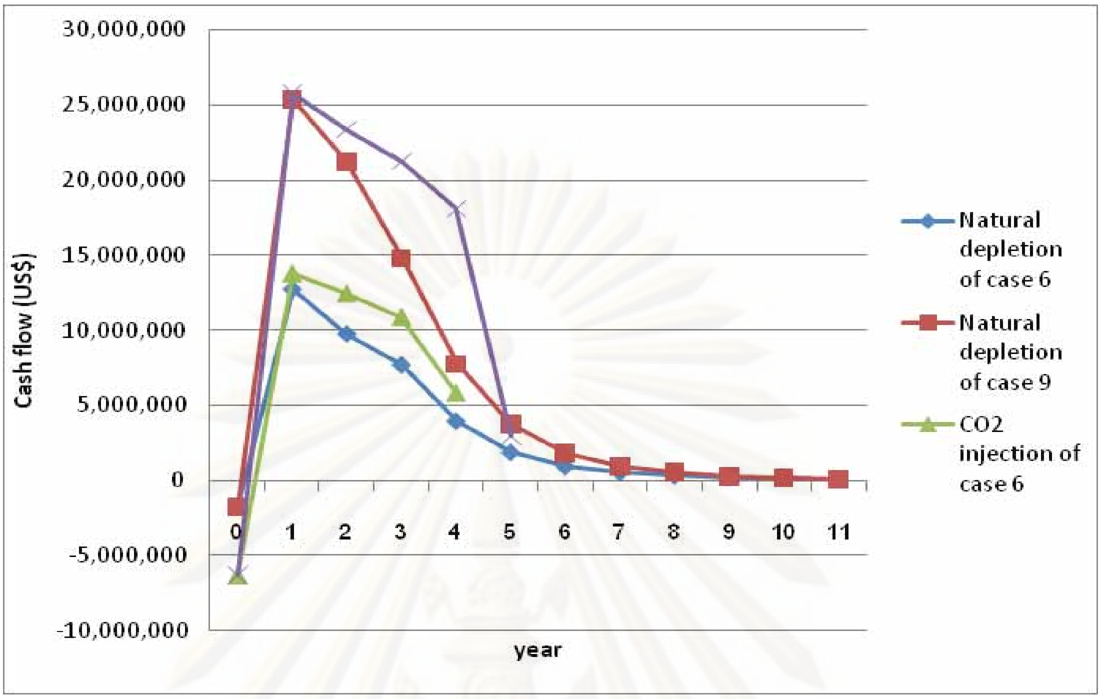

Figure 5.61: Cash flow for selected cases.

From the economic analysis, the results can be summarized as follows**:**

(a) From Figure 5.60, we can see that the NPV of producing with CO_2 injection is higher than producing with natural depletion in case 6 and case 9. There is 0.9% gain in NPV for case 6 and 13% gain in NPV for case 9 when producing with CO_2 injection.

(b) The reservoir fluid in case 9 has moderate-high maximum liquid dropout (15%). The liquid dropout occurs very fast when producing by natural depletion. Thus, CO_2 injection effectively improves the condensate recovery by revaporizing the liquid dropout around the wellbore.

(c) The reservoir fluid in case 6 has low maximum liquid dropout (2%). So, the reservoir fluid in this case can be effectively recovered by natural depletion. Then, the NPV of producing with CO_2 injection is almost the same as producing with natural depletion. Therefore, CO_2 injection does not improve the condensate recovery and gain the NPV in this case.

CHAPTER VI

CONCLUSIONS AND RECOMMENDATIONS

In this chapter, the conclusions of the effect of the reservoir fluid compositions on CO_2 injection in gas condensate reservoir are illustrated in terms of hydrocarbon recovery and economic analysis.

6.1 Conclusions

Based on the input data used in this study and simulation results obtained from ECLIPSE 300 reservoir simulator, hydrocarbon recovery enhancement and economic analysis of CO_2 injection in gas condensate reservoirs can be concluded as follows:

6.1.1 Hydrocarbon Recovery Enhancement by CO_2 Injection

(a) CO_2 injection can revaporize the liquid dropout around the wellbore and increase the condensate recovery by keeping the reservoir pressure high.

(b) When CO_2 concentration increases, the dew point pressure of the new mixture decreases. This mechanism will assist in revaporizing the liquid dropout in the reservoir. The reservoir fluid with high dew point pressure or low maximum liquid dropout is more difficult to completely revaporize once it is dropped out in the reservoir.

(c) The breakthrough time is not much affected by the reservoir fluid composition. It is greatly affected by the injection rate. Increasing the injection rate accelerates the breakthrough time.

(d) In all cases, producing with CO_2 injection has lower gas recovery than producing with natural depletion. When producing with natural depletion, most of the reservoir fluid is produced as gas but the produced reservoir fluid is changed from gas to condensate when producing with CO_2 injection.

(e) In order to gain maximum condensate recovery, the liquid dropout around the wellbore has to be completely revaporized. If we start injecting CO_2

too late, the liquid dropout around wellbore will not be completely revaporized before the CO_2 content in the produced gas reaches its limit of 23%. And, if we start injecting CO_2 too early, CO_2 breakthrough time will be accelerated, resulting in short production life and low gas and condensate recovery. The dew point pressure and maximum liquid dropout has an effect on the optimum time to start CO_2 injection. The reservoir fluid which has high dew point pressure or low maximum liquid dropout requires earlier CO_2 injection than the reservoir fluid which has low dew point pressure or high maximum liquid dropout.

(f) In the case that we cannot start CO_2 injection early in order to completely revaporize the liquid dropout around the wellbore, injection with a rate higher than the production rate is an option. If the injection rate is lower than the optimum rate, the liquid dropout around the wellbore will not be completely revaporized before the CO_2 content in the produced gas reaches its limit of 23%. And, if the injection rate is higher than the optimum rate, CO_2 breakthrough time will be accelerated, resulting in short production life and low gas and condensate recovery. The optimum injection rate of CO_2 seems to depend on the maximum liquid dropout of the reservoir fluid. The reservoir fluid which has moderate-high maximum liquid dropout should be injected at the lower rate than the reservoir fluid which has low maximum liquid dropout.

6.1.2 Economic analysis of CO_2 Injection

(a) When the reservoir fluid has low maximum liquid dropout, the NPV of producing with CO_2 injection is almost the same as producing with natural depletion. This reservoir fluid can be effectively recovered by natural depletion and the CO_2 injection cannot recover much condensate in the reservoir. Therefore, CO_2 injection does not gain the NPV.

(b) When the reservoir fluid has moderate-high maximum liquid dropout, the NPV of producing with CO_2 injection is higher than producing with natural depletion. In a reservoir with moderate-high maximum liquid dropout, the liquid blockage problem is much more severe. So, CO_2 injection can help recover condensate in the reservoir effectively.

6.2 Recommendations

In this study, performance of CO_2 injection for different reservoir compositions fluid was studied. The optimum time and rate which can provide the maximum condensate recovery were investigated. The phase behavior of each case was also studied in order to understand the effect of increasing CO_2 concentration. The economic evaluation was also perform in order to study the feasibility of CO_2 injection.

However, the conclusions are made from simulation results which come from a hypothetical model which has homogeneous reservoir properties, no dip angle, and immobile reservoir water. The field results may be different due to the effect of the parameters mentioned above. Future works should study the influence of these parameters for more understanding on mechanism and performance of CO_2 injection into a gas condensate reservoir.

References

[1] Chaback, J.J., and Willium, M.L. p-x Behavior of a Rich-Gas-Condensate Reservoir Fluid in Admixture of CO_2 and (N_2 + CO_2). Paper SPE 24132 Presented at the 1992 SPE/DOE Symposium on Enhanced Oil Recovery held Tulsa April 1992.

[2] Shtepani, E. CO_2 Sequestration in Depleted Gas/Condensate Reservoirs. Paper SPE 102284 Presented at the 2006 SPE Annual Technical Conference and Exhibition held in San Antonio, Texas, U.S.A. September 2006.

[3] Zaitsev, I.Y., Dmitrievsky, S.A., Norvik, H. etc. Compositional Modelling and PVT Analysis of Pressure Maintenance effect in Gas Condensate Field: Comparative Study. Paper SPE 36923 Peresented at the 1996 SPE European Petroleum Conference held in Milan, Italy. 22 – 24 October 1996.

[4] Ahmed, T., Evans, J., Kwan, R., and Vivian, T. Wellbore Liquid Blockage in Gas Condensate Reservoir. Paper SPE 51050 Presented at the 1998 SPE Eastern Regional Meeting, Pittsburgh, PA. 9-11 November 1998.

[5] Morokane, D., Logmo-Ngog, A.B., and Sarkar, R. Applicability of Timely Gas Injection in Gas Condensate Fields To Improve Well Productivity. Paper SPE 75147 Peresented at the SPE/DOE Improved Oil Recovery Symposium held in Tulsa, Oklahoma. 13 – 17 April 2002.

[6] Phakphum Tangkaprasert. Enhancing hydrocarbon recovery from gas condensate reservoir via carbon dioxide injection. Master's Thesis, Department of Mining and Petroleum engineering Chulalongkorn University. 2008.

[7] Shi, C., and Horne, R.N. Improved Recovery in Gas-Condensate Reservoirs Considering Compositional Variations. Paper SPE 115786 Presented at the 2008 SPE Annual Technical Conference and Exhibition held in Denver, Colorado, U.S.A. 21-24 September 2008.

[8] Chang, Y., Coats, B.K., and Nolen, J.S. A Compositional Model for CO_2 Floods Including CO_2 Solubility in Water. SPE Reservoir Evaluation & Engineering, 155-160. April 1998.

[9] Fan, L., Billy, W., and Jamaluddin, A. etc. Understanding Gas-Condensate Reservoirs. 2006.

[10] Yisheng, F., Baozhu, L., Yongle, H. etc. Condensate Gas Phase Behavior and Development. Paper SPE 50925 Peresented at the 1998 SPE International Conference and Exhibition in China held in Beijing. 2– 6 November 1998.

[11] Nemeth, L.K., and Kennedy, H.T. A correlation of Dewpoint Pressure With Fluid Composition and Temperature. Paper SPE 1147 Presented at SPE 41st Annual Fall Meeting held in Dallas, Texas, U.S.A. 1966.

[12] Van Der Waal, J.D. On the Continuity of the Gaseous and liquid States (doctoral dissertation). Universiteit Leiden. 1873.

[13] Redlich, O., and Kwong, J. N. S. On the Thermodynamics of Solution. V-An Equation of State. Fugacities of Gaseous Solutions, 1949

[14] Soave, G. Equilibrium Constants from a Modified Redlich-Kwong Equation of State, 1972

[15] Peng, D., and Robinson, DB. A New Two-Constant Equation of State. Industrial and Engineering Chemistry: Fundamentals 15, 1976

[16] Forrest F.Craig, JR. The Reservoir Engineering Aspects of Waterflooding. Monograph Volume 3 of the Henry L.Doherty series. New York, U.S.A: Millet the printer, 1980.

[17] Chaibhorn Kittirattanapaiboon. Effect of reservoir fluid composition on gas recycling in gas condensate reservoirs. Master's Thesis, Department of Mining and Petroleum engineering Chulalongkorn University. 2007.

[18] Gas Processors Association. ENGINEERING DATA BOOK FPS VERSION volume I & II (Electronic), 1998.

[19] Schlumberger Information Solutions. ECLIPSE Reference Manual 2006.1 and ECLIPSE Technical Description 2006.1, 2004.

[20] William D. McCain, JR. The Properties of Petroleum Fluids. Second edition. Oklahoma, Oklahoma, 1989.

APPENDICES

APPENDIX A

A-1) Reservoir model

The reservoir model is generated by input the required data in Eclipse simulator. The geological model composes of number of cells or blocks in X, Y and Z directions and in this study, the number of block is 15 x 15 x 3

A-2) Case Definition

Simulator: Compositional

Model Dimensions: Number of cells in the x direction 15

Number of cells in the y direction 15

Number of cells in the z direction 3

Grid type: Cartesian

Geometry type: Block Centered

Oil-Gas-Water Options: Water, Gas Condensate (ISGAS), CO_2 in Aqueous Phase

Number of Components: 16

Pressure Saturation Options (Solution Type): AIM

A-3) Reservoir properties

Grid

Properties: Active grid blocks X (15) = 1

Y (15) = 1

Z (8) = 1

Porosity = 0.165

Permeability k-x = 10.85 mD

k-y = 10.85 mD

k-z = 1.27 mD

X Grid block sizes = 150 ft

Y Grid block sizes = 150 ft

Z Grid block sizes = 40 ft

Depth of Top face (Top layer) = 8,000 ft

Cartesian Local Grid Refinement

LGR Name	**LGR Coordinate**			**Number of refined cells**		
	I	**J**	**K**	**X**	**Y**	**Z**
Producer	1-2	1-2	1-3	8	8	3

PVT Table

Fluid Densities at Surface Conditions	Oil density	49.99914	lb/ft3
	Water density	62.42797	lb/ft3
	Gas density	0.04947417	lb/ft3

A-4) Miscellaneous

Specify properties of water-CO2 system *(SOLUBILI)

Press (psia)	**VisCmp (scf /stb)**	**FVF (rb /stb)**	**Viscos (cp)**	**Cmprss (/psi)**
14.7	1.6022420	1.061622788	0.227468152	0.0000036657
200	20.6106981	1.065858529	0.227474803	0.0000036528
400	38.8621564	1.069524352	0.227494866	0.0000036389
600	55.0491457	1.072945944	0.227528304	0.0000036250
800	69.4314589	1.075976959	0.227575117	0.0000036111
1000	82.2365873	1.078668411	0.227635305	0.0000035972
1200	93.6629441	1.081064376	0.227708868	0.0000035833
1400	103.8831835	1.083202904	0.227795806	0.0000035694
1600	113.0473766	1.085116834	0.22789612	0.0000035555
1800	121.2859265	1.086834526	0.228009808	0.0000035416
2000	128.7121799	1.088380496	0.228136872	0.0000035277
2200	135.4247293	1.089775966	0.228277311	0.0000035138
2400	141.5094212	1.091039337	0.228431125	0.0000034999
2600	147.0410961	1.092186586	0.228598314	0.0000034860
2800	152.0850902	1.093231617	0.228778878	0.0000034720
3000	156.6985265	1.094186548	0.228972817	0.0000034581
3200	160.9314247	1.095061958	0.229180132	0.0000034442
3400	164.8276528	1.095867106	0.229400821	0.0000034303
3600	168.4257452	1.096610103	0.229634886	0.0000034164
3800	171.7596043	1.097298074	0.229882326	0.0000034025

A-5) Schedule

Production

LGR Well Specification (Prod1) [WELSPECL]

Well	PROD 1
Group	1
LGR	PRODUCER
I Location	1
J Location	1
Datum depth	8,120 ft
Preferred Phase	GAS
Inflow Equation	STD
Automatic Shut-In instruction	SHUT
Cross flow	YES
Density calculation	SEG
Type of Well Model	STD

Amalgamated LGR Well Comp Data (Prod1) [COMPDATL]

Well	PROD 1
LGR	PRODUCER
K Upper	1
K Lower	3
Open/Shut Flag	OPEN
Wellbore ID	6.125 in
Direction	Z

Production Well Control (Prod1) [WCONPROD]

Well	PROD 1
Open/Shut Flag	OPEN
Control	GRAT
Gas rate	10,000 MSCF/D
BHP target	14.7 psia
THP target	200 psia
VFP Pressure Table	1

Production Well Economics Limit [WECON]

Well	PROD 1
Minimum oil rate	13.32 STB/D
Minimum gas rate	100 MSCF/D
Workover procedure	NONE
End run	YES
Quantity for Economic Limit	RATE
Secondary Workover Procedure	NONE

Production Vertical Flow Performance [VFPPROD]

VFP Table Number	1
Datum Depth	8,120 ft
Flow Rate Definition	GAS
Water Fraction Definition	WGR
Gas Fraction Definition	GOR
Fixed Pressure Definition	THP
Table Units	FIELD
Tabulated Quantity Definition	BHP

Injection

Well Specification (Inj1) [WELSPECS]

Well	INJ 1
I Location	15
J Location	15
Datum depth	8,120 ft
Preferred Phase	GAS
Inflow Equation	STD
Automatic Shut-In instruction	SHUT
Cross flow	YES
Density calculation	SEG
Type of Well Model	STD

Well Connection Data (Inj1) [COMPDAT]

Well	INJ 1
K Upper	1
K Lower	3
Open/Shut Flag	SHUT
Wellbore ID	6.125 in
Direction	Z

Injection Well Control (Inj1) [WCONINJE]

Well	INJ 1
Injector type	GAS
Open/Shut Flag	SHUT
Control Mode	RATE
Gas Surface Rate	10,000 MSCF/D

Nature of Injection Gas (Inj1) [WINJGAS]

Well	INJ 1
Injector fluid	STREAM
Well stream	1

Injection Gas Composition [WELLSTRE]

Well stream	1
Comp 10	1

APPENDIX B

B-1) Phase behavior

The phase behavior of gas condensate reservoir generated from PVTi program (ECLIPSE 300 adds on).

CASE 1

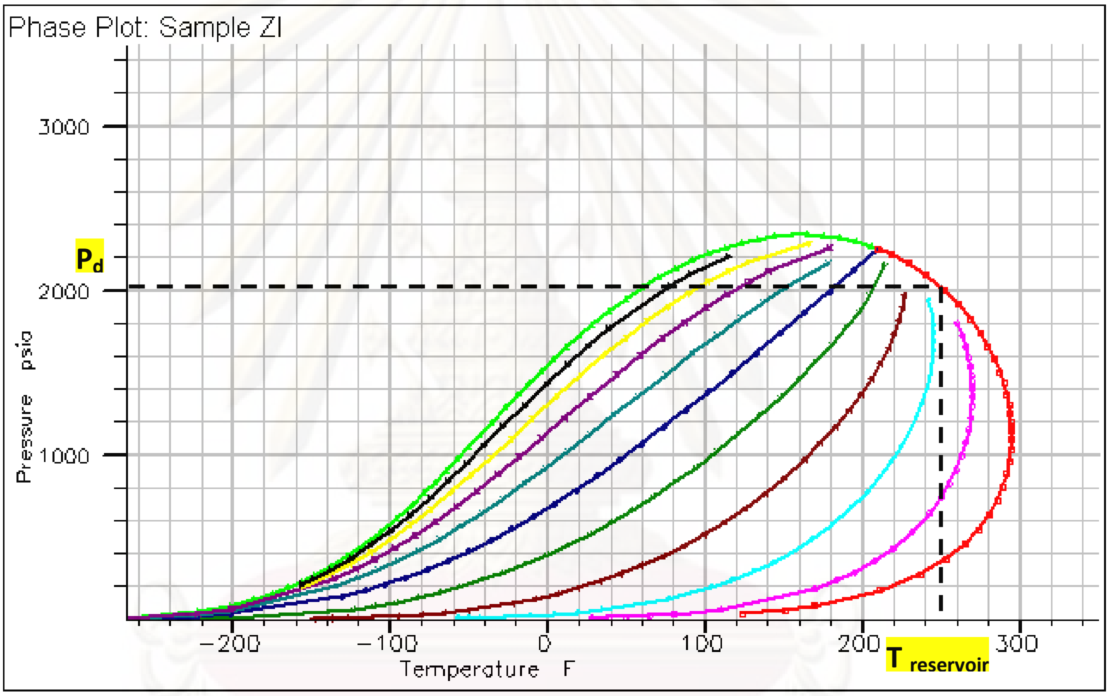

CASE 2

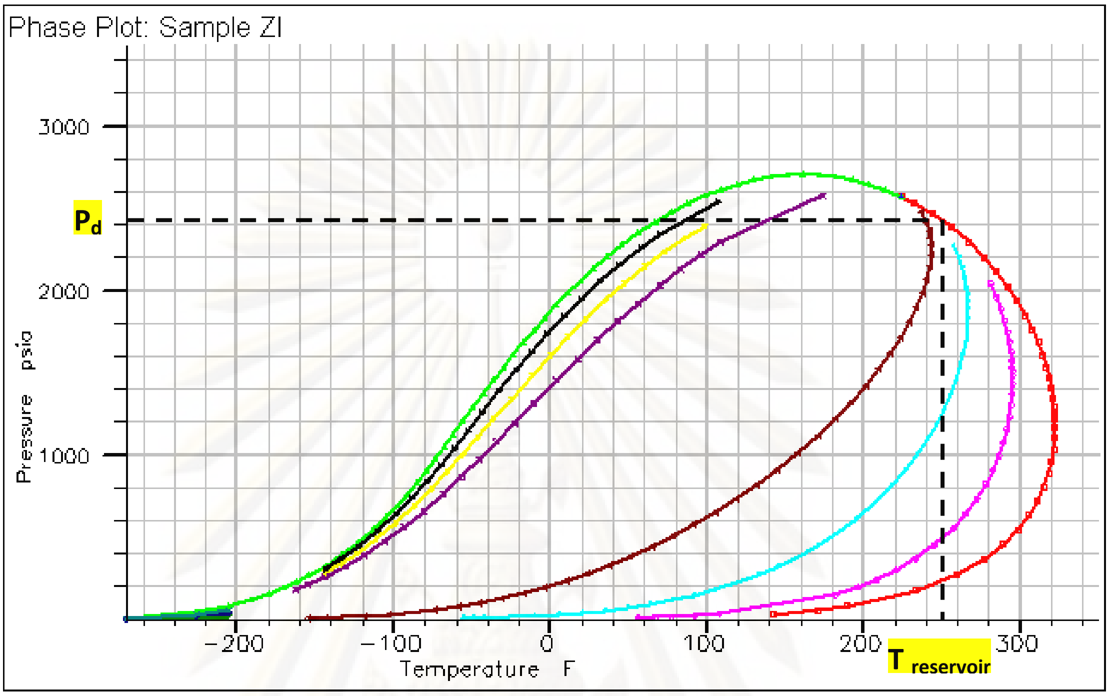
Phase Plot: Sample ZI
3000
2000
1000
Pressure psia
Pd
-200
-100
0
100
200
300
Temperature F
T reservoir

CASE 3

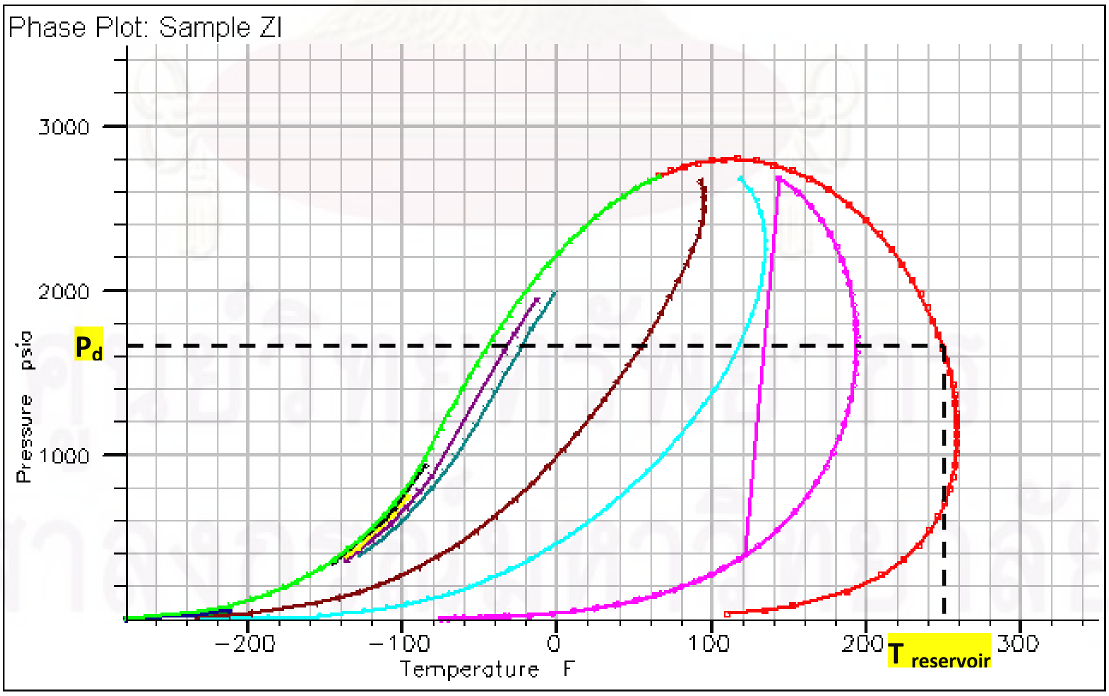
Phase Plot: Sample ZI
3000
2000
1000
Pressure psia
Pd
-200
-100
0
100
200
300
Temperature F
T reservoir

CASE 4

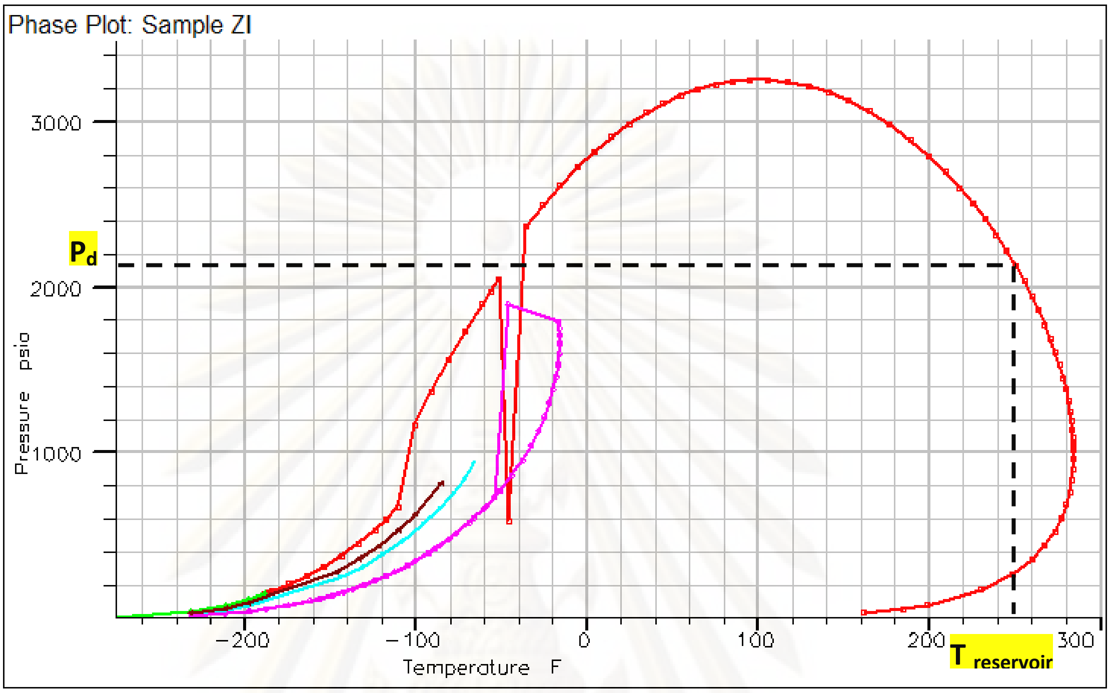
Phase Plot: Sample ZI
Pressure psia
3000
2000
1000
Pd
-200
-100
0
100
200
300
Temperature F
T reservoir

CASE 5

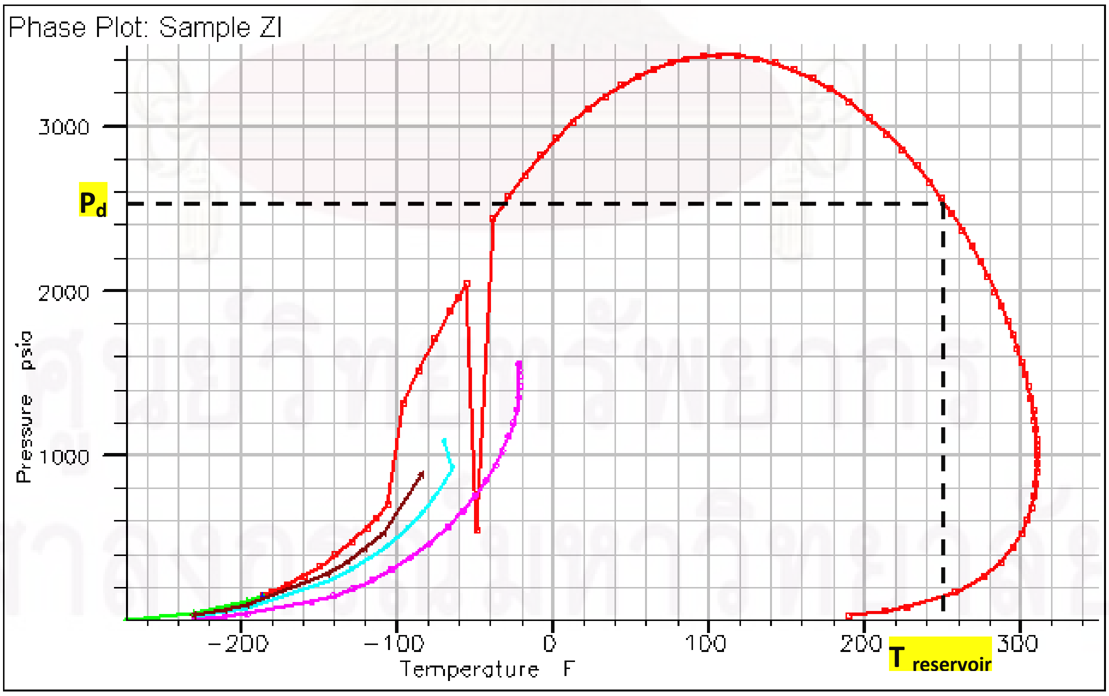
Phase Plot: Sample ZI
Pressure psia
3000
2000
1000
Pd
-200
-100
0
100
200
300
Temperature F
T reservoir

CASE 6

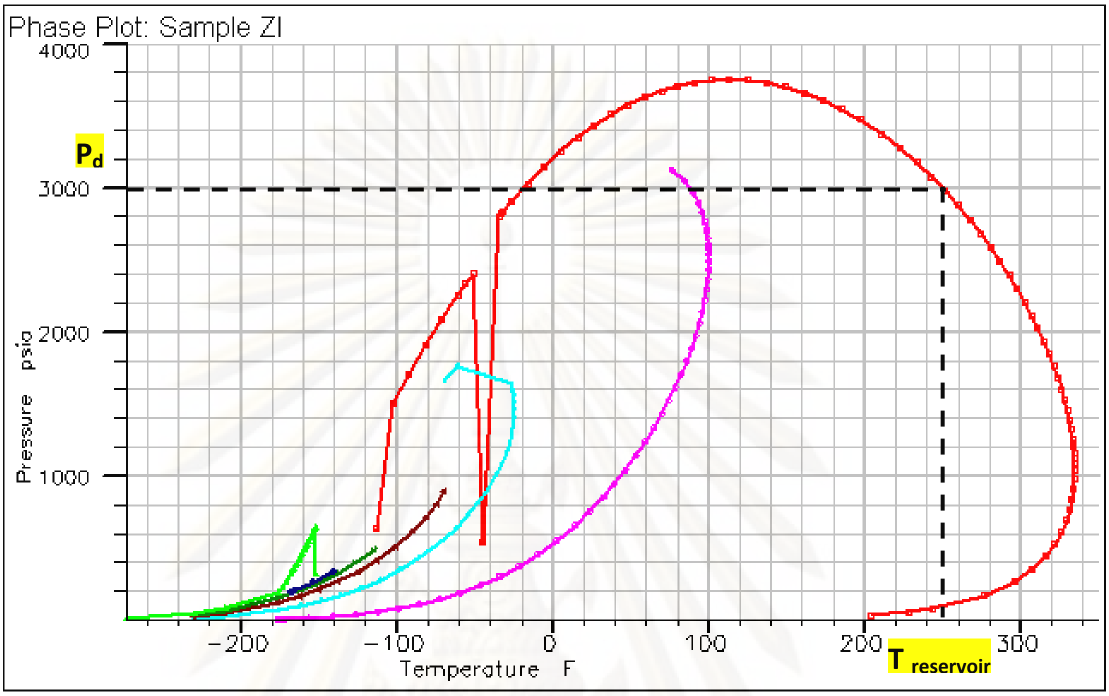
Phase Plot: Sample ZI
4000
3000
2000
1000
Pd
Pressure psia
-200
-100
0
100
200
300
Temperature F
T reservoir

CASE 7

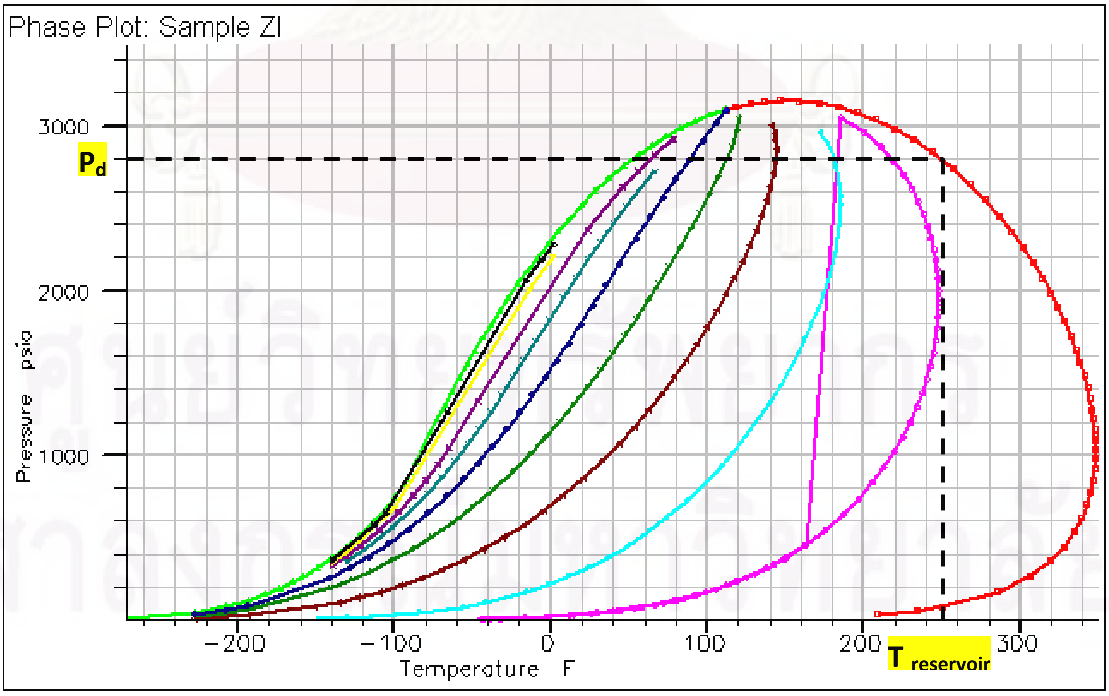
Phase Plot: Sample ZI
3000
2000
1000
Pd
Pressure psia
-200
-100
0
100
200
300
Temperature F
T reservoir

CASE 8

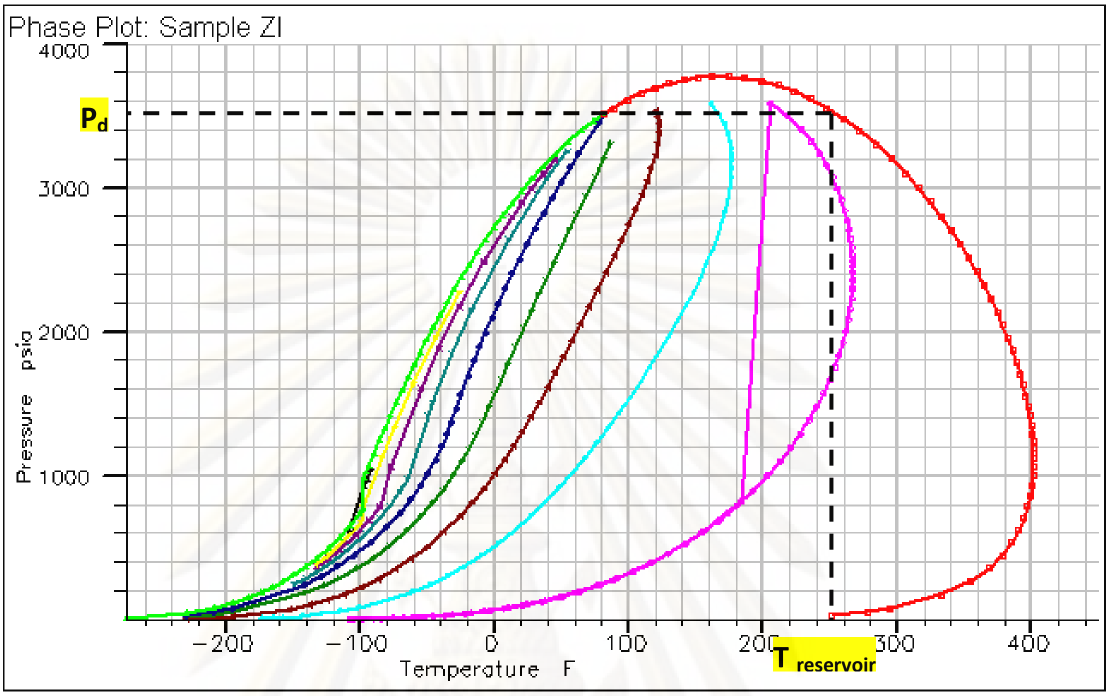
Phase Plot: Sample ZI
4000
3000
2000
1000
Pd
Pressure psia
-200
-100
0
100
200
300
400
Temperature F
T reservoir

CASE 9

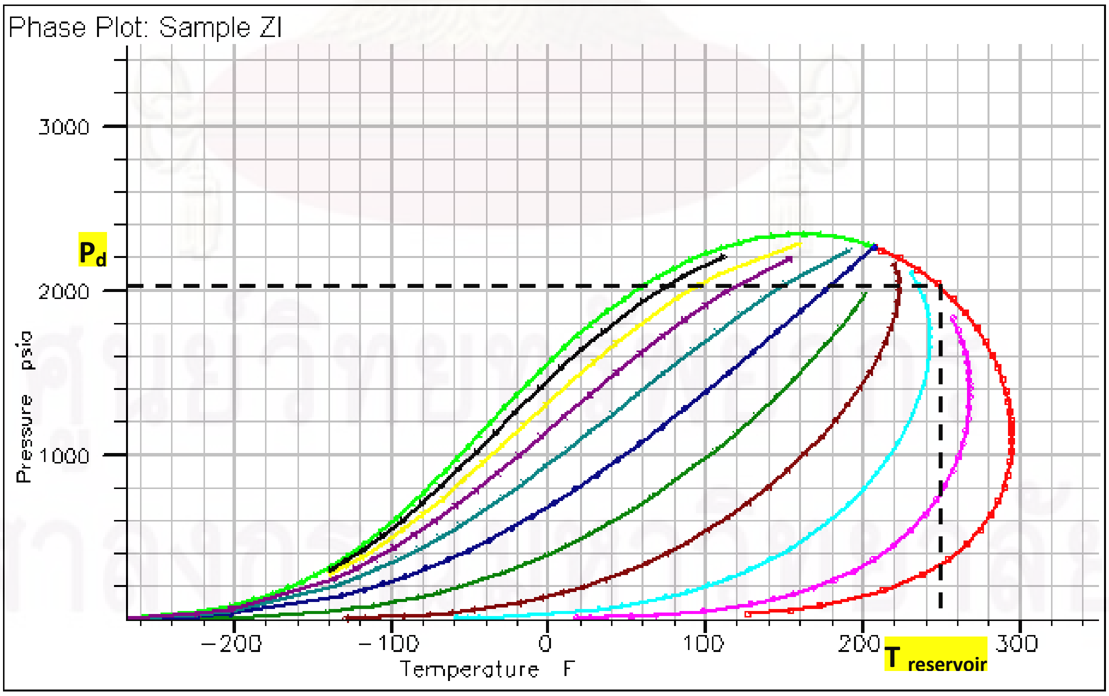
Phase Plot: Sample ZI
3000
2000
1000
Pd
Pressure psia
-200
-100
0
100
200
300
Temperature F
T reservoir

CASE 10

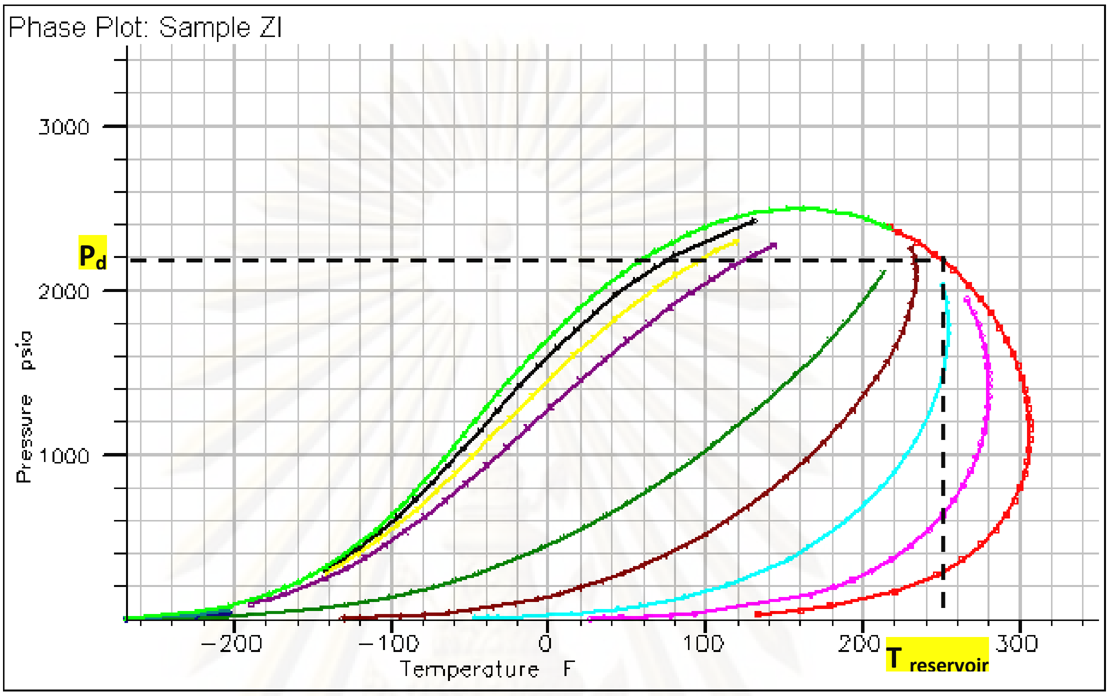
Phase Plot: Sample ZI
3000
2000
1000
P_d
Pressure psia
−200
−100
0
100
200
300
Temperature F
$T_{reservoir}$

B-2) Binary interaction coefficient

The binary interaction coefficient between components calculated from PVTi program (ECLIPSE 300 adds on).

	N_2	CO_2	C1	C2	C3	i-C4	n-C4	i-C5	n-C5	C6	C7	C8	C9	C10	C11	C12+
N_2	0	0	0.0106	0.0100	0.0100	0	0	0	0	0	0	0	0	0	0	0
CO_2	0	0	0.0153	0.0100	0.0100	0	0	0	0	0	0	0	0	0	0	0
C1	0.0106	0.0153	0	0	0	0.0196	0.0196	0.0238	0.0238	0.0288	0.0343	0.0377	0.0401	0.0419	0.0435	0.0450
C2	0.0100	0.0100	0	0	0	0.0100	0.0100	0.0100	0.0100	0.0100	0.0100	0.0100	0.0100	0.0100	0.0100	0.0100
C3	0.0100	0.0100	0	0	0	0.0100	0.0100	0.0100	0.0100	0.0100	0.0100	0.0100	0.0100	0.0100	0.0100	0.0100
i-C4	0	0	0.0196	0.0100	0.0100	0	0	0	0	0	0	0	0	0	0	0
n-C4	0	0	0.0196	0.0100	0.0100	0	0	0	0	0	0	0	0	0	0	0
i-C5	0	0	0.0238	0.0100	0.0100	0	0	0	0	0	0	0	0	0	0	0
n-C5	0	0	0.0238	0.0100	0.0100	0	0	0 22	0	0	0	0	0	0	0	0
C6	0	0	0.0288	0.0100	0.0100	0	0	0	0	0	0	0	0	0	0	0
C7	0	0	0.0343	0.0100	0.0100	0	0	0	0	0	0	0	0	0	0	0
C8	0	0	0.0377	0.0100	0.0100	0	0	0	0	0	0	0	0	0	0	0
C9	0	0	0.0401	0.0100	0.0100	0	0	0	0	0	0	0	0	0	0	0
C10	0	0	0.0419	0.0100	0.0100	0	0	0	0	0	0	0	0	0	0	0
C11	0	0	0.0435	0.0100	0.0100	0	0	0	0	0	0	0	0	0	0	0
C12+	0	0	0.0450	0.0100	0.0100	0	0	0	0	0	0	0	0	0	0	0

APPENDIX C

C-1) Vertical Flow Performance (VFPi)

The vertical flow performance is used in study the aspects of pressure traverse calculations along well of production.

CASE 1

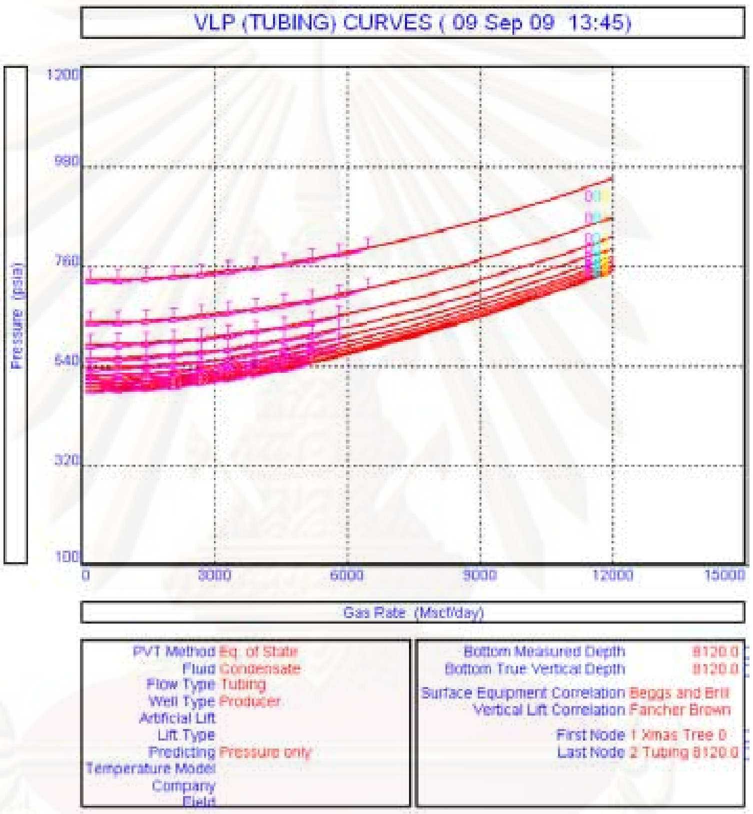

PVT Method Eq. of State
Fluid Condensate
Flow Type Tubing
Well Type Producer
Artificial Lift
Lift Type
Predicting Pressure only
Temperature Model
Company
Field

Bottom Measured Depth 8120.0
Bottom True Vertical Depth 8120.0
Surface Equipment Correlation Beggs and Brill
Vertical Lift Correlation Fancher Brown
First Node 1 Xmas Tree 0
Last Node 2 Tubing 8120.0

CASE 2

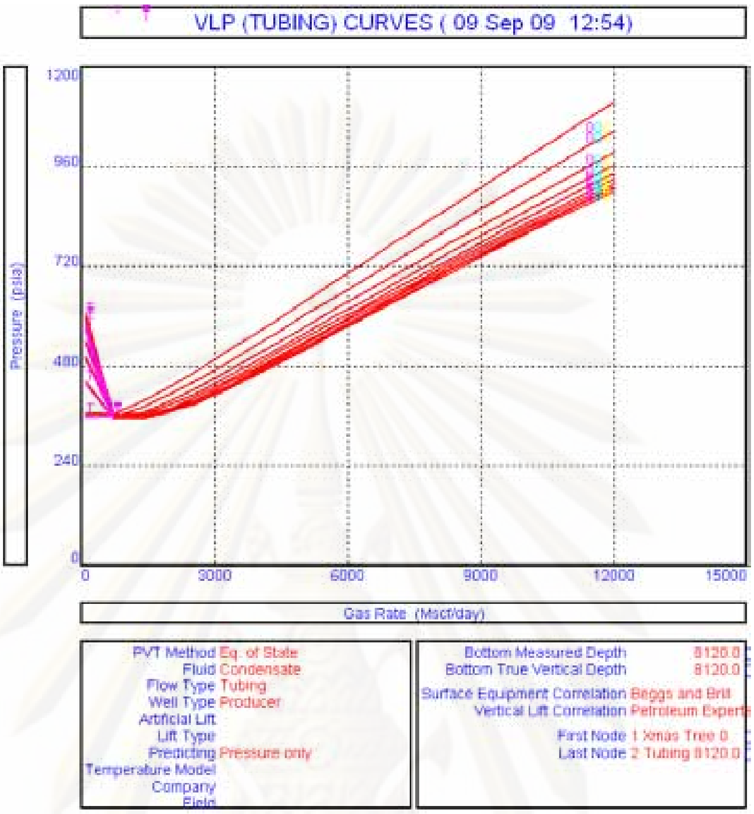

VLP (TUBING) CURVES (09 Sep 09 12:54)

PVT Method Eq. of State
Fluid Condensate
Flow Type Tubing
Well Type Producer
Artificial Lift
Lift Type
Predicting Pressure only
Temperature Model
Company
Field

Bottom Measured Depth 8120.0
Bottom True Vertical Depth 8120.0
Surface Equipment Correlation Beggs and Brill
Vertical Lift Correlation Petroleum Expert
First Node 1 Xmas Tree 0
Last Node 2 Tubing 8120.0

CASE 3

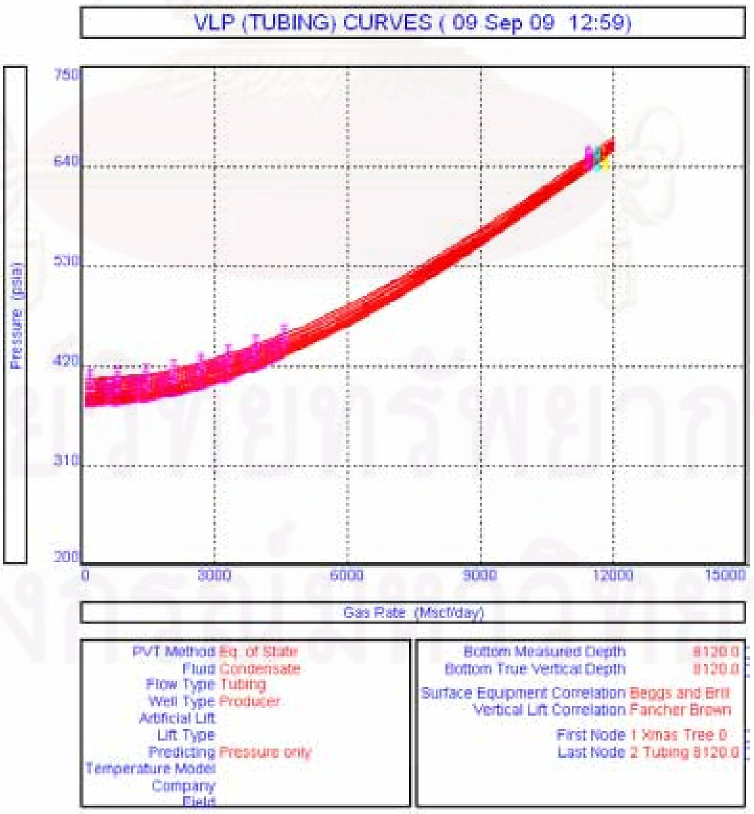

VLP (TUBING) CURVES (09 Sep 09 12:59)

PVT Method Eq. of State
Fluid Condensate
Flow Type Tubing
Well Type Producer
Artificial Lift
Lift Type
Predicting Pressure only
Temperature Model
Company
Field

Bottom Measured Depth 8120.0
Bottom True Vertical Depth 8120.0
Surface Equipment Correlation Beggs and Brill
Vertical Lift Correlation Fancher Brown
First Node 1 Xmas Tree 0
Last Node 2 Tubing 8120.0

CASE 4

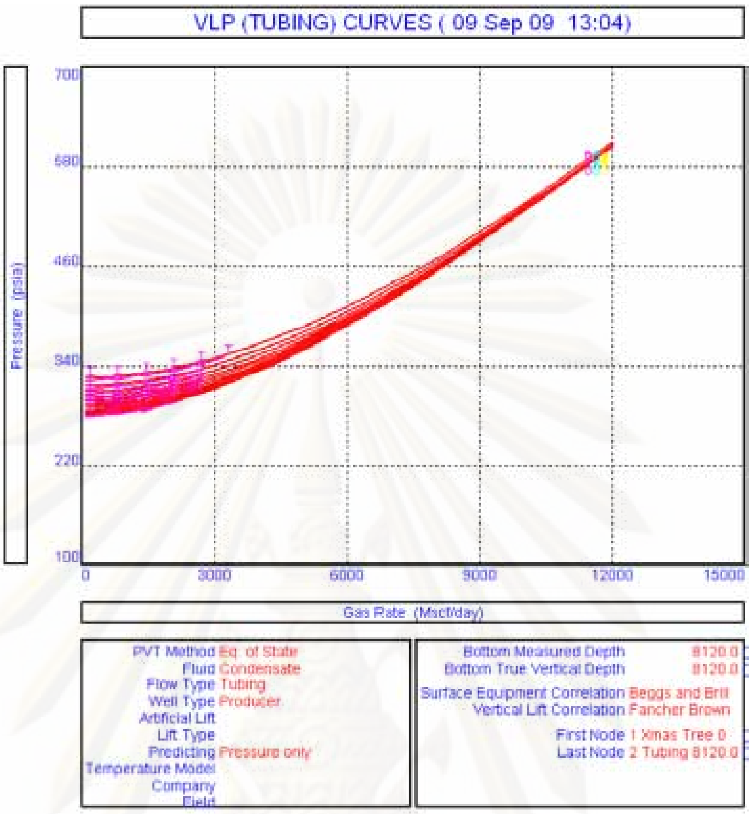

PVT Method Eq. of State
Fluid Condensate
Flow Type Tubing
Well Type Producer
Artificial Lift
Lift Type
Predicting Pressure only
Temperature Model
Company
Field

Bottom Measured Depth 8120.0
Bottom True Vertical Depth 8120.0
Surface Equipment Correlation Beggs and Brill
Vertical Lift Correlation Fancher Brown
First Node 1 Xmas Tree 0
Last Node 2 Tubing 8120.0

CASE 5

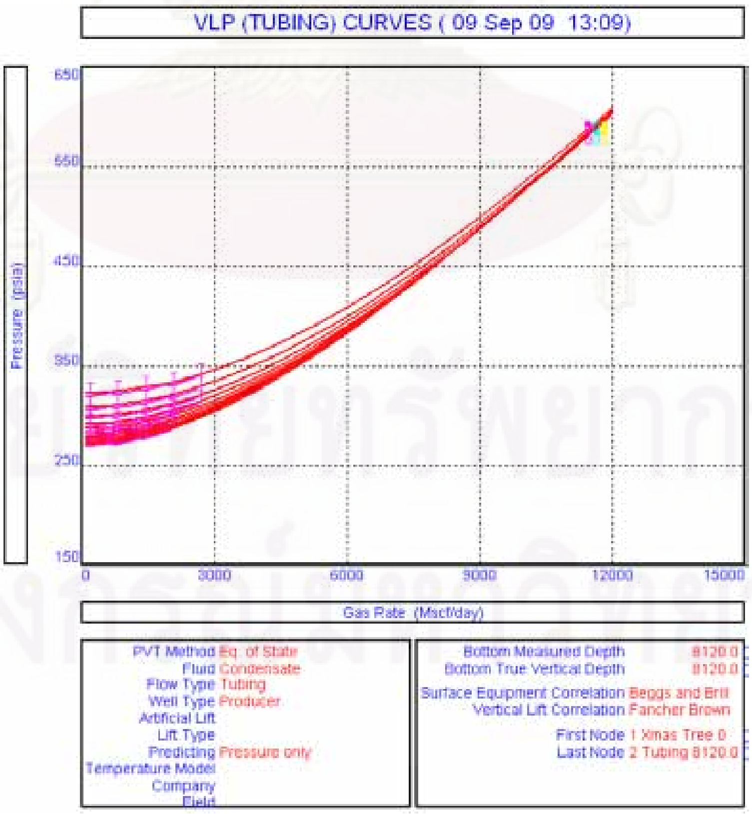

PVT Method Eq. of State
Fluid Condensate
Flow Type Tubing
Well Type Producer
Artificial Lift
Lift Type
Predicting Pressure only
Temperature Model
Company
Field

Bottom Measured Depth 8120.0
Bottom True Vertical Depth 8120.0
Surface Equipment Correlation Beggs and Brill
Vertical Lift Correlation Fancher Brown
First Node 1 Xmas Tree 0
Last Node 2 Tubing 8120.0

CASE 6

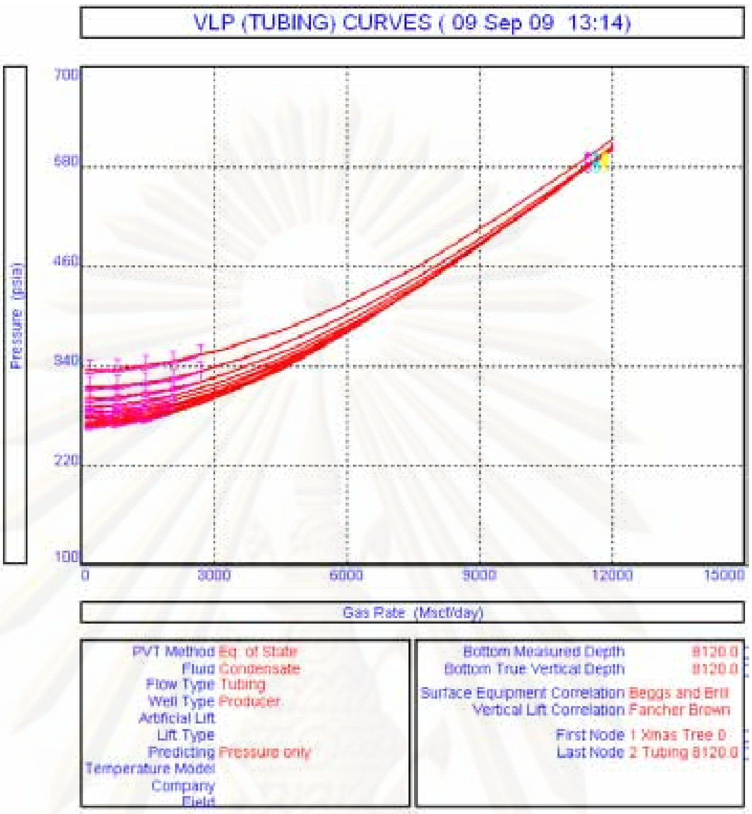

PVT Method Eq. of State
Fluid Condensate
Flow Type Tubing
Well Type Producer
Artificial Lift
Lift Type
Predicting Pressure only
Temperature Model
Company
Field

Bottom Measured Depth 8120.0
Bottom True Vertical Depth 8120.0
Surface Equipment Correlation Beggs and Brill
Vertical Lift Correlation Fancher Brown
First Node 1 Xmas Tree 0
Last Node 2 Tubing 8120.0

CASE 7

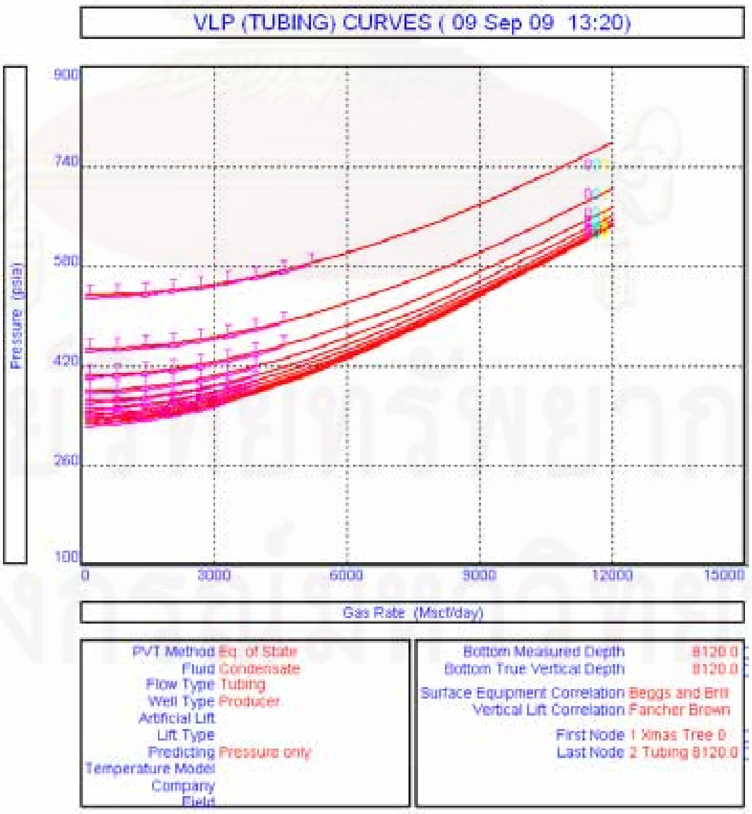

PVT Method Eq. of State
Fluid Condensate
Flow Type Tubing
Well Type Producer
Artificial Lift
Lift Type
Predicting Pressure only
Temperature Model
Company
Field

Bottom Measured Depth 8120.0
Bottom True Vertical Depth 8120.0
Surface Equipment Correlation Beggs and Brill
Vertical Lift Correlation Fancher Brown
First Node 1 Xmas Tree 0
Last Node 2 Tubing 8120.0

CASE 8

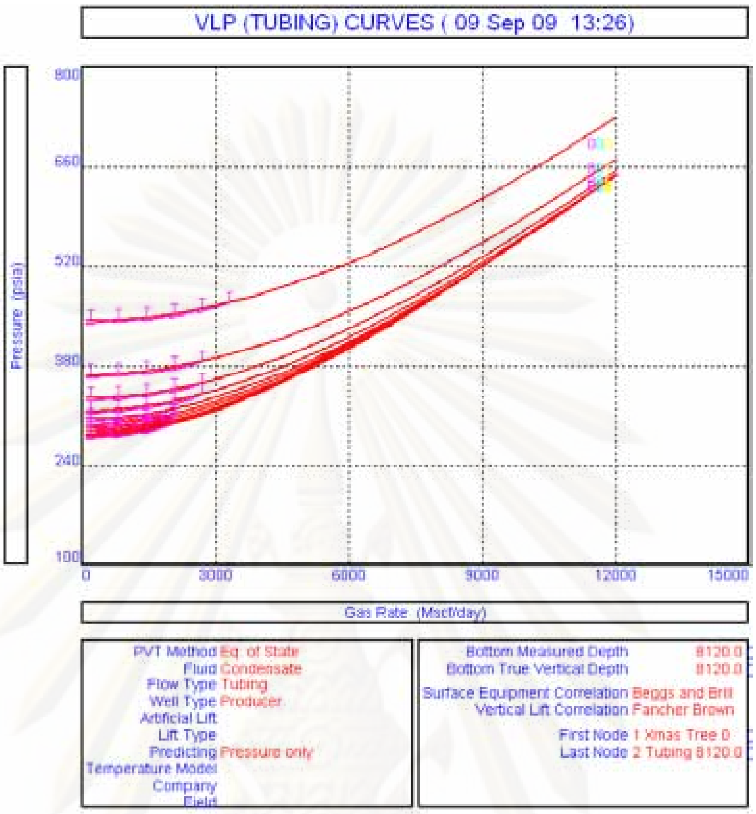

PVT Method Eq. of State
Fluid Condensate
Flow Type Tubing
Well Type Producer
Artificial Lift
Lift Type
Predicting Pressure only
Temperature Model
Company
Field

Bottom Measured Depth 8120.0
Bottom True Vertical Depth 8120.0
Surface Equipment Correlation Beggs and Brill
Vertical Lift Correlation Fancher Brown
First Node 1 Xmas Tree 0
Last Node 2 Tubing 8120.0

CASE 9

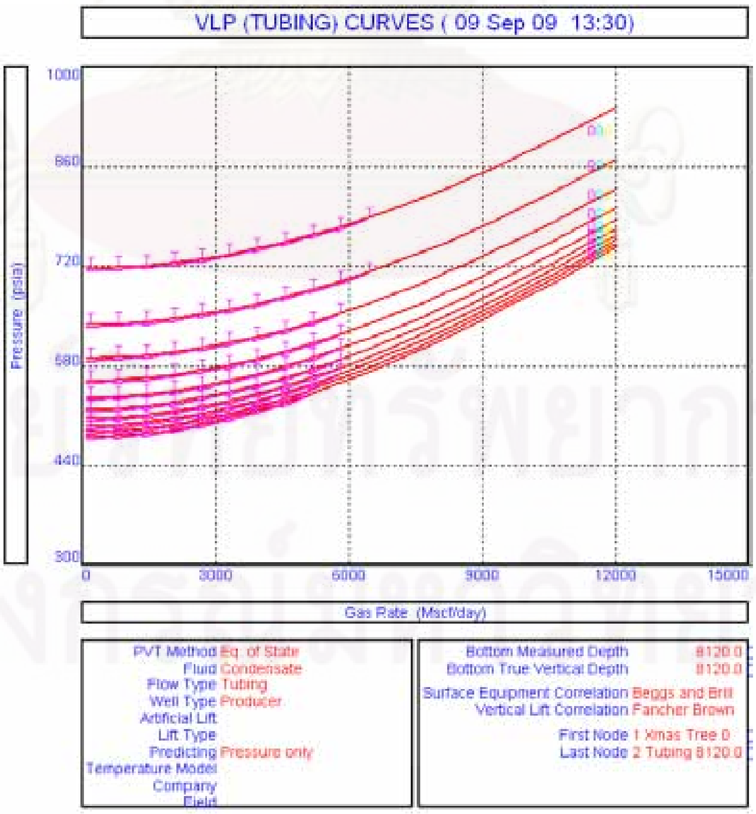

PVT Method Eq. of State
Fluid Condensate
Flow Type Tubing
Well Type Producer
Artificial Lift
Lift Type
Predicting Pressure only
Temperature Model
Company
Field

Bottom Measured Depth 8120.0
Bottom True Vertical Depth 8120.0
Surface Equipment Correlation Beggs and Brill
Vertical Lift Correlation Fancher Brown
First Node 1 Xmas Tree 0
Last Node 2 Tubing 8120.0

CASE 10

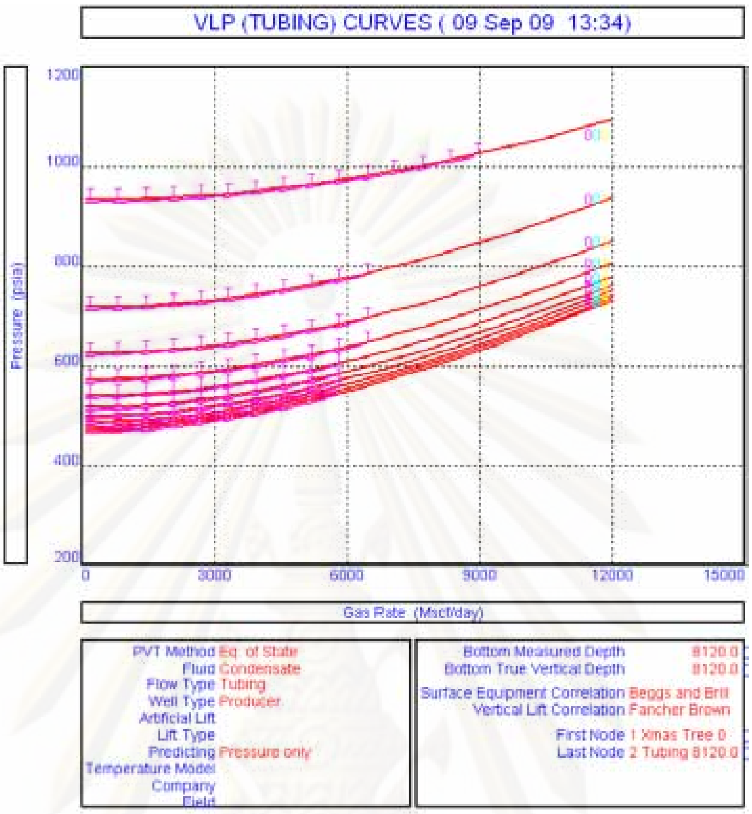

PVT Method Eq. of State
Fluid Condensate
Flow Type Tubing
Well Type Producer
Artificial Lift
Lift Type
Predicting Pressure only
Temperature Model
Company
Field

Bottom Measured Depth 8120.0
Bottom True Vertical Depth 8120.0
Surface Equipment Correlation Beggs and Brill
Vertical Lift Correlation Fancher Brown
First Node 1 Xmas Tree 0
Last Node 2 Tubing 8120.0

APPENDIX D

D-1) Compressor specification and Cost

Compressor Spec

Type	: Reciprocating
Design capacity	: 14.0 MMSCF/D
Operating capacity	: 12.5 MMSCF/D
Operating suction pressure	: 275 psig
Operating discharge pressure	: 1,350 psig (Δp = 1,075 psig)
Operating temperature	: 50 °C
Estimated required power	: 1,400 HP

Cost estimation of compressor

Items	**Cost[1] (1000 US$)**
PDS Tariff	
- Detailed design	25.0
- Construction	30.0
- Project management	25.0
Materials	1,760
- Compressor package	
- Compressor frame and cylinders	
- F&G lube system	
- Pulsation dampener and separator	
- Air cooler	
- Gas engine driver	
- Skid	
- Water cooling system	
- PLC control unit	
- Drawings	
- Transportation and insurance for major equipment	137.5
- Foundation and grouting work	100.0
- Mechanical modification	50.0
- Instrumentation (replace the aging facility)	25.0

Items	Cost[1] (1000 US$)
- Electrical modification (hook-up to power supply from the existing facility)2 - Soft starter panel, 110 kW, IP55 for fan motor - Cables - RCU - Small distribution board - Lightings - Splice box - Accessories	112.5
- Modification of fire and gas detection system - New sensor units (5 sets) - Modification of existing fire and gas alarm panel - Software	30.0
- Commissioning spare parts3	0.0
- Other bulks	25.0
Construction and Commissioning Cost	
- Civil work	20.0
- Mechanical work	37.5
- Electrical work4	20.0
- Instrument work	5.0
- Third party inspection of K-3850 at the factory	15.0
- Installation, commissioning, and training (vendor)	60.0
- Contingency (10%)	247.75
Total	2,725.25

The above costs form part of BI 5DXX

Notes: Cost for electrical facility has been based on the estimated electrical consumption (by the air cooler fan) of 90-110 kW.

D-2) Electrical/Power consumption calculations

Pumping power is defined as the time-rate of pumping work. It is related to pumping rate and pressure by

$$\text{power} = \frac{\text{work}}{\text{time}} = q\Delta p$$

The customary unit of power for combustion engines is horsepower (HP) and for electrical motors is the kilowatt (kw). The power units are related by

$$1\ \text{HP} = 0.746\ \text{kw}$$

The approximate compressor power

$$P = 0.23\, q_g \left[\left(\frac{p_2}{p_1}\right)^{0.2} - 1\right]$$

where

q_g is gas compression rate, mscf/D

p_1 is compressor suction pressure, psia

p_2 is compressor discharge pressure, psia

P is compression power, HP

Injection Rate ; q (Mscf/D)	**Power (HP)**	**Power (kw)**	**Consumption Total Power Cost(USD/Year) EGAT Power**
10000	835.78	598.42	235,394.46

D-3) Calculation of Btu for produced gas

Case 6

Component	**Mole Fraction y_j**	**Gross Heating value, (Btu/scf) L_{cj}**	**y_j*L_{cj}**	**Compressibility Factor at Standard Conditions**	
				z_j	**$y_j(1\text{-}zj)^{0.5}$**
C1	0.834	1010.0	842.340	0.9980	0.037298
C2	0.072	1769.6	127.411	0.9919	0.006480
C3	0.0274	2516.1	68.941	0.9825	0.003625
i-C4	0.0054	3251.9	17.560	0.9711	0.000918
n-C4	0.009	3262.3	29.361	0.9667	0.001642
i-C5	0.0042	4000.9	16.804	0.9480	0.000958
n-C5	0.003	4008.9	12.027	0.9420	0.000722
C6	0.0058	4755.9	27.584	0.9100	0.001740
C7+	0.0326	5502.5	179.382	0.8520	0.012541
N2	0.0047	0.0	0	0.9875	0.000525
CO2	0.0019	0.0	0	0.9943	0.000143
	1.0000		**1321.410**		**0.066593**

$Z = 1 - (\sum y_j (1-z_j)^{0.5})^2$

$Z = 1 - (0.066593)^2$

$= 0.995565$

$L_c = L_{c\ ideal} \ / \ z$

$L_c = (1321.410\ \text{Btu/scf}) / 0.995565$

Btu / scf = 1327.2966

Case 9

Component	Mole Fraction y_j	Gross Heating value, (Btu/scf) L_{cj}	y_j*L_{cj}	Compressibility Factor at Standard Conditions	
				z_j	$y_j(1-zj)^{0.5}$
C1	0.6072	1010.0	613.272	0.9980	0.027155
C2	0.081	1769.6	143.338	0.9919	0.007290
C3	0.0637	2516.1	160.276	0.9825	0.008427
i-C4	0.0398	3251.9	129.426	0.9711	0.006766
n-C4	0.0445	3262.3	145.172	0.9667	0.008120
i-C5	0.0291	4000.9	116.426	0.9480	0.006636
n-C5	0.0252	4008.9	101.024	0.9420	0.006069
C6	0.0179	4755.9	85.131	0.9100	0.005370
C7+	0.0885	5502.5	486.971	0.8520	0.034047
N2	0.0013	0.0	0	0.9875	0.000145
CO2	0.0018	0.0	0	0.9943	0.000136
	1.0000		**1981.035**		**0.110161**

$Z = 1 - (\sum y_j (1-z_j)^{0.5})^2$

$Z = 1 - (0.110161)^2$

$= 0.987865$

$L_c = L_{c\ ideal} / z$

$L_c =$ (1981.035 Btu/scf) / 0.987865

Btu / scf = 2500.3714

Appendix E

E-1) Cash flow of production with natural depletion

Case 6

Year	Gross Revenue (US$)		5% Royalties (US$)	Power Consum. (US$)	Capex (US$)	Depletiation (US$)	Taxes (US$)	Net Income (US$)	Present Value (US$)
	Gas	Oil							
0	-	-	-	-	1,800,000	-	-	- 1,800,000	-1,800,000
1	16,952,425	11,533,429	576,671	235,394		360,000	13,656,894	14,016,894	12,742,631
2	16,952,425	6,908,932	345,447	235,394		360,000	11,460,258	11,820,258	9,768,808
3	16,509,753	4,070,502	203,525	235,394		360,000	9,890,668	10,250,668	7,701,478
4	9,426,821	2,080,212	104,011	235,394		360,000	5,403,814	5,763,814	3,936,762
5	4,779,107	1,124,380	56,219	235,394		360,000	2,625,937	2,985,937	1,854,032
6	2,775,813	719,958	35,998	235,394			1,612,189	1,612,189	910,039
7	1,762,880	494,273	24,714	235,394			998,523	998,523	512,400
8	1,191,927	354,785	17,739	235,394			646,789	646,789	301,732
9	835,355	260,034	13,002	235,394			423,497	423,497	179,604
10	604,788	194,830	9,742	235,394			277,241	277,241	106,889
11	312,152	102,898	5,145	235,394			87,256	87,256	30,583

Case 9

Year	Gross Revenue (US$)		5% Royalties (US$)	Power Consum. (US$)	Capex (US$)	Depletiation (US$)	Taxes (US$)	Net Income (US$)	Present Value (US$)
	Gas	Oil							
0	-	-	-	-	1,800,000	-	-	- 1,800,000	-1,800,000
1	31,937,500	25,000,975	1,250,049	235,394		360,000	27,546,516	27,906,516	25,369,560
2	31,937,500	20,329,541	1,016,477	235,394		360,000	25,327,585	25,687,585	21,229,409
3	31,200,540	8,472,518	423,626	235,394		360,000	19,327,019	19,687,019	14,791,149
4	18,623,439	4,135,027	206,751	235,394		360,000	10,978,160	11,338,160	7,744,116
5	9,452,625	2,440,034	122,002	235,394		360,000	5,587,631	5,947,631	3,693,011
6	5,209,558	1,538,341	76,917	235,394			3,217,793	3,217,793	1,816,361
7	3,025,461	969,888	48,494	235,394			1,855,730	1,855,730	952,283
8	1,819,186	616,522	30,826	235,394			1,084,744	1,084,744	506,041
9	1,106,621	388,474	19,424	235,394			620,139	620,139	262,999
10	681,896	244,526	12,226	235,394			339,401	339,401	130,854
11	338,135	122,693	6,135	235,394			109,649	109,649	38,431

E-2) Cash flow of production with 23% CO_2 limit

Case 6

Year	Gross Revenue (US$)		5% Royalties (US$)	Power Consum. (US$)	Capex (US$)	Depletiation (US$)	Taxes (US$)	Net Income (US$)	Present Value (US$)
	Gas	Oil							
0	-	-	-	-	6,325,250	-	-	- 6,325,250	-6,325,250
1	16,952,418	12,949,094	647,455	235,394		1,265,050	13,876,806	15,141,856	13,765,324
2	16,951,183	12,751,248	637,562	235,394		1,265,050	13,782,212	15,047,262	12,435,754
3	16,651,458	11,874,475	593,724	235,394		1,265,050	13,215,882	14,480,932	10,879,739
4	9,076,174	7,303,554	365,178	235,394		1,265,050	7,257,053	8,522,103	5,820,711

Case 9

Year	Gross Revenue (US$)		5% Royalties (US$)	Power Consum. (US$)	Capex (US$)	Depletiation (US$)	Taxes (US$)	Net Income (US$)	Present Value (US$)
	Gas	Oil							
0	-	-	-	-	6,325,250	-	-	- 6,325,250	-6,325,250
1	31,937,441	25,000,975	1,250,049	235,394		1,265,050	27,093,961	28,359,011	25,780,919
2	31,937,325	24,914,809	1,245,740	235,394		1,265,050	27,052,974	28,318,024	23,403,326
3	31,928,345	24,929,512	1,246,476	235,394		1,265,050	27,055,468	28,320,518	21,277,624
4	30,364,732	22,729,692	1,136,485	235,394		1,265,050	25,228,748	26,493,798	18,095,620
5	5,342,437	3,315,954	165,798	235,394		1,265,050	3,496,074	4,761,124	2,956,284

Vitae

Patamaporn Thitaram was born on July 7th, 1982 in Bangkok, Thailand. She received her Bachelor of Engineering in Chemical Engineering from the Faculty of Engineering, King Mongkut's University of Technology Thonburi in 2004. She has been a graduate student in the Master's Degree Program in Petroleum Engineering of the Department of Mining and Petroleum Engineering, Chulalongkorn University since 2007.